Physics – Uspekhi **44** (3) 221 – 253 (2001)

REVIEWS OF TOPICAL PROBLEMS

PACS numbers: **31.10.+z**, **31.25.–v**, 34.20.Cf, **34.70.+e**

Atomic structure and the resonant charge exchange process

B M Smirnov

DOI: 10.1070/PU2001v044n03ABEH000826

Contents

Abstract. Inaccuracies in the atomic shell model due to the neglect of electron correlation and some relativistic effects are examined. The asymptotic behavior of atomic valence electrons is considered, and the accuracy of the asymptotic coefficient of the electron wave function is evaluated with account for the model errors. The coupling of the electron orbital momenta and spins in atomic particles, molecules, and colliding particles is discussed. The resonant charge exchange process is analyzed in terms of the asymptotic theory, with the inverse of the typical ion – atom separation being used in the small-parameter expansion of the cross section. The influence of atomic shell model errors — via the valence electron asymptotic coefficient — on the accuracy of the charge exchange cross section is discussed. The relation between the cross section and the specifics of the moment addition law for an ion – atom collision event is elucidated. The accuracy-estimated values of cross sections for the slow-collision resonant charge exchange are given for most elements in the periodic table.

B M Smirnov Institute for High Temperatures, Russian Academy of Sciences, ul. Izhorskaya 13/19, 127412 Moscow, Russian Federation
Tel./Fax (7-095) 190 42 44
E-mail: smirnov@oivtran.iitp.ru

Received 11 August 2000
Uspekhi Fizicheskikh Nauk **171** (3) 233 – 266 (2001)
Translated by B M Smirnov; edited by A Radzig

1. Introduction

The atomic shell model [1 – 5] is a convenient model for the atomic structure, which describes the main features of the physics of atoms. This model includes a one-electron approach with an exchange interaction between electrons due to the Pauli exclusion principle [6] and spin – orbit interactions for individual electrons. The errors of this model result from neglecting the correlations between electrons and from ignoring other relativistic interactions. If we calculate the interaction potential of atomic particles and the cross section of collisional processes within the framework of the atomic shell model for atomic particles, the errors of the latter model will be extended to these parameters. Below we analyze this problem for the ion – atom exchange interaction potential at large separations that determines the cross section of the resonant charge exchange process at low collision energies.

The character of momentum addition is of importance both for atoms or molecules and for collisional processes of atomic particles. Within the framework of the atomic shell model, we have two schemes of coupling of electron orbital momenta and spins into the total atomic momentum (*LS*-coupling and *jj*-coupling schemes), depending on the relation between the exchange interaction of electrons and the spin – orbit interaction. The *LS*-scheme of coupling of electron momenta provides a high accuracy for the relative positions of atomic energy levels of a given electron shell in the case of light atoms. For heavy atoms, when the *jj*-coupling scheme is preferable, the accuracy in determination of energy levels is worse and strongly drops with increasing atomic number.

This is due to additional relativistic effects with respect to the spin – orbit interaction, and the role of these relativistic interactions increases with increasing nuclear charge. This will be shown for simple examples.

In molecules, the rotational energy is added to the above two interactions, and this leads to six limiting cases of momentum addition, which are known as the cases of Hund coupling scheme [7, 8]. In the case of collisions of atomic particles, the character of momentum addition becomes more complex because some of the interaction potentials depend on time. We consider slow collisions, when the velocity of colliding particles is small compared to a typical electron velocity, so that electrons are redistributed in the course of collision in accordance with the variations of atomic fields. Then the evolution of colliding atomic particles may be connected with parameters of the quasi-molecule, that is the system of colliding atoms for fixed nuclei, and the internuclear distance of colliding particles is a parameter in the wave function of the quasi-molecule. In this case the number of limiting cases of momentum coupling is the same as for molecules (i.e. they relate to different cases of Hund coupling scheme), but different limiting cases correspond to different regions of the particle trajectory [9 – 11].

Though a general method of momentum addition for colliding particles is cumbersome, the coupling schemes are simplified for certain collisional processes with participation of slow atomic particles. This applies to quasi-resonant processes in atomic collisions which are characterized by large cross sections in comparison to a typical atomic cross section. This means that the transition proceeds at large separations between atomic particles that allows one to connect the electronic terms of the quasi-molecule consisting of colliding particles and to express the cross section of the process under consideration through the parameters of free atomic particles. This also simplifies the character of momentum addition for colliding particles.

Below we consider this problem for the resonant charge exchange process in slow collisions involving an ion and the parent atom. This process results in the transition of a valence electron from the field of one atomic core to another. The transition proceeds at large separations between the colliding ion and atom that allows one to construct an asymptotic theory of this process [12 – 14]. Then the cross section of this process is given in the form of an expansion over a small parameter which is an inverse value with respect to a typical separation for this transition. The simple character of the electron transition in this process simplifies the analysis of the momentum coupling schemes in the theory of resonant charge exchange in slow collisions. The demonstration of this fact is the goal of this paper. An additional aim of the paper is the determination of the errors following from standard atomic models and the evaluation of the accuracy of the asymptotic theory. The subsequent analysis shows that the accuracy of the evaluated cross sections is usually determined by the accuracy of atomic wave functions for valence electrons of atoms.

2. Atomic shell model

2.1 Schemes of coupling of electron momenta in atoms

The atomic shell model considers an atom to consist of a heavy Coulomb center and bound electrons, and the action of other electrons and the Coulomb center on a test electron is changed by an effective self-consistent field which does not depend on the coordinates of the other electrons, but takes into account the exchange interaction between electrons. Therefore, the behavior of electrons is described by the Hartree – Fock equations [2, 4, 5, 15 – 17]. The atomic shell model distributes electrons over electron shells, so that because of the spherically symmetric form of a self-consistent field, each shell is characterized by the principal quantum number and angular electron momentum. According to the Pauli exclusion principle, only one electron can be found in each state of each electron shell, and this state is also defined by the projections of the angular momentum and spin of an electron onto a given direction.

Below we use two schemes of coupling of electron momenta in an atom, so that in the case of the *LS*-coupling scheme the state of an individual electron is characterized by the electron orbital momentum and spin, and we neglect the spin – orbit interaction in constructing the atom's electron shell. Until we neglect the relativistic interactions, the electronic terms of an atom are described by the quantum numbers L, the total atomic orbital momentum, and S, the total atomic spin. The momenta are added into the total atomic momentum J, so that an atomic state is characterized by the quantum numbers L, S, J, M_J, where M_J is the projection of the total atomic momentum J onto a quantization axis.

In the second case of momentum addition, when relativistic interactions are dominant, the state of an individual electron is characterized by its total momentum j which is a sum of the orbital momentum of this electron and its spin. The electron momenta of individual electrons are composed into the total atomic momentum J, and an atomic state is characterized by the quantum numbers J, M_J and also by the total electron momenta of individual electrons. This is the *jj*-coupling scheme for the coupling of electron momenta into the total atomic momentum J.

Let us consider the character of the valence electron shell filling using the example of valence p-electrons. This is of interest for two reasons. First, such atoms occupy a certain part of the periodic table of elements and, second, the coupling of orbital and spin momenta is of importance in this case. We start from the *LS*-scheme of coupling of electron momenta, and within the framework of this scheme we construct the electron shell p^n. This shell includes n identical electrons whose orbital electron momentum is one, and they are located in the self-consistent field of the Coulomb center and other electrons. We demonstrate the shell structure using the example of an atom with a p^2-electron shell, and Fig. 1 shows the method of distributing these two electrons over 6 possible states which differ by projections of the electron

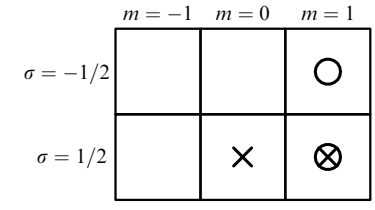

Figure 1. Distribution of valence p-electrons for atoms of the fourth group of the periodic table of elements over cells of the electron shell for states with the maximum atomic spin (open circles) and maximum atomic orbital momentum (crosses) [18].

orbital momentum and spin. According to the Pauli exclusion principle, only one electron can be placed in one cell, so that the total number of possible states is $C_6^2 = 15$ in this case. Let us distribute electrons throughout the states. First we extract the state with the maximum orbital momentum, which is indicated by open circles in Fig. 1 [18]. Take a direction of the quantization axis such that the projection of the orbital momentum of each electron onto this axis is equal to one. Then the projection of the total atomic orbital momentum onto this axis equals 2, and according to the Pauli exclusion principle the total spin projection is zero. The electronic term of this state is ^{1}D, and the statistical weight relative to this state (the number of projections of the atomic orbital momentum) is 5. Next, let us construct the state with the maximum projection of the total spin. We obtain that the spin projection is one, and the total orbital momentum projection is also one. This state corresponds to the term ^{3}P which includes 9 states with different projections of the atomic orbital momentum and its spin. Therefore, the selected terms ^{1}D and ^{3}P include 14 $(5+9)$ states from the total number of 15, and the additional state is ^{1}S. Hence, the electronic terms of atoms of the fourth group of the periodic table of elements with the valence shell p^2 are ^{3}P, ^{1}D, ^{1}S, and the same terms relate to atoms of the sixth group of the periodic table of elements with the valence shell p^4 (two p-holes).

The electron shell for the *jj*-scheme of coupling of electron momenta has a lower symmetry than in the case of the *LS*-scheme. In this case each electron can have the momentum 1/2 or 3/2. The total number of states for an electron shell with a given number of valence electrons is identical for both schemes as well as the total momentum of electrons. Table 1 lists the electronic terms of atoms in the case of filling the p-electron shells within the framework of the *LS*- and *jj*-coupling schemes. Note that the Pauli exclusion principle, which requires a certain symmetry of the total wave function of electrons, restricts the total number of possible electronic terms.

Table 1. Electron shells of atoms with p-valent electrons.

LS-shell	*LS*-term	*J*	*jj*-shell	*J*
p	^{2}P	1/2	$[1/2]^1$	1/2
	^{2}P	3/2	$[3/2]^1$	3/2
p^2	^{3}P	0	$[1/2]^2$	0
	^{3}P	1	$[1/2]^1[3/2]^1$	1
	^{3}P	2	$[1/2]^1[3/2]^1$	2
	^{1}D	2	$[3/2]^2$	2
	^{1}S	0	$[3/2]^2$	0
p^3	^{4}S	3/2	$[1/2]^2[3/2]^1$	3/2
	^{2}D	3/2	$[1/2]^1[3/2]^2$	3/2
	^{2}D	5/2	$[1/2]^1[3/2]^2$	5/2
	^{2}P	1/2	$[1/2]^1[3/2]^2$	1/2
	^{2}P	3/2	$[3/2]^3$	3/2
p^4	^{3}P	2	$[1/2]^1[3/2]^3$	2
	^{3}P	0	$[1/2]^2[3/2]^2$	0
	^{3}P	1	$[1/2]^1[3/2]^3$	1
	^{1}D	2	$[1/2]^2[3/2]^2$	2
	^{1}S	0	$[3/2]^4$	0
p^5	^{2}P	3/2	$[1/2]^2[3/2]^3$	3/2
	^{2}P	1/2	$[1/2]^1[3/2]^4$	1/2
p^6	^{1}S	0	$[1/2]^2[3/2]^4$	0

Due to the high accuracy of spectroscopic measurements, it is convenient to compare the atomic energy levels according to different models with the spectroscopic data for these levels [19–21], and this comparison allows one to ascertain the reality of these models. In particular, let us compare the position of the lower energy levels of atoms with the p^2-shell of valence electrons. Then both the *LS*- and *jj*-coupling schemes lead to an identical sequence for the total momentum of electrons, which is $J = 0, 1, 2, 2, 0$. The lightest atom with this electron shell is carbon, $C(2p^2)$, and the positions of its excitation energies are 0, 0.002, 0.005, 1.264 and 2.654 eV, respectively. This corresponds to the *LS*-coupling scheme where there are three terms ^{3}P, ^{1}D, ^{1}S with a weak splitting of the lowest one. The electron excitation energies for the heaviest atom with this electron shell, $Pb\,(6p^2)$, are 0, 0.969, 1.320, 2.660, 3.653 eV. It is difficult to divide them into levels and sublevels, i.e. this situation corresponds to an intermediate coupling scheme.

Thus, the above schemes of coupling of electron momenta allow one sequentially to construct an atom consisting of a heavy Coulomb center and electrons which are located in the self-consistent field of this center and other electrons. Within the framework of these schemes, we neglect the correlations between the positions of individual electrons (except an exchange interaction due to the Pauli exclusion principle), and relativistic interactions involving different electrons. What is the accuracy of such a scheme? The simplest way to estimate the error relative to neglecting the correlations between electrons consists in the analysis of a two-electron atom or ion. In this case the one-electron approximation leads to the Hartree–Fock equations [15–17] for the wave function of electrons. The energy of the ground state and lower excited states in this system can also be determined on the basis of the variational method [22–25] which allows us to find the optimal electron wave functions [21, 22]. Comparison of the calculated and measured electron energies gives the error of the one-electron approximation. In particular, the analysis of the helium atom in the ground [23, 26–28] and lower excited states [23, 29–31] which are determined on the basis of the variational principle [22–25] give an error of the order of 1–2% for the total electron energy. This corresponds to an error of several percent for the electron wave function. Hence, correlations between electrons can make a significant contribution to some atomic parameters.

Ignoring the electron correlation in the atom, which corresponds to the Hartree–Fock approach, can lead to a certain error both in the positions of atomic levels and various atomic parameters. Especially, the correlation between electron positions is of importance for those parameters which are determined by a small overlapping of wave functions. These correlations are of importance for the rates of forbidden radiative transitions and for the lifetimes of autoionizing states. Alongside the correlation of electrons, the shell scheme of atomic structure under consideration neglects some relativistic interactions such as the interaction of an electron spin with the fields created by other electrons. We consider the validity of such assumptions below on the basis of simple examples.

2.2 Lower excited states of rare gas atoms

The above *LS*- and *jj*-coupling schemes do not account for the variety of possible interactions in a real atom. One can demonstrate this for an atom which has two valence

electrons. In this case the following four schemes of coupling of electron momenta into the total atomic momentum are possible [5]:

$$\begin{aligned}
&\mathbf{l}_1+\mathbf{l}_2=\mathbf{L}\,, \quad \mathbf{s}_1+\mathbf{s}_2=\mathbf{S}\,, \quad \mathbf{S}+\mathbf{L}=\mathbf{J} \quad (LS\text{-coupling})\,,\\
&\mathbf{l}_1+\mathbf{s}_1=\mathbf{j}_1\,, \quad \mathbf{l}_2+\mathbf{s}_2=\mathbf{j}_2\,, \quad \mathbf{j}_1+\mathbf{j}_2=\mathbf{J} \quad (jj\text{-coupling})\,,\\
&\mathbf{l}_1+\mathbf{l}_2=\mathbf{L}\,, \quad \mathbf{L}+\mathbf{s}_1=\mathbf{K}\,, \quad \mathbf{K}+\mathbf{s}_2=\mathbf{J} \quad (LK\text{-coupling})\,,\\
&\mathbf{l}_1+\mathbf{s}_1=\mathbf{j}_1\,, \quad \mathbf{j}_1+\mathbf{l}_2=\mathbf{K}\,, \quad \mathbf{K}+\mathbf{s}_2=\mathbf{J} \quad (JK\text{-coupling})\,.
\end{aligned} \tag{2.1}$$

Here, $\mathbf{l}_1, \mathbf{l}_2$ are the orbital momenta of electrons, and $\mathbf{s}_1, \mathbf{s}_2$ are their spins. Restricting ourselves to the *LS*- and *jj*-coupling schemes, we assume the combinations $\hat{\mathbf{l}}_1\hat{\mathbf{s}}_1, \hat{\mathbf{l}}_2\hat{\mathbf{s}}_2, \hat{\mathbf{l}}_1\hat{\mathbf{l}}_2, \hat{\mathbf{s}}_1\hat{\mathbf{s}}_2$ to be the strongest in the Hamiltonian of electrons and neglect some relativistic interactions. Below we shall try to understand the validity of this approximation from the analysis of positions of the lower excited states in rare gas atoms, which are formed from the ground electronic state with the filled electron shell $n\mathrm{p}^6$ by the transition of one electron from this shell into the state $(n+1)\mathrm{s}$. Thus, the excited states of rare gas atoms under consideration are characterized by one p-hole in the outer valence shell and one excited s-electron. In this case, within the framework of *LS*- and *jj*-coupling schemes, one can find the positions of energy levels analytically and compare these positions with real ones. From this one can determine the accuracy of this assumption for different atoms numerically.

Let us consider the peculiarities of coupling of electron momenta into the total atomic momentum for the electron shell $n\mathrm{p}^5(n+1)\mathrm{s}$. An inert gas ion has the electron shell $n\mathrm{p}^5$ and the ground state $^2\mathrm{P}_{3/2}$. We denote by Δ_f the fine-structure splitting of ion levels, i.e. the distance between levels of the $^2\mathrm{P}_{3/2}$ and $^2\mathrm{P}_{1/2}$ ion states, and this will be used as a typical energy of spin – orbit interaction for excited atoms. There are 4 different energy levels for the lower atomic states. If we use the *LS*-coupling scheme, these states are $^3\mathrm{P}_2, ^3\mathrm{P}_1, ^3\mathrm{P}_0, ^1\mathrm{P}_1$. We set these states in order of the atomic excitation in accordance with the Hund rule. Within the framework of the *jj*-coupling scheme, the sequence of states is the following:

$$\mathrm{s}\left[\frac{3}{2}\right]_2, \quad \mathrm{s}\left[\frac{3}{2}\right]_1, \quad \mathrm{s}'\left[\frac{1}{2}\right]_0, \quad \mathrm{s}'\left[\frac{1}{2}\right]_1.$$

This notation is close to the usual notation of addition of momenta for the case of *jj*-coupling, which usually has the form $[j_1, j_2]_J$ and denotes that addition of momenta j_1 and j_2 yields the total momentum J. So-called Pashen notation is often used for excited atoms of rare gases for simplicity. Then the above states in order of excitation of the atom are denoted as $1\mathrm{s}_5$, $1\mathrm{s}_4$, $1\mathrm{s}_3$, and $1\mathrm{s}_2$. Below we take the energy of the state $1\mathrm{s}_5$ to be zero and denote the difference of excitation energies between this state and the others as ε_4, ε_3 and ε_2, so that, for example, ε_2 is the difference of energies for levels $1\mathrm{s}_2$ and $1\mathrm{s}_5$ (see Fig. 2 [18]).

Table 2 contains some parameters of the lower excited states for atoms of inert gases [19 – 21]. Below we briefly analyze these data. Along with the energies of these states, in Table 2 the ratio is given for the difference in the energies of the lowest states of the shells 2p and 1s in the Pashen notation (or the $[n\mathrm{p}^5(n+1)\mathrm{p}]$ and $[n\mathrm{p}^5(n+1)\mathrm{s}]$ shells in the usual notation) to the energy difference for the highest and lowest states of the shell 1s. This ratio demonstrates the degree of interaction between electron shells for a given atom.

Table 2. Energy parameters of lower excited states in atoms of inert gases.

Atom	Δ_f, cm^{-1}	ε_3/Δ_f	ε_4/Δ_f	$(\varepsilon_2-\varepsilon_3)/\Delta_f$	$(\varepsilon_{2\mathrm{p}}-\varepsilon_5)/(\varepsilon_2-\varepsilon_5)$
Ne	780.3	0.996	0.54	0.09	7.7
Ar	1432.0	0.984	0.43	0.10	4.9
Kr	5370.1	0.972	0.18	0.13	1.9
Xe	10537	0.866	0.11	0.11	1.01

	Energy levels		
jj-notation	*LS*-notation	Pashen notation	Number of states
$(n+1)\mathrm{s}'[1/2]_1^0$	$^1\mathrm{P}_1$	$1\mathrm{s}_2$	3
$(n+1)\mathrm{s}'[1/2]_0^0$	$^3\mathrm{P}_0$	$1\mathrm{s}_3$	1
$(n+1)\mathrm{s}\ [3/2]_1^0$	$^3\mathrm{P}_1$	$1\mathrm{s}_4$	3
$(n+1)\mathrm{s}\ [3/2]_2^0$	$^3\mathrm{P}_2$	$1\mathrm{s}_5$	5

Figure 2. Notation of the lower excited levels in atoms of inert gases [18].

One can extract two terms from the Hamiltonian which describe the considered electronic states of a given atom:

$$\hat{H} = -a\hat{\mathbf{l}}\hat{\mathbf{s}}_1 - b\,\hat{\mathbf{s}}_1\hat{\mathbf{s}}_2\,, \tag{2.2}$$

where $\hat{\mathbf{l}}$ is the operator of the orbital momentum of the atomic core, $\hat{\mathbf{s}}_1$ is the spin operator of the core, and $\hat{\mathbf{s}}_2$ is the spin operator of an excited valence s-electron. Here and below we use the Hartree atomic units $\hbar = m_\mathrm{e} = e^2 = 1$, if the units are not indicated specially. The first term relates to the spin – orbit interaction for the core, the second term corresponds to the exchange interaction of an excited electron with the atomic core. In the case $a \ll b$, the *LS*-coupling scheme holds true, and if $a \gg b$, the *jj*-coupling scheme is valid. The determination of the level positions for an excited atom can be done analytically, and then we express the positions of three levels with respect to the lowest one through two parameters a and b. If we find the values of these parameters from the positions of two levels, comparison between the calculated positions of the third term with its measured value allows us to check the validity of this assumption numerically. Moreover, if we take the parameter a from the splitting of ion levels, we can use two free parameters to check the assumptions.

Let us introduce the total momentum of the electron and core, $\hat{\mathbf{J}} = \hat{\mathbf{l}} + \hat{\mathbf{s}}_1 + \hat{\mathbf{s}}_2$, which is the quantum number because this operator commutes with the Hamiltonian. The total number of states of the electron shell under consideration is the product of the number of projections of the atomic core orbital momentum (3), projections of the atomic core spin (2) and projections of the excited electron spin (2), i.e. the total number of states is equal to 12. These states relate to the total momentum $J = 0, 1, 2$, and there are two different levels for $J = 1$. As is seen, the total number of projections of the total momentum, i.e. the total number of states, is equal to 12.

In order to find the positions of the 4 energy levels, it is necessary to construct the wave functions of these states from the wave functions of the orbital momenta and spins. We denote by ψ_m the wave function of the atomic core with a projection m of the orbital momentum onto a given direction. Correspondingly, the wave functions χ_+, χ_- relate to the spin

projections $1/2$ and $-1/2$ of the atomic core onto a given direction, and the wave functions η_+, η_- describe spin states of the excited electron with the spin projections $1/2$ and $-1/2$. The atomic wave function consists of products of the above wave functions, and we have 12 different combinations of such products. Our task is to find eigenfunctions of the Hamiltonian that requires the application of operators of the angular momentum and spins. We have the following relations for the orbital momentum operator [4, 32, 33]:

$$\hat{l}_z\psi_m = m\psi_m\,, \quad \hat{l}_+\psi_{-1} = \sqrt{2}\,\psi_0\,, \quad \hat{l}_+\psi_0 = \sqrt{2}\,\psi_1\,, \quad \hat{l}_+\psi_1 = 0\,,$$

$$\hat{l}_-\psi_{-1} = 0\,, \qquad \hat{l}_-\psi_0 = \sqrt{2}\,\psi_{-1}\,, \quad \hat{l}_-\psi_1 = \sqrt{2}\,\psi_0\,,$$

where $\hat{l}_+ = \hat{l}_x + \mathrm{i}\hat{l}_y$, $\hat{l}_- = \hat{l}_x - \mathrm{i}\hat{l}_y$, and we use $l = 1$. We have identical relations for the spin operators [4, 32, 33]:

$$\hat{s}_{1z}\chi_+ = \frac{1}{2}\,\chi_+\,, \qquad \hat{s}_{1z}\chi_- = -\frac{1}{2}\,\chi_-\,, \qquad \hat{s}_{1+}\chi_+ = 0\,,$$

$$\hat{s}_{1-}\chi_+ = \chi_-\,, \qquad \hat{s}_{1+}\chi_- = \chi_+\,, \qquad \hat{s}_{1-}\chi_- = 0\,,$$

and the same relations for the operator $\hat{\mathbf{s}}_2$. Here $\hat{s}_+ = \hat{s}_x + \mathrm{i}\hat{s}_y$, and $\hat{s}_- = \hat{s}_x - \mathrm{i}\hat{s}_y$.

Let us denote the wave function of an atomic state with total momentum J and projection M by Ψ_{JM}. Take the state with $J = 2$, $M = 2$, whose wave function is $\Psi_{22} = \psi_1\chi_+\eta_+$, and evaluate the energy of this state. We have

$$\hat{H}\Psi_{22} = -a\hat{l}_z\hat{s}_{1z}\Psi_{22} - b\hat{s}_{1z}\hat{s}_{2z}\Psi_{22} = \varepsilon_5\Psi_{22}\,, \tag{2.3}$$

where the energy of this state ε_5 (we denote it in Pashen notation as $1s_5$) is equal to

$$\varepsilon_5 = -\frac{a}{2} - \frac{b}{4}\,. \tag{2.4}$$

This energy corresponds to states with $J = 2$ and any momentum projection onto a given direction.

Next, we construct the wave function of the state with $J = 0$ as a result of coupling of the orbital momentum $\hat{\mathbf{l}}$ and the total spin $\hat{\mathbf{s}}_1 + \hat{\mathbf{s}}_2$, which has the form

$$\Psi_{00} = \frac{1}{\sqrt{3}}\,\psi_1\chi_-\eta_- + \frac{1}{\sqrt{3}}\,\psi_{-1}\chi_+\eta_+ - \frac{1}{\sqrt{6}}\,\psi_0\chi_+\eta_- - \frac{1}{\sqrt{6}}\,\psi_0\chi_-\eta_+\,. \tag{2.5}$$

Then we obtain equations

$$\hat{\mathbf{l}}\hat{\mathbf{s}}_1\Psi_{00} = -\Psi_{00}\,, \qquad \hat{\mathbf{s}}_1\hat{\mathbf{s}}_2\Psi_{00} = \frac{1}{4}\,\Psi_{00}\,, \qquad \hat{H}\Psi_{00} = \varepsilon_3\Psi_{00}\,.$$

The energy of this state as the eigenvalue of the Hamiltonian is given by

$$\varepsilon_3 = a - \frac{b}{4}\,. \tag{2.6}$$

In order to determine the energies of states with $J = 1$, let us consider the states with the momentum projection $M = 1$. The wave functions of these states can be constructed from $\varphi_1 = \psi_0\chi_+\eta_+$, $\varphi_2 = \psi_1\chi_-\eta_+$, and $\varphi_3 = \psi_1\chi_+\eta_-$. Extracting from these functions the wave function for the state $J = 2$, $M = 1$, which has the form

$$\Phi_1 = \Psi_{21} = \frac{1}{\sqrt{2}}\,\varphi_1 + \frac{1}{2}\,\varphi_2 + \frac{1}{2}\,\varphi_3\,, \tag{2.7}$$

we arrive at

$$\hat{\mathbf{l}}\hat{\mathbf{s}}_1\Psi_{21} = \frac{1}{2}\,\Psi_{21}\,, \qquad \hat{\mathbf{s}}_1\hat{\mathbf{s}}_2\Psi_{21} = \frac{1}{4}\,\Psi_{21}\,, \qquad \hat{H}\Psi_{21} = \varepsilon_5\Psi_{21}\,.$$

The energy ε_5 is the eigenvalue for this wave function and is given by formula (2.4). Taking two other wave functions to be normalized to unity, orthogonal to this function and orthogonal each to other, we get

$$\Phi_2 = -\frac{1}{\sqrt{2}}\,\varphi_1 + \frac{1}{2}\,\varphi_2 + \frac{1}{2}\,\varphi_3\,, \qquad \Phi_3 = \frac{1}{\sqrt{2}}\,\varphi_2 - \frac{1}{\sqrt{2}}\,\varphi_3\,. \tag{2.8}$$

Next, we have

$$\hat{\mathbf{l}}\hat{\mathbf{s}}_1\Phi_2 = -\frac{1}{2}\,\Phi_2 - \frac{1}{\sqrt{2}}\,\Phi_3\,, \qquad \hat{\mathbf{l}}\,\hat{\mathbf{s}}_1\Phi_3 = -\frac{1}{\sqrt{2}}\,\Phi_3\,,$$

$$\hat{\mathbf{s}}_1\hat{\mathbf{s}}_2\Phi_2 = \frac{1}{4}\,\Phi_2\,, \qquad \hat{\mathbf{s}}_1\hat{\mathbf{s}}_2\Phi_3 = -\frac{3}{4}\,\Phi_3\,.$$

Calculating the matrix elements of the Hamiltonian on the basis of these relations, we obtain the following secular equation for the eigenvalues of the Hamiltonian:

$$\begin{vmatrix} \dfrac{a}{2} - \dfrac{b}{4} - \varepsilon & \dfrac{a}{\sqrt{2}} \\ \dfrac{a}{\sqrt{2}} & \dfrac{3}{4}\,b - \varepsilon \end{vmatrix} = 0\,.$$

The solution of this equation gives the state energies

$$\varepsilon_{2,4} = \frac{1}{4}(a+b) \pm \frac{1}{4}\sqrt{9a^2 - 4ab + 4b^2}\,. \tag{2.9}$$

In the limiting case $b = 0$, when one can neglect the exchange interaction, we have $\varepsilon_4 = -a/2$, $\varepsilon_2 = a$ (i.e. $\varepsilon_4 = \varepsilon_5$, and $\varepsilon_2 = \varepsilon_3$). In the other limiting case $a = 0$, when one can neglect the spin–orbit interaction, we have $\varepsilon_4 = -b/4$, $\varepsilon_2 = 3b/4$, i.e. $\varepsilon_4 = \varepsilon_5 = \varepsilon_3$ and the exchange splitting is equal to b.

Let us take the position of the lowest excited level of an inert gas atom as zero ($\varepsilon_5 = 0$). Then from the obtained formulas it follows for the positions of the other energy levels:

$$\varepsilon_{2,4} = \frac{3}{4}\,a + \frac{1}{2}\,b \pm \frac{1}{4}\,\sqrt{9a^2 - 4ab + 4b^2}\,, \qquad \varepsilon_3 = \frac{3}{2}\,a\,. \tag{2.10}$$

Table 3 contains the results which follow from comparison of this formula with the positions of energy levels ε_2, ε_3, ε_4 for real inert gas atoms. In this table Δ_f is the fine-structure splitting of levels for the corresponding free ion. As is seen, this value is close to ε_3 (see also Table 2). The exchange interaction parameter b according to the above formulas is $b = \varepsilon_4 + \varepsilon_2 - \varepsilon_3$. As follows from the data of Table 3, the exchange interaction parameter slowly depends on the sort of atom. Table 3 also gives the values of $(9a^2/4 + b^2 - ab)^{1/2}$ which according to the obtained formulas equals the difference $\varepsilon_2 - \varepsilon_4$. Comparison of these values and also the ion fine-structure splitting Δ_f with $\varepsilon_3 = 3a/2$ for real atoms shows that the above Hamiltonian includes the main part of the interaction for the lower excited states of rare gas atoms. In addition, Table 3 contains the ratio b/a which characterizes the method of addition of momenta in the atom. In the limiting case $b \gg a$, this leads to the LS-scheme of coupling of

Table 3. Energy parameters of the first excited states of rare gas atoms (all the energy parameters are expressed in cm^{-1}).

Atom	Δ_f	ε_3	b	b/a	$\varepsilon_2 - \varepsilon_4$	$\sqrt{9a^2/4 + b^2 - ab}$	x	c_3^2
Ne	780	777	1488	2.9	1430	1430	−1.67	0.071
Ar	1432	1410	1453	1.5	1649	1653	−0.72	0.207
Kr	5370	5220	1600	0.46	4930	4923	0.038	0.481
Xe	10537	9129	1966	0.32	9140	8674	0.16	0.423

momenta, and in the limiting case $a \gg b$ the *jj*-scheme of momentum addition takes place. As is seen, in the argon and krypton cases we come up against an intermediate case of coupling, and the Hamiltonian (2.2) well describes the positions of energy levels for these atoms.

Note that along with the positions of the $1s_2$ and $1s_4$ energy levels, the above operations allow us to find expressions for the wave functions of these states. Indeed, representing the wave functions Ψ_2 and Ψ_4 of these states in the form

$$\Psi_2 = c_2\Phi_2 + c_3\Phi_3\,, \qquad \Psi_4 = -c_3\Phi_2 + c_2\Phi_3\,,$$

we get from the Schrödinger equations $\hat{H}\Psi_{2,4} = \varepsilon\Psi_{2,4}$ the set of equations for the coefficients of these wave functions:

$$\big(\langle\Phi_2\hat{H}\Phi_2\rangle - \varepsilon\big)c_2 + \langle\Phi_2\hat{H}\Phi_3\rangle c_3 = 0\,,$$
$$\langle\Phi_3\hat{H}\Phi_2\rangle c_2 + \big(\langle\Phi_3\hat{H}\Phi_3\rangle - \varepsilon\big)c_3 = 0\,.$$

Here we account for the wave functions Φ_i as well as coefficients c_i being real quantities. This is the secular set of equations for determination of the energy levels. Simultaneously, this allows one to find the expansion coefficients. Indeed, introducing

$$x = \frac{\langle\Phi_2\hat{H}\Phi_2\rangle - \langle\Phi_3\hat{H}\Phi_3\rangle}{\langle\Phi_3\hat{H}\Phi_2\rangle} = \frac{1}{2\sqrt{2}}\left(1 - \frac{2b}{a}\right) = \frac{1}{2\sqrt{2}}\left(1 - \frac{3b}{\Delta_f}\right) \tag{2.11}$$

and accounting for the normalization condition $c_2^2 + c_3^2 = 1$, we get

$$c_{2,3}^2 = \frac{\sqrt{1+x^2} \pm x}{2\sqrt{1+x^2}}\,. \tag{2.12}$$

Table 3 contains the values of these parameters for the excited atoms under consideration.

Now let us analyze the results obtained for this problem, which are given in Table 3. From this it follows that the assumption used is valid while relativistic interactions are not large. Even in the krypton case the ion doublet splitting and the difference of energies of levels $1s_3$ and $1s_5$ differ by 2.8%, whereas in the xenon case this difference is about 13%. Next, under the assumptions used the relative positions of levels $1s_2$ and $1s_4$ differ from the real value by 0.14% in the krypton case, while in the xenon case this difference is above 5%. We may conclude that the accuracy of the approach is higher, the smaller the relativistic corrections to the atomic energy, and the error in this model increases nonlinearly with respect to relativistic interactions. Hence, additional relativistic interactions are significant when the condition of the *jj*-coupling scheme is valid. In addition, the interaction of the 1s and 2p shells in the Pashen notation, that is stronger for xenon than for other rare gas atoms, also influences the accuracy of the model. Note that this interaction between shells, which mixes shells $np^5(n+1)s$ and $np^5(n+1)p$ as a result of the exchange interaction between electrons, influences the parameter b which is responsible for the exchange interaction in the atom. Because an $(n+1)$p-excited electron interacts weakly with internal electrons, interaction between shells does not act on the fine-structure splitting of levels in the atomic core, that is, the interaction between shells does not influence the spin–orbit interaction of the atomic core. Therefore, the deviation of the difference $\varepsilon_3 - \varepsilon_5$ from the fine-structure splitting of ion levels for xenon may be related to additional relativistic effects.

2.3 Radiation from the first excited states of rare gas atoms

The analysis of first excited states in rare gas atoms is useful because it gives analytical expressions for atomic parameters, so that their comparison with real parameters allows us to find the accuracy of the approximation. Above we used this for the determination of energy levels. Now we continue this analysis for the determination of radiative parameters of the lower excited states in rare gas atoms where correlation effects can be more essential. The electron shell for these excited states of rare gas atoms is $np^5(n+1)s$, and radiative transitions $np^5(n+1)s \to np^6$ are allowed in the dipole approximation to the interaction between these atomic states and the radiation field. But only two of the four states in this group are resonantly excited states. Below we extract these states and find the parameters of these radiative transitions. For this goal we represent the wave function of electrons for the excited atom in the form

$$\Psi_{JM} = \sum_{m,\sigma_1,\sigma_2} \begin{bmatrix} \frac{1}{2} & 1 & j \\ \sigma_1 & m-\sigma_1 & m \end{bmatrix} \begin{bmatrix} \frac{1}{2} & j & J \\ \sigma_2 & m & M \end{bmatrix} \psi_m\,\chi_{\sigma_1}\eta_{\sigma_2}\,. \tag{2.13}$$

Here, σ_1, σ_2, $m-\sigma_1$ are the projections of the spin of the atomic core, the spin of the valence electron and the orbital momentum of the atomic core onto a given direction, respectively, j is the total momentum of the atomic core, and J is the total atomic momentum. Though this expression is written within the framework of the *jj*-coupling scheme, it is valid in the general case too, because the total atomic momentum J is a quantum number. Dividing the atom into the atomic core and valence electron, we represent the wave function of the ground atomic state as a combination of products of their spin and spatial wave functions. In the general case this is not correct, but because the electron shell for the ground atomic state is filled, spins of the valence electron and atomic core have opposite directions, and the total spin is zero. This allows one to represent the total wave function for the ground atomic state as a product of the spatial and spin wave functions of electrons, that is, the atomic wave function for the ground state has the form

$$\Phi = \varphi_0\,\frac{1}{\sqrt{2}}(\chi_+\eta_- - \chi_-\eta_+)\,, \tag{2.14}$$

where $\chi_+, \chi_-, \eta_+, \eta_-$ are the spin wave functions of the atomic core and valence electron with the spin projection $\pm 1/2$ onto

a given direction; φ_0 is the spatial wave function for the ground state of an atom which consists of an atomic core and valence electron. We used above the assumption that the total spin of the atom in the ground state equals zero. The probability of radiative transition per unit time is proportional to the square of the matrix element of the atomic dipole moment operator which does not depend on electron spins. Hence it is convenient to project the wave function of the excited state (2.13) onto the spin wave function of the ground state (2.14). This gives

$$\langle \Psi_{JM}|\Phi\rangle = \frac{1}{\sqrt{2}}\begin{bmatrix} \frac{1}{2} & 1 & j \\ \frac{1}{2} & M & M+\frac{1}{2}\end{bmatrix}\begin{bmatrix} \frac{1}{2} & j & J \\ -\frac{1}{2} & M+\frac{1}{2} & M\end{bmatrix} - \frac{1}{\sqrt{2}}\begin{bmatrix} \frac{1}{2} & 1 & j \\ -\frac{1}{2} & M & M-\frac{1}{2}\end{bmatrix}\begin{bmatrix} \frac{1}{2} & j & J \\ \frac{1}{2} & M-\frac{1}{2} & M\end{bmatrix}. \quad (2.15)$$

Below we will show that this quantity goes to zero for the states $1s_3$ and $1s_5$. Let us take a quantization axis for the lowest excited state, $1s_5$ or $[3/2]_2$ state, such that the momentum projection onto this axis is $M = 2$. Then all the Clebsch–Gordan coefficients in formula (2.15) except the last one are equal to zero because their momentum projections exceed their values, and the matrix element becomes zero. This results from the symmetry of the wave function. Indeed, the wave function (2.13) for $M = 2$ takes the form $\Psi_{22} = \psi_{+1}\chi_+\eta_+$, i.e. the total spin wave function of the valence electron and atomic core corresponds to their total spin $S = 1$, while the spin of the ground atomic state is zero. For the $1s_3$ or $[1/2]_0$ state formula (2.15) assumes the form

$$\langle \Psi_{00}|\Phi\rangle = \frac{1}{\sqrt{2}}\left(\begin{bmatrix} \frac{1}{2} & 1 & \frac{1}{2} \\ \frac{1}{2} & 0 & \frac{1}{2}\end{bmatrix}\begin{bmatrix} \frac{1}{2} & \frac{1}{2} & 0 \\ -\frac{1}{2} & \frac{1}{2} & 0\end{bmatrix} - \begin{bmatrix} \frac{1}{2} & 1 & \frac{1}{2} \\ -\frac{1}{2} & 0 & -\frac{1}{2}\end{bmatrix}\begin{bmatrix} \frac{1}{2} & \frac{1}{2} & 0 \\ \frac{1}{2} & -\frac{1}{2} & 0\end{bmatrix}\right).$$

As is seen, the second term in this expression equals the first and eliminates it. Thus, the states $1s_5$ and $1s_3$ are metastable states and dipole radiative transitions from these states to the ground state are forbidden.

The radiative lifetime of an excited state is inversely proportional to the square of the matrix element of the dipole moment operator of the atom:

$$\frac{1}{\tau_f} \sim \left|\langle 0|\mathbf{D}|f\rangle\right|^2, \quad (2.16)$$

where indices 0, f refer to the ground and the considered excited states. For the wave function of the ground atomic state we use formula (2.14), and the wave function of the lowest excited state with the projection of the total momentum 2 onto a given direction has the form

$$\Psi_5 = \psi_1\chi_+\eta_+,$$

where ψ_1 is the spatial wave function of the core and test electron with a projection of one of the angular momentum onto a given direction. As is seen, the matrix element $\langle \Psi_0|\mathbf{D}|\Psi_5\rangle = 0$ because of the orthogonality of spin wave functions in accordance with formula (2.15).

Using formula (2.5) for the wave function of the state $1s_3$ one finds

$$\Psi_2 = \frac{1}{\sqrt{3}}\psi_1\chi_-\eta_- + \frac{1}{\sqrt{3}}\psi_{-1}\chi_+\eta_+ - \frac{1}{\sqrt{6}}\psi_0\chi_+\eta_- - \frac{1}{\sqrt{6}}\psi_0\chi_-\eta_+,$$

and it is seen that the matrix element $\langle \Psi_0|\mathbf{D}|\Psi_3\rangle = 0$ because of the orthogonality of spin wave functions of the core and a test electron. Thus, the states $1s_5$, $1s_3$ are metastable and are characterized by an infinite radiative lifetime with respect to dipole radiation.

For determination of the radiative lifetimes of the states $1s_4$ and $1s_2$ we use the wave functions of these states according to formulas (2.7), (2.8). First we write down the dipole moment operator of the atom in the form

$$\mathbf{D} = \sum_m (\mathbf{i}\sin\theta_m\cos\phi_m + \mathbf{j}\sin\theta_m\sin\phi_m + \mathbf{k}\cos\theta_m) r_m,$$

where $\mathbf{i}, \mathbf{j}, \mathbf{k}$ are the unit vectors directed along the axes x, y, z, respectively, and the subscript m corresponds to mth electron whose spherical coordinates are r_m, θ_m, Φ_m. Because the basis wave functions have the form

$$\varphi_1 = \psi_0\chi_+\eta_+, \qquad \varphi_2 = \psi_1\chi_-\eta_+, \qquad \varphi_3 = \psi_1\chi_+\eta_-,$$

we obtain for matrix elements:

$$\langle \Psi_0|\mathbf{D}|\varphi_1\rangle = 0, \qquad \langle \Psi_0|\mathbf{D}|\varphi_2\rangle = C(-\mathbf{i} + \mathrm{i}\mathbf{j}),$$
$$\langle \Psi_0|\mathbf{D}|\varphi_3\rangle = C(\mathbf{i} - \mathrm{i}\mathbf{j}).$$

Thus, the rate of the radiative transition is determined by the amplitude of the wave function Φ_3 entering the wave function of the excited state. From this we get the ratio of the radiative lifetimes of the resonantly excited states:

$$\frac{\tau(1s_2)}{\tau(1s_4)} = \frac{c_2^2}{c_3^2} = \frac{\sqrt{1+x^2}-|x|}{\sqrt{1+x^2}+|x|}, \quad (2.17)$$

where the parameter x is given by formula (2.11). Table 4 contains the measured radiative lifetimes $\tau(1s_2)$ and $\tau(1s_4)$ of resonantly excited states in rare gas atoms [21, 34], the ratio of these quantities, and an evaluated ratio of the lifetimes if the exchange and spin–orbit interactions are taken into account. Comparison between these values shows their accuracy within the framework of the assumptions made. Analysis of the data from Table 4 shows that the measured and calculated radiative lifetimes of the lower resonantly excited states of rare gas atoms differ more strongly than the energies of excited levels. Indeed, the correlation effects are of importance for radiative atomic parameters that creates an additional source of error for the atomic model under

Table 4. Radiative lifetimes for lower resonantly excited states of rare gas atoms.

Atom	$\tau(1s_2)$, ns	$\tau(1s_4)$, ns	$\tau(1s_2)/\tau(1s_4)$	c_2^2/c_3^2
Ne	1.6	25	16	13
Ar	2.0	10	5	3.8
Kr	3.2	3.5	1.1	1.1
Xe	3.5	3.6	1.0	1.4

consideration — both for light and heavy atoms. As follows from the data of Table 4, this error is estimated as $\sim 10-20\%$ with respect to the radiative parameters.

Thus, the analysis of energy levels for the lower excited electron shell in rare gas atoms and their radiative parameters demonstrates the general positions of the atomic shell model. This model, along with the interaction of electrons with the Coulomb center and Coulomb interaction between electrons, also includes the exchange interaction between electrons due to the Pauli exclusion principle and spin – orbit interaction for valence electrons. In the limiting cases, depending on the ratio between two last interactions, the *LS*- or *jj*-coupling schemes of momenta are realized. The atomic shell model neglects the correlation between electrons, which occurs due to the violation of the one-electron approach. The correlation between electrons is not significant for the atomic energy parameters, but it is more essential for radiative atomic parameters, and becomes of importance for two-electron and many-electron transitions in atomic particles.

2.4 Correlations between atomic electrons

Thus, in the atomic shell model which uses a one-electron approach, we encounter two types of errors in atomic parameters. The first type relates to some relativistic interactions, additional to the spin – orbit interaction of individual electrons, and the scale of such errors was discussed above. The second type of error is caused by correlation effects in the atomic shell model. These effects follow from the one-electron approach which accounts for the electron correlation due to the Pauli exclusion principle only.

The character of correlation effects has mostly been studied for a two-electron atom [5]. For their analysis, alongside the coordinates of the two electrons r_1, r_2 , the relative distance between electrons $r_{12} = |\mathbf{r}_1 - \mathbf{r}_2|$ is introduced into the consideration. In combination with the variational principle for the ground and lower excited states of a two-electron atom, the introduction of r_{12} into the trial wave function of electrons allows one to improve the accuracy of the variational method for the atomic energy by taking into account the correlation effects [26, 27, 35, 36]. In particular, usage of the trial wave function for the ground state of the helium atom, which includes the distance between electrons r_{12} and uses 1024 varying parameters [37], allows one to account for the correlation effects there with a high accuracy. The other method of such a type introduces the relative distance between electrons in the Schrödinger equation [38], and this allows one to account for the correlation effects in a more compact way. The use of 52 varying parameters for the ground state of the helium atom within the framework of this approach [39] provides the same accuracy for correlation effects as the above-mentioned calculation with 1024 varying parameters.

The above analysis of radiative parameters of rare gas atoms testifies to the error arising from neglecting the correlation effects. But for two-electron transitions the correlation effects are principle. The analysis of autoionizing states with two excited electrons shows the molecule-like character of electron correlations [40 – 45]. This provided the basis for the configuration interaction method [46 – 49] which also suits stable two-electron atoms and allows one to calculate various parameters, such as the atomic energies, oscillator strengths, and quadrupole momenta, accounting for the electron correlations. Other methods exist for this goal [49], but we will not consider them, because our task is only to estimate corrections to the energies and interaction potentials of atomic particles due to the correlations between electrons. The quantitative characteristic of corrections due to electron correlations is the overlap integral for the Hartree – Fock wave function Ψ_{HF} which corresponds to the one-electron approach and the wave function Ψ_{CI} of the configuration interaction method that accounts for electron correlations. These overlap integrals are given in Table 5 for some states of alkali-earth atoms with two excited electrons [50, 51].

Table 5. Square of the overlap integral $|\langle\Psi_{\mathrm{CI}}|\Psi_{\mathrm{HF}}\rangle|^2$ for the Hartree – Fock wave function Ψ_{HF} and the wave function Ψ_{CI} of the configuration interaction method for alkali-earth atoms [50, 51].

Atom	Be	Be	Be	Be	Be	Be	Be
Shell	$2s^2$	2s2p	2s2p	2s3s	2s3s	$2p^2$	$2p^2$
Term	^{1}S	^{3}P	^{1}P	^{3}S	^{1}S	^{1}D	^{3}P
$\lvert\langle\Psi_{\mathrm{CI}}\rvert\Psi_{\mathrm{HF}}\rangle\rvert^2$	0.89	0.99	0.92	0.97	0.95	0.72	0.99
Atom	Mg	Mg	Mg	Mg	Mg	Mg	Mg
Shell	$3s^2$	3s3p	3s3p	3s4s	3s4s	3s3d	$3p^2$
Term	^{1}S	^{3}P	^{1}P	^{3}S	^{1}S	^{1}D	^{3}P
$\lvert\langle\Psi_{\mathrm{CI}}\rvert\Psi_{\mathrm{HF}}\rangle\rvert^2$	0.92	0.98	0.93	0.96	0.92	0.65	0.98
Atom	Ca	Ca	Ca	Ca	Ca	Ca	Ca
Shell	$4s^2$	4s4p	4s3d	4s4p	4s5s	4s5s	$4p^2$
Term	^{1}S	^{3}P	^{1}D	^{1}P	^{3}S	^{1}S	^{3}P
$\lvert\langle\Psi_{\mathrm{CI}}\rvert\Psi_{\mathrm{HF}}\rangle\rvert^2$	0.92	0.96	0.85	0.85	0.96	0.92	0.88
Atom	Sr	Sr	Sr	Sr	Sr	Sr	Sr
Shell	$5s^2$	5s5p	5s4d	5s5p	5s6s	$5p^2$	5s6s
Term	^{1}S	^{3}P	^{1}D	^{1}P	^{3}S	^{3}P	^{1}S
$\lvert\langle\Psi_{\mathrm{CI}}\rvert\Psi_{\mathrm{HF}}\rangle\rvert^2$	0.92	0.93	0.83	0.68	0.72	0.57	0.59
Atom	Ba	Ba	Ba	Ba	Ba	Ba	Ba
Shell	$6s^2$	6s5d	6s6p	6s6p	$5d^2$	$5d^2$	6s7s
Term	^{1}S	^{1}D	^{3}P	^{1}P	^{3}P	^{1}S	^{3}S
$\lvert\langle\Psi_{\mathrm{CI}}\rvert\Psi_{\mathrm{HF}}\rangle\rvert^2$	0.92	0.88	0.89	0.53	0.83	0.76	0.92

The development of the atomic shell model was simultaneous with the creation of quantum mechanics [52 – 54]. This model includes the basic features of the behavior of bound electrons which are located in the field of the nuclear Coulomb center. The atomic shell model allowed one to check the postulates of quantum mechanics. As a model, the atomic shell model leads to errors of two types for atomic parameters, those due to correlations of electrons and those owing to relativistic interactions, additional to the spin – orbit interactions for individual electrons. As follows from the above analysis, these errors are not essential if we determine the positions of atomic energy levels in light atoms. In the case of energy parameters of heavy atoms and radiative atomic parameters these errors may be significant.

3. Wave function of valence electrons

3.1 Fractional parentage scheme of the atom

The atomic shell model corresponds to a one-electron description of the atom. Then the wave function of atomic

electrons is a combination of products of one-electron wave functions. This combination takes into account the symmetry of the electron wave function with respect to permutation of electrons. In reality, the radial symmetry of atomic fields and the character of addition of momenta of individual electrons to the total atomic momenta simplifies the construction of the atomic wave function. Our task is now to construct the atomic wave function by extraction of one valence electron from the total wave function of electrons, which is made on the basis of the fractional parentage scheme of the atom [1, 3, 55]. The connection between the total wave function of electrons and the wave function of a test valence electron is more complicated if the relativistic interactions are small and the atom has a higher symmetry. This connection within the framework of the *LS*-coupling scheme takes the form [1, 3, 55]

$$\Psi_{LSM_LM_S}(1,2,\ldots,n) = \frac{1}{\sqrt{n}}\,\hat{P}\sum_{lmsm_s\mu\sigma} G_{ls}^{LS}(l_e,n)\,, \begin{bmatrix} l_e & l & L \\ \mu & m & M_L \end{bmatrix}\begin{bmatrix} \frac{1}{2} & s & S \\ \sigma & m_s & M_S \end{bmatrix}\psi_{l_e\frac{1}{2}\mu\sigma}(1)\Psi_{lsmm_s}(2,\ldots,n)\,. \tag{3.1}$$

Here, n is the number of valence electrons, the operator $\hat{P}$ transposes positions and spins of a test electron, which is described by the argument 1, and other valence electrons, L, S, M_L, M_S are the quantum numbers of the atom, l, s, m, m_s are the quantum numbers of the atomic core, l_e, $\frac{1}{2}$, μ, σ are the quantum numbers of an extracted valence electron, and $G_{ls}^{LS}(l_e,n)$ is the fractional parentage coefficient or the Racah coefficient [1, 3] which is responsible for the connection of an extracting electron with the atomic core in the formation of the atom. It is of importance that the removal of one valence electron from the atom leaves a finite number of states for the atomic core. Table 6 lists the magnitudes of fractional parentage coefficients for s- and p-electron shells [1, 3, 21, 55]. In the cases of d- and f-electrons, several different states of the atom can be characterized by the same values of L and S. In order to distinguish them, one more quantum number v, the state seniority, is introduced [5, 56]. Below we will be guided by s- and p-valence electrons and exclude the seniority parameter from consideration.

Table 6. Fractional parentage coefficients for valence s- and p-electron shells. The electron shells of the atom and atomic core are indicated along with their electronic terms.

Electron shell		G_{ls}^{LS}	Electron shell		G_{ls}^{LS}
Atom	Atomic core		Atom	Atomic core	
$s(^2S)$	(^1S)	1	$p^3(^2P)$	$p^2(^1S)$	$\sqrt{2}/3$
$s^2(^1S)$	$s(^2S)$	1	$p^4(^3P)$	$p^3(^4S)$	$-1/\sqrt{3}$
$p(^2P)$	(^1S)	1		$p^3(^2D)$	$\sqrt{5/12}$
$p^2(^3P)$	$p(^2P)$	1		$p^3(^2P)$	$-1/2$
$p^2(^1D)$	$p(^2P)$	1	$p^4(^1D)$	$p^3(^4S)$	0
$p^2(^1S)$	$p(^2P)$	1		$p^3(^2D)$	$\sqrt{3/4}$
$p^3(^4S)$	$p^2(^3P)$	1		$p^3(^2P)$	$-1/2$
	$p^2(^1D)$	0	$p^4(^1S)$	$p^3(^4S)$	0
	$p^2(^1S)$	0		$p^3(^2D)$	0
$p^3(^2D)$	$p^2(^3P)$	$1/\sqrt{2}$		$p^3(^2P)$	1
	$p^2(^1D)$	$-1/\sqrt{2}$	$p^5(^2P)$	$p^4(^3P)$	$\sqrt{3/5}$
	$p^2(^1S)$	0		$p^4(^1D)$	$1/\sqrt{3}$
$p^3(^2P)$	$p^2(^3P)$	$-1/\sqrt{2}$		$p^4(^1S)$	$1/\sqrt{15}$
	$p^2(^1D)$	$-\sqrt{5/18}$	$p^6(^1S)$	$p^5(^2P)$	1

The fractional parentage coefficients satisfy the condition which follows from the normalization of the wave function:

$$\sum_{lsv}\left[G_{ls}^{LS}(l_e,n,v)\right]^2 = 1\,. \tag{3.2}$$

The number of electrons in a filled electron shell is equal to $4l_e+2$. From the symmetry between electrons and holes, the analogy follows between the case of removal of one vacancy from a shell containing $n+1$ vacancies and $4l_e+3-n$ electrons, and the case of removal of one electron from the shell containing n electrons. This correspondence is expressed by the formula

$$G_{ls}^{LS}(l_e,n) = (-1)^{L+l+S+s-l_e-1/2} \times\left[\frac{n(2s+1)(2l+1)}{(4l_e+3-n)(2S+1)(2L+1)}\right]^{1/2} G_{ls}^{LS}(l_e,4l_e+3-n)\,. \tag{3.3}$$

The mathematical formalism based on the Clebsch–Gordan coefficients and the fractional parentage coefficients occupies a central place in the theory of atoms. This formalism allows one to take into account the symmetry of atomic particles when analyzing their properties.

In the *jj*-coupling case, the fractional parentage scheme is simpler. Indeed, in the case of the *LS*-coupling scheme, an atomic state is characterized by the quantum numbers L, M_L, S, M_S in neglecting relativistic interactions, and the fractional parentage scheme includes 11 quantum numbers: L, M_L, S, M_S for the atom, l, m, s, m_s for an ion, and l_e, m, σ for a test electron. In the case of the *jj*-coupling scheme, these quantum numbers are the total momenta of the atom, ion, electron and their projections onto the quantization axis. Hence, in this case instead of formula (3.1) we arrive at

$$\Psi_{JM_J}(1,2,\ldots,n) = \frac{1}{\sqrt{n}}\,\hat{P}\sum_{J'M_{J'}m_j}\begin{bmatrix} j & J' & J \\ m_j & M_{J'} & M_J \end{bmatrix} \times\psi_{jm_j}(1)\Psi_{J'M_{J'}}(2,\ldots,n) \tag{3.4}$$

that means the ion and electron momenta are composed to the total atomic momentum within the framework of a given electron shell of the atom. Here, jm_j, $J'M_{J'}$, JM_J are the quantum numbers of the electron, the atomic core, and the atom, which include the total atomic momentum and its projection onto the selected direction. Thus, a decrease in the atomic symmetry lowers the complexity of the atomic fractional parentage scheme.

3.2 Asymptotic behavior of atomic wave functions

The atomic fractional parentage scheme allows one to extract one valence electron from an electron shell consisting of several identical electrons. This is of importance for one-electron atomic parameters, including the ion–atom exchange interaction at large separations, which is determined by the transition of one valence electron from one core to another. This interaction is determined by the positions of a valence electron far from the core, and we shall find below the asymptotic expression for the wave function of a valence electron at large distances from the core. Within the framework of the one-electron approxima-

tion, we represent the wave function of a given electron with quantum numbers $lm\frac{1}{2}\sigma$ in the following form

$$\psi_{lm\frac{1}{2}\sigma} = R_l(r)\,Y_{lm}(\theta,\varphi)\chi_\sigma\,, \tag{3.5}$$

where $R_l(r)$ is the radial wave function, $Y_{lm}(\theta,\varphi)$ is the electron angular wave function, χ_σ is the electron spin function, and r,θ,φ are the spherical coordinates of this electron. In the course of removal of an electron from the atom, only the radial wave function varies. Hence, below we concentrate our attention on the radial electron wave function and find its asymptotic expression. Because at large distances from the atom an exchange interaction of electrons in the atom is not essential, we neglect this effect. Next, the self-consistent field potential far from the atom coincides with the Coulomb field of the atomic core. Thus, the Schrödinger equation for the radial function of a test valence electron located far from the core has the form

$$\frac{1}{r}\frac{\mathrm{d}^2}{\mathrm{d}r^2}(rR_l) + \left[2\varepsilon - \frac{2Z}{r} + \frac{l(l+1)}{r^2}\right]R_l(r) = 0\,, \tag{3.6}$$

where Z is the core charge. Introducing the electron energy by the relation $\varepsilon = -I = -\gamma^2/2$, where I is the atomic ionization potential, we obtain the asymptotic solution of this equation at large r:

$$R_l(r) = Ar^{Z/\gamma-1}\exp(-r\gamma)\,, \qquad r\gamma \gg 1\,, \qquad r\gamma^2 \gg Z\,. \tag{3.7}$$

We consider below the asymptotic behavior of valence electrons in atoms ($Z = 1$) and negative ions ($Z = 0$). The asymptotic coefficient A is determined by the electron behavior in an internal atomic region where the electron considered is located and formula (3.7) is violated. This coefficient can be obtained by comparison of the asymptotic wave function (3.7) with that at middle distances from the nucleus. Indeed, numerical methods of solution of the Schrödinger equation enable us to determine the electron wave function in a region where electrons are mostly located. Such a solution gives rise to an error at large distances from the nucleus, because these electron positions give a small contribution to the atomic energy. An increase in the accuracy of the electron wave function makes it correct over a wider range of electron distances from the center. Then there is a range of distances of a test valence electron from the center where, on the one hand, the asymptotic expression (3.7) is valid and, on the other hand, a numerical wave function is correct. Comparing the wave functions in this region, one can find the parameter A. Table 7 contains recommended asymptotic parameters for the wave function of valence electrons in atoms [21], which were obtained on the basis of numerical calculations [57, 58] for the wave functions. These parameters are contained in formula (3.7) for the asymptotic expression of the radial wave function of a valence electron.

Note that if the Coulomb interaction of an electron with the atomic core takes place in the basic region of electron location, i.e. normalization of the wave function is determined by this range of distances from the core, we have the following expression for the asymptotic coefficient of a valence s-electron [14, 21, 59]:

$$A = \frac{\gamma^{3/2}(2\gamma)^{1/\gamma}}{\Gamma(1/\gamma)}\,. \tag{3.8}$$

Table 7. Asymptotic parameters of valence electrons.

Atom (state)	Shell	γ	A	Atom (state)	Shell	γ	A
He (^{1}S)	$1s^2$	1.344	2.9	Ge (^{3}P)	$4p^2$	0.762	1.3
Li (^{2}S)	2s	0.630	0.82	As (^{4}S)	$4p^3$	0.850	1.6
Be (^{1}S)	$2s^2$	0.828	1.6	Se (^{3}P)	$4p^4$	0.847	1.5
B (^{2}P)	2p	0.781	0.88	Br (^{2}P)	$4p^5$	0.932	1.8
C (^{3}P)	$2p^2$	0.910	1.3	Kr (^{1}S)	$4p^6$	1.014	2.1
N (^{4}S)	$2p^3$	1.034	1.5	Rb (^{2}S)	5s	0.554	0.48
O (^{3}P)	$2p^4$	1.000	1.3	Sr (^{1}S)	$5s^2$	0.647	0.86
F (^{2}P)	$2p^5$	1.132	1.6	Ag (^{2}S)	5s	0.746	1.2
Ne (^{1}S)	$2p^6$	1.259	1.8	Cd (^{1}S)	$5s^2$	0.813	1.6
Na (^{2}S)	3s	0.615	0.74	In (^{2}P)	5p	0.652	0.58
Mg (^{1}S)	$3s^2$	0.750	1.3	Sn (^{3}P)	$5p^2$	0.735	1.0
Al (^{2}P)	3p	0.663	0.61	Sb (^{4}S)	$5p^3$	0.797	1.7
Si (^{3}P)	$3p^2$	0.774	1.1	Te (^{3}P)	$5p^4$	0.814	1.6
P (^{4}S)	$3p^3$	0.878	1.6	I (^{2}P)	$5p^5$	0.876	1.9
S (^{3}P)	$3p^4$	0.873	1.1	Xe (^{1}S)	$5p^6$	0.944	2.2
Cl (^{2}P)	$3p^5$	0.976	1.8	Cs (^{2}S)	6s	0.535	0.41
Ar (^{1}S)	$3p^6$	1.076	2.0	Ba (^{1}S)	$6s^2$	0.619	0.78
K (^{2}S)	4s	0.565	0.52	Au (^{2}S)	6s	0.823	1.6
Ca (^{1}S)	$4s^2$	0.670	0.95	Hg(^{1}S)	$6s^2$	0.876	1.9
Cu (^{2}S)	4s	0.754	1.3	Tl (^{2}P)	6p	0.670	0.55
Zn (^{1}S)	$4s^2$	0.831	1.7	Pb (^{3}P)	$6p^2$	0.738	1.1
Ga (^{2}P)	4p	0.664	0.60	Bi (^{4}S)	$6p^3$	0.732	1.4

This expression can also be used for the p-electron as an upper limit for the asymptotic coefficient.

3.3 Determination of the asymptotic coefficient

We now demonstrate the method of determining the asymptotic coefficient A using the example of the helium atom in the ground state. This analysis permits us to estimate the reliability of this information. As a basis we use the one-electron wave functions which depend only on electron distances from the nuclei and follow from the variational principle. The simplest electron wave function has the hydrogen-like form

$$\Psi(r_1,r_2) = C\exp\bigl[-Z_{\mathrm{eff}}(r_1+r_2)\bigr]\,, \qquad C = \frac{Z_{\mathrm{eff}}^6}{\pi^2}\,,$$

where r_1, r_2 are the distances of the electrons from the nucleus, and $Z_{\mathrm{eff}} = 27/16$ follows from the variational principle for the helium atom in the ground state. Then the electron density $\rho(r)$ which is normalized by the relation

$$\int_0^\infty \rho(r)r^2\,\mathrm{d}r = 2\,,$$

at a large distance r from the center is written as

$$\rho(r) = 2\int_0^\infty \bigl|\Psi(r_1,r)\bigr|^2 r_1^2\,\mathrm{d}r_1 = 8Z_{\mathrm{eff}}^3\exp(-2Z_{\mathrm{eff}}r)$$
$$= 38.4\exp(-3.375r)\,.$$

We compare this quantity with the asymptotic density which according to formula (3.7) has the form

$$\rho(r) = 2A^2r^{-0.511}\exp(-2.687r)\,.$$

The comparison gives for the asymptotic coefficient:

$$A^2(r) = 19.2r^{0.511}\exp(-0.688r)\,. \tag{3.9}$$

Note that this wave function, which follows from the variational principle, leads to the ionization potential

$I = 23.06$ eV instead of the accurate value 24.56 eV. If we use the trial wave function in the form

$$\Psi(r_1, r_2) = C\left[\exp(-\alpha r_1 - \beta r_2) - \exp(-\beta r_1 - \alpha r_2)\right],$$

then we obtain from the variational principle: $\alpha = 1.189$, $\beta = 2.183$ [23, 31] and the ionization potential is $I = 23.83$ eV that is closer to the accurate value. This gives for the electron density far from the atomic center:

$$\begin{aligned}\rho(r) &= 4\left[\frac{1}{\alpha^3\beta^3} + \frac{64}{(\alpha+\beta)^6}\right]^{-1} \\ &\times \left[\frac{\exp(-2\alpha r)}{\beta^3} + \frac{16\exp\left[-(\alpha+\beta)r\right]}{(\alpha+\beta)^3} + \frac{\exp(-2\beta r)}{\alpha^3}\right] \\ &= 3.817\exp(-2.378r) + 16.57\exp(-3.372r) \\ &+ 23.62\exp(-4.366r),\end{aligned}$$

and the asymptotic coefficient squared is equal to

$$A^2(r) = r^{0.511}\left[1.908\exp(0.309r) + 8.286\exp(-0.685r) + 11.81\exp(-1.679r)\right]. \quad (3.10)$$

The variation of the asymptotic coefficient over the range under consideration gives an estimate of its accuracy. One more method to evaluate the accuracy relates to the use of the next terms in the expansion of the wave function (3.7) in a small parameter $1/r$. In particular, in the helium case we now obtain for the asymptotic coefficient:

$$A_1^2 = \frac{A_0^2}{1 + 0.095/r}, \quad (3.11)$$

where the subscript indicates an approach to the asymptotic wave function, and the quantity A_0 was calculated above.

From these results one can find a range of distances where the function $A(r)$ weakly varies with r (see Fig. 3). This takes place near the minimum of $A(r)$, which occurs at $r = 1.65$ for $A_0(r)$ and $r = 1.55$ for $A_1(r)$. Function (3.9) has a maximum at $r = 0.75$. From this analysis it follows that the simple wave function leads to a significant error. Indeed, taking the region $r = 0.4-2.6$, we find that the asymptotic coefficient according to formula (3.10) is $A = 2.98 \pm 0.05$ in this range, and according to formula (3.11) it is $A = 2.87 \pm 0.07$, so that on the basis of these data we obtain

$$A = 2.9 \pm 0.1. \quad (3.12)$$

Formula (3.9) gives $A = 2.8 \pm 0.3$ in this range, i.e. the use of a simple wave function increases the error several times. This example shows that the identical wave functions of the same valence electrons lead to a significant error.

It is clear that an error in the Hartree–Fock wave functions is transferred to the asymptotic coefficient A. Next, the use of the simplified versions of the Hartree–Fock wave functions increases the error in the asymptotic coefficient, which is found on the basis of such wave functions as was demonstrated for the helium atom. In particular, the standard exponential approximation for one-electron wave functions [57, 58, 60] is accompanied by a significant error in the asymptotic coefficient. Moreover, for such wave functions the above method of determination of the asymptotic coefficient can lead to a monotonic dependence $A(r)$ that hampers the extraction of a range of distances r suitable for determining the asymptotic coefficient and its error by comparison of the asymptotic and approximated wave functions. This is true for the above-discussed helium case.

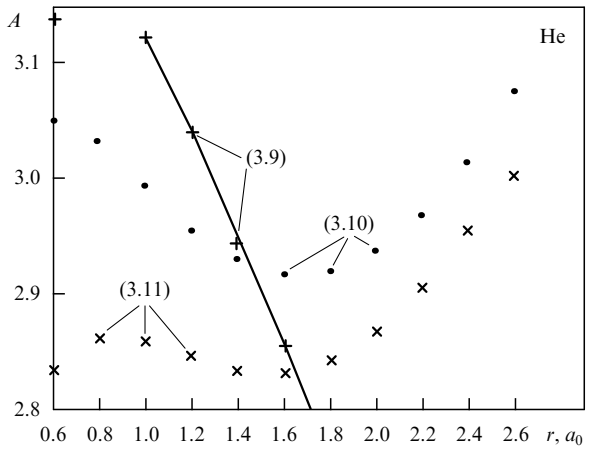

Figure 3. Determination of the asymptotic coefficient A of the electron wave function for the helium atom on the basis of formulas (3.9)–(3.11).

3.4 Asymptotic wave function of electrons in a negative ion

Negative ions are the bound states of electrons with neutral atomic particles [61, 62]. The binding energy of a valence electron is called the electron affinity of an atom or molecule and is denoted EA. The asymptotic expression for the wave function of a valence electron in a negative ion according to Eqn (3.7) is

$$R(r) = \frac{A}{r}\exp(-r\gamma), \quad (3.13)$$

where $\gamma = \sqrt{2\mathrm{EA}}$. Note that the atoms with filled electron shells, as atoms of alkali-earth metals and atoms of rare gases, do not usually form negative ions. Most elements have only one state of the negative ion, and stable negative ions of elements of group IV of the periodic table can be found in three different electronic states. Figure 4 contains information about the electron affinity of the atoms. The basic data of this figure are taken from Ref. [63], and the data of Refs [64–69] are also included in Fig. 4. The accuracy of the data is such that the error is one or several units in the last significant figure. The word 'absent' is used in the cases where a stable atomic negative ion does not exist. Notice that the most accurate contemporary method to measure the EA is based on determination of the threshold of electron photodetachment from negative ions by laser radiation. Schematically, this method has two versions. In the first case, a beam of negative ions is irradiated by a tuned laser, and the threshold photon energy for this process is found. In the second case, the laser frequency is fixed and the distribution of released electrons over kinetic energy is measured, so that the maximum kinetic energy for a given direction of motion is detected. These methods of determining the threshold of the photodetachment process are joined with taking into account additional factors which improve the accuracy of the results. In particular, the threshold form of the photodetachment cross section is used and the wavelength for the photodetachment threshold is compared with the known wavelengths of resonant radiative transitions in atoms. Such a calibration

Periodic table of elements — negative ions

Period	Group I	Group II	Group III	Group IV	Group V	Group VI	Group VII	Group VIII		
1	$1s^2\ {}^1S_0$ $_1$**H** 0.75420 Hydrogen	$2s\ {}^2S_{1/2}$ abs. $_2$**He** Helium								
2	$2s^2\ {}^1S_0$ $_3$**Li** 0.6180 Lithium	$2p\ {}^2P_{1/2}$ $_4$**Be** abs. Beryllium	$2p^2\ {}^3P_0$ 0.27972 $_5$**B** Boron	$2p^3$ ${}^4S_{3/2}$ 1.2621 $_6$**C** ${}^2D_{3/2}$ 0.033 Carbon	$2p^4\ {}^3P_0$ abs. $_7$**N** Nitrogen	$2p^5\ {}^2P_{3/2}$ 1.4611103 $_8$**O** Oxygen	$2p^6\ {}^1S_0$ 3.401190 $_9$**F** Fluorine	$2p^6 3s\ {}^2S_{1/2}$ abs. $_{10}$**Ne** Neon		
3	$3s^2\ {}^1S_0$ $_{11}$**Na** 0.54793 Sodium	$3p\ {}^2P_{1/2}$ $_{12}$**Mg** abs. Magnesium	$3p^2$ ${}^3P_0$ 0.4328 $_{13}$**Al** ${}^1D_2$ 0.11 Aluminium	$3p^3$ ${}^4S_{3/2}$ 1.385 ${}^2D_{3/2}$ 0.5272 $_{14}$**Si** ${}^2D_{5/2}$ 0.5255 ${}^2P_{1/2}$ 0.029 Silicon	$3p^4\ {}^3P_0$ 0.7465 $_{15}$**P** Phosphorus	$3p^5\ {}^2P_{3/2}$ 2.077104 $_{16}$**S** Sulfur	$3p^6\ {}^1S_0$ 3.61269 $_{17}$**Cl** Chlorine	$3p^6 4s\ {}^2S_{1/2}$ abs. $_{18}$**Ar** Argon		
4	$4s^2\ {}^1S_0$ $_{19}$**K** 0.5015 Potassium	$4p\ {}^2P_{1/2}$ $_{20}$**Ca** 0.0245 Calcium	$3d4s^24p$ $_{21}$**Sc** ${}^3F_2$ 0.19 Scandium ${}^3D_1$ 0.04	$3d^34s^2\ {}^4F_{3/2}$ $_{22}$**Ti** 0.08 Titanium	$3d^44s^2\ {}^5D_0$ $_{23}$**V** 0.52 Vanadium	$3d^54s^2\ {}^6S_{5/2}$ $_{24}$**Cr** 0.66 Chromium	$3d^64s^2\ {}^5D_4$ $_{25}$**Mn** abs. Manganese	$3d^74s^2\ {}^4F_{9/2}$ $_{26}$**Fe** 0.151 Iron	$3d^84s^2\ {}^3F_4$ $_{27}$**Co** 0.662 Cobalt	$3d^94s^2\ {}^2D_{5/2}$ $_{28}$**Ni** 1.16 Nickel
	$3d^{10}4s^2\ {}^1S_0$ 1.235 $_{29}$**Cu** Copper	$4p\ {}^2P_{1/2}$ abs. $_{30}$**Zn** Zinc	$4p^2\ {}^3P_0$ 0.43 $_{31}$**Ga** Gallium	${}^4S_{3/2}$ 1.2327 $4p^3$ ${}^2D_{3/2}$ 0.4014 $_{32}$**Ge** ${}^2D_{5/2}$ 0.3773 Germanium	$4p^4\ {}^3P_0$ 0.81 $_{33}$**As** Arsenic	$4p^5\ {}^2P_{3/2}$ 2.02067 $_{34}$**Se** Selenium	$4p^6\ {}^1S_0$ 3.363590 $_{35}$**Br** Bromine	$4p^6 5s\ {}^2S_{1/2}$ abs. $_{36}$**Kr** Krypton		
5	$5s^2\ {}^1S_0$ $_{37}$**Rb** 0.48592 Rubidium	$5p\ {}^2P_{1/2}$ $_{38}$**Sr** 0.048 Strontium	$4d5s^25p$ $_{39}$**Y** ${}^3F_2$ 0.31 Yttrium ${}^3D_1$ 0.16	$4d^35s^2\ {}^4F_{3/2}$ $_{40}$**Zr** 0.43 Zirconium	$4d^45s^2\ {}^5D_0$ $_{41}$**Nb** 0.89 Niobium	$4d^55s^2\ {}^6S_{5/2}$ $_{42}$**Mo** 0.748 Molibdenum	$4d^65s^2\ {}^5D_4$ $_{43}$**Tc** 0.6 Technetium	$4d^75s^2\ {}^4F_{9/2}$ $_{44}$**Ru** 1.0 Ruthenium	$4d^85s^2\ {}^3F_4$ $_{45}$**Rh** 1.137 Rhodium	$4d^95s^2\ {}^2D_{5/2}$ $_{46}$**Pd** 0.562 Palladium
	$4d^{10}5s^2\ {}^1S_0$ 1.302 $_{47}$**Ag** Silver	$5p\ {}^2P_{1/2}$ abs. $_{48}$**Cd** Cadmium	$5p^2\ {}^3P_0$ 0.40 $_{49}$**In** Indium	${}^4S_{3/2}$ 1.1121 $5p^3$ ${}^2D_{3/2}$ 0.3976 $_{50}$**Sn** ${}^2D_{5/2}$ 0.3046 Tin	${}^3P_2$ 1.047 $5p^4$ ${}^3P_1$ 0.714 $_{51}$**Sb** ${}^3P_0$ 0.700 ${}^1D_2$ 0.131 Antimony	$5p^5\ {}^2P_{3/2}$ 1.9708 $_{52}$**Te** Tellurium	$5p^6\ {}^1S_0$ 3.05904 $_{53}$**I** Iodine	$5p^6 6s\ {}^2S_{1/2}$ abs. $_{54}$**Xe** Xenon		
6	$6s^2\ {}^1S_0$ $_{55}$**Cs** 0.47163 Cesium	$6p\ {}^2P_{1/2}$ $_{56}$**Ba** 0.15 Barium	$5d^26s^2\ {}^3F_2$ $_{57}$**La** 0.5 Lanthanum	$5d^36s^2\ {}^4F_{3/2}$ $_{72}$**Hf** abs. Hafnium	$5d^46s^2\ {}^5D_0$ $_{73}$**Ta** 0.32 Tantalum	$5d^56s^2\ {}^6S_{5/2}$ $_{74}$**W** 0.815 Tungsten	$5d^66s^2\ {}^5D_4$ $_{75}$**Re** 0.2 Rhenium	$5d^76s^2\ {}^4F_{9/2}$ $_{76}$**Os** 1.1 Osmium	$5d^86s^2\ {}^3F_4$ $_{77}$**Ir** 1.5638 Iridium	$5d^96s^2\ {}^2D_{5/2}$ $_{78}$**Pt** 2.128 Platinum
	$5d^{10}6s^2\ {}^1S_0$ 2.30863 $_{79}$**Au** Gold	$6p\ {}^2P_{1/2}$ abs. $_{80}$**Hg** Mercury	$6p^2\ {}^3P_0$ 0.4 $_{81}$**Tl** Thallium	$6p^3\ {}^4S_{3/2}$ 0.364 $_{82}$**Pb** Lead	$6p^4\ {}^3P_0$ 0.95 $_{83}$**Bi** Bismuth	$6p^5\ {}^2P_{3/2}$ 1.9 $_{84}$**Po** Polonium	$6p^6\ {}^1S_0$ 2.8 $_{85}$**At** Astatine	$6p^6 7s\ {}^2S_{1/2}$ abs. $_{86}$**Rn** Radon		
7	$7s^2\ {}^1S_0$ $_{87}$**Fr** 0.46 Francium									

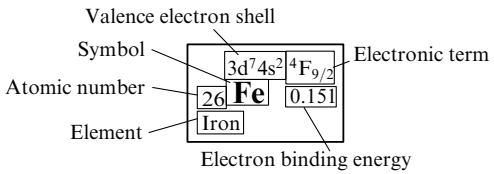

Figure 4. Electron affinity of atoms for elements of the periodic table. There may be an error in the last digit. Abbreviation 'abs.' is used for 'absent' (see the text).

allows one to improve the accuracy of the threshold wavelength. As a result, the laser method provides a high accuracy for the electron affinities obtained, and other methods for determination of electron affinities can compete with the laser method only in the case of complex molecules.

The asymptotic coefficient for the wave function of a valence electron in a negative ion can be found by means of the standard method which was described in the previous section. We now do this operation for the hydrogen negative ion where two bound electrons are located in the proton Coulomb field. Take the Chandrasekhar wave function of electrons [65]:

$$\Psi(r_1, r_2) = C\big[\exp(-\alpha r_1 - \beta r_2) - \exp(-\beta r_1 - \alpha r_2)\big] \times \big(1 + c|\mathbf{r}_1 - \mathbf{r}_2|\big)\,, \tag{3.14}$$

and the variational principle gives the following parameters of this wave function: $\alpha = 1.039$, $\beta = 0.283$, $c = 0$ for the two-parameter form of the wave function, and $\alpha = 1.075$, $\beta = 0.478$, $c = 0.312$ if we use three parameters. The electron affinity of the hydrogen atom is 0.367 eV in the first case and 0.705 eV in the second one, instead of the accurate value 0.754 eV.

Repeating the operations of the previous section, we obtain for the asymptotic coefficient squared:

$$A^2(r) = r^2\big[0.0695\exp(-0.096r) + 0.540\exp(-0.852r) + 3.44\exp(-1.608r)\big] \tag{3.15}$$

in the first case, and

$$A^2(r) = r^2\big[(0.102 + 0.0411r + 0.0064r^2)\exp(-0.486r) + (0.660 + 0.218r + 0.0341r^2)\exp(-1.063r) + (2.20 + 0.468r + 0.0729r^2)\exp(-1.68r)\big] \tag{3.16}$$

in the second. Figure 5 depicts the asymptotic coefficients obtained on the basis of these formulas. As a result, we have $A = 1.07 \pm 0.03$ on the basis of formula (3.15), and $A = 1.19 \pm 0.01$ if we use formula (3.16) and r ranges in both cases from 2 up to 5. Here, the statistical error is indicated only, and the real accuracy of this asymptotic coefficient is worse. Nevertheless, the accuracy of the asymptotic coefficient for a negative ion is usually better than that for an atom because of the absence of interaction of a weakly bound electron with its core outside the atom. Both formulas (3.15) and (3.16) give for the asymptotic coefficient $A = 1.13 \pm 0.06$ in the range $r = 2-5$.

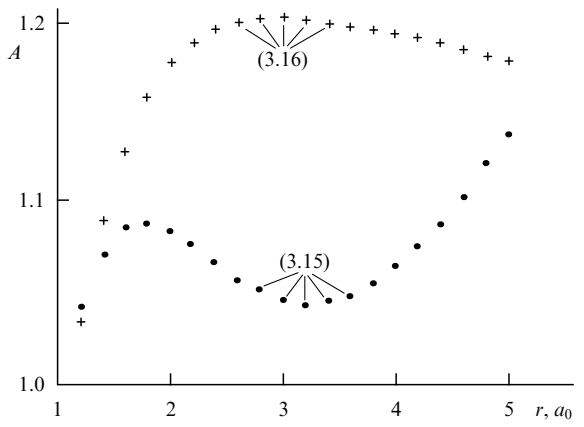

Figure 5. Determination of the asymptotic coefficient A of the electron wave function for the hydrogen negative ion on the basis of formulas (3.16) and (3.15).

For determination of the asymptotic coefficient one can fall back on that the electron affinity of atoms is relatively small. This means that an atomic size is small compared to the size of the negative ion. Then expression (3.13) is valid in the basic region of electron location, and from the normalization condition of the electron wave function we have

$$A = \sqrt{2\gamma}\,. \tag{3.17}$$

This is a rough approximation because the atomic region gives a contribution to the normalization integral. One can improve the correctness of this relation using additional information from the scattering of a slow electron by the atom. Indeed, let us consider the finite radius model for the electron–atom interaction, so that the wave function of a weakly bound electron equals zero for $r < r_0$, where r_0 is the effective atomic radius. Because the interaction of a valence electron with the atom is absent for $r > r_0$, the solution of the Schrödinger equation for $r > r_0$ is given by formula (3.13), and from the normalization of this wave function we have

$$A = \sqrt{2\gamma}\,\exp(\gamma r_0)\,. \tag{3.18}$$

As is seen, this effect must be taken into account even for small values of the parameter γr_0.

For determination of the parameter r_0 one can apply to the identical behavior of a free and bound electron outside the atom near its boundary. Indeed, the wave function of a slow free s-electron outside the coverage of an atomic field takes the form [4, 71]

$$R_q(r) = \frac{1}{r}\sin(qr - \delta_0)\,,$$

where q is the electron wave vector, r is the electron distance from the atom, and the scattering phase of s-electron δ_0 is equal to $\delta_0 = -Lq$ at a small electron wave vector, where L is the scattering length for a slow electron on the atom. This relation is valid for a slow electron $q \ll 1$ and is the definition of the scattering length L. As follows, the logarithmic derivative of this wave function on the atomic surface is

$$\left.\frac{\mathrm{d}\ln\big[rR_q(r)\big]}{\mathrm{d}r}\right|_{r=r_0} = \frac{1}{r_0 - L}\,, \tag{3.19}$$

and the logarithmic derivative of a bound electron wave function on the atomic surface according to formula (3.13) is equal to

$$\left.\frac{\mathrm{d}\ln\big[rR_q(r)\big]}{\mathrm{d}r}\right|_{r=r_0} = -\gamma\,. \tag{3.20}$$

Because inside an atom and in the vicinity of its boundary the behavior of free and bound electrons is identical, the logarithmic derivatives of their wave functions coincide on the atomic boundary, giving [72]

$$r_0 = L - \frac{1}{\gamma}\,. \tag{3.21}$$

In particular, in the case of the hydrogen negative ion we have $L = 5.8$, $\gamma = 0.235$, so that $r_0 = 1.55$, and according to formula (3.18) we have $A = 1.0$ in rough accordance with the above result.

This finite radius model of an atom accounts for the exchange interaction of a free or weakly bound electron with internal electrons. This interaction acts inside the atom only, while the polarization electron – atom interaction can be of importance far from the atom. The polarization interaction determines the expansion of the cross section of electron – atom scattering at small electron energies [73]. We now account for the influence of the polarization interaction with the atom on the wave function of a weakly bound s-electron on the basis of the method of Ref. [74] and the role of the polarization interaction for the asymptotic coefficient of the weakly bound electron in negative ions. The radial wave function of this electron satisfies the Schrödinger equation

$$\frac{\mathrm{d}^2}{\mathrm{d}r^2}\left[rR(r)\right] + \left(\frac{\alpha}{r^4} - \gamma^2\right) rR(r) = 0\,, \tag{3.22}$$

where α is the atomic polarizability. This wave function satisfies the boundary condition

$$\left.\frac{\mathrm{d}\ln\left[rR(r)\right]}{\mathrm{d}r}\right|_{r=0} = -\frac{1}{L}\,. \tag{3.23}$$

Introducing a reduced variable $x = r(\gamma^2/\alpha)^{1/4}$ and the small parameter $\beta = (\alpha\gamma^2)^{1/4}$ of the perturbation theory, we rewrite the above Schrödinger equation in the form

$$\frac{\mathrm{d}^2\varphi}{\mathrm{d}x^2} + \beta^2\left(\frac{1}{x^4} - 1\right)\varphi = 0\,,$$

where $\varphi = rR(r)$. Taking into account $\beta \ll 1$ and following paper [74], we use the perturbation operator of the perturbation theory in the form

$$V = \begin{cases} -\beta^2\,, & x \leqslant 1\,, \\ \dfrac{\beta^2}{x^4}\,, & x \geqslant 1\,. \end{cases}$$

Then the Schrödinger equation in the zero approximation is given by

$$\begin{aligned} &\frac{\mathrm{d}^2\varphi}{\mathrm{d}x^2} + \frac{\beta^2}{x^4}\,\varphi = 0\,, \qquad x \leqslant 1\,, \\ &\frac{\mathrm{d}^2\varphi}{\mathrm{d}x^2} - \beta^2\varphi = 0\,, \qquad x \geqslant 1\,. \end{aligned} \tag{3.24}$$

This equation has the following solutions [74]

$$\begin{aligned} &\varphi = Cx\sin\left(\frac{\beta}{x} + \delta\right), \qquad x \leqslant 1\,, \\ &\varphi = A\exp(-\beta x)\,, \qquad x \geqslant 1\,. \end{aligned} \tag{3.25}$$

and in the case $x \geqslant 1$ this electron wave function coincides with that of formula (3.13).

The phase δ in expression (3.25) of the wave function can be determined from the behavior of a free electron under the assumption that in the region of action of an atomic field the wave functions of free and weakly bound electrons are identical. The wave function of a free electron outside the atom is

$$\varphi = \mathrm{const}\,(r - L)\,, \tag{3.26}$$

where L is the electron scattering length. The wave function of a slow electron outside the atom satisfies the Schrödinger equation

$$\frac{\mathrm{d}^2\varphi}{\mathrm{d}r^2} + \frac{\alpha}{r^4}\,\varphi = 0\,,$$

and its solution is given by formula (3.25):

$$\varphi = Cx\sin\left(\frac{\beta}{x} + \delta\right).$$

This function is transformed into $\varphi = C(\beta + \delta x)$ at large $x \gg \beta$, that is $r \gg \sqrt{\alpha}$. Comparing this expression for the electron wave function with that of formula (3.26), we find for the phase δ in formula (3.25):

$$\delta = -\frac{\sqrt{\alpha}}{L} = -\frac{\beta^2}{\gamma L}\,. \tag{3.27}$$

In principle, the solution of the Schrödinger equation allows us to connect the values L, γ, α by equalizing the logarithmic derivatives of the wave functions (3.25) at $x = 1$. This operation holds true for $\beta \ll 1$, when the polarization interaction is relatively weak in the basic region of location of a weakly bound electron. As a result, we obtain

$$\tan(\beta + \delta) = \frac{\beta}{1 + \beta}\,. \tag{3.28}$$

Comparing the solution of this equation with formula (3.27), one can find the electron scattering length

$$L = \beta\left[\gamma\left(1 - \frac{1}{\beta}\arctan\frac{\beta}{1+\beta}\right)\right]^{-1}. \tag{3.29}$$

In the limit $\beta \to 0$ this gives $L = 1/\gamma$, as we have from formula (3.21) for $r_0 = 0$.

Table 8 contains the parameters of alkali metal atoms: the polarizability [75] and the scattering length L [71] if the total electron and atomic spin is zero, and also the scattering length calculated on the basis of formula (3.29) under the assumption that $\beta \ll 1$ and the polarization interaction acts on the weakly bound electron and atom outside the atomic boundary. The comparison between the electron scattering lengths of Table 8 shows that this model is not true. Moreover, this model cannot explain that the scattering length becomes negative for heavy alkali metal atoms. This contradiction

Table 8. Parameters of alkali metal atoms and their interaction with electrons.

Ion (state)	γ	L	α	β	L [formula (3.29)]	$\bar{r}$	A [formulas (3.18), (3.30)]
$H^-(1^1S)$	0.235	5.8	4.5	0.706	6.8	1.5	1.0
$Li^-(2^1S)$	0.213	3.6	162	1.65	12	3.9	1.5
$Na^-(3^1S)$	0.201	4.2	162	1.60	12	4.2	1.5
$K^-(4^1S)$	0.192	0.4	290	1.81	14	5.2	1.7
$Rb^-(5^1S)$	0.189	(−1.8)	320	1.84	14	5.6	1.8
$Cs^-(6^1S)$	0.188	−4.0	400	1.94	15	6.3	2.0

for the electron scattering lengths is not connected with a simplified solution of equation (3.22). The main reason is that the polarization interaction is formed at large distances, and another character of interaction takes place in the region of a weakly bound electron.

Taking things altogether, we neglect the interaction between a weakly bound electron and a residual atom in a negative ion outside the atom. We assume that the weakly bound electron cannot penetrate inside the atom due to the exchange interaction with internal electrons. Then we use the finite radius model for determining the asymptotic coefficient of a weakly bound electron, and the asymptotic coefficient is given by formula (3.18) with $r_0 = \bar{r}$, where $\bar{r}$ is the mean atomic radius. Table 8 contains values of this parameter [21] for alkali metal atoms and also the asymptotic coefficient of their negative ions, which are calculated in this way.

Thus, from the above analysis we obtained that the wave function of valence electrons in the atom on neglecting relativistic interactions is determined by the fractional parentage scheme, and the behavior of a weakly bound valence electron far from the atomic core is described by its binding energy and the asymptotic coefficient which characterizes the amplitude of the electron wave function far from the core. The asymptotic coefficient in turn is determined by the exchange interaction of this electron with electrons of the core, which results in electron repulsion from the core.

4. Ion – atom exchange interaction

4.1 Exchange interaction between the ion and parent one-electron atom at large separations

The exchange interaction potential of atomic particles is determined by the overlapping of the electron wave functions which reside on different atomic centers. Below we determine the exchange interaction potential of an ion with the parent atom, which is connected with the transition of a valence electron from the field of one ion to the field of another, and the nature of this interaction is illustrated in Fig. 6. We first consider the case when the valence electron is found in an s-state so that the system has two states composed from states related to location of the electron in the field of the first and second ion (see Fig. 6).

Let us denote the electron wave function centered on the first nucleus by ψ_1, and the wave function centered on the second nucleus by ψ_2. The electron Hamiltonian has the form

$$\hat{H} = -\frac{1}{2}\Delta + V(r_1) + V(r_2) + \frac{1}{R}\,. \tag{4.1}$$

Here, R is the distance between atomic cores, r_1, r_2 are the distances of the electron from the corresponding nucleus, $V(r)$ is the electron – ion interaction potential, and far from the ion this potential is the Coulomb one: $V(r) = -1/r$. We use the symmetry of the problem, so that the symmetry plane is perpendicular to the line joining the nuclei and bisects it, and the electron reflection with respect to this plane conserves the electron Hamiltonian. Hence, the electron eigenstates can be divided into even and odd ones, depending on whether their wave functions conserve or change their sign as a result of reflection with respect to the symmetry plane. Evidently, at large separations these wave functions are the following compositions of ψ_1 and ψ_2 which correspond to the location of the electron in the field of the corresponding atomic core:

$$\psi_g = \frac{1}{\sqrt{2}}(\psi_1 + \psi_2)\,, \qquad \psi_u = \frac{1}{\sqrt{2}}(\psi_1 - \psi_2)\,. \tag{4.2}$$

These wave functions are appropriate to the interacting ion and atom and satisfy the Schrödinger equations

$$\hat{H}\psi_g = \varepsilon_g\psi_g\,, \qquad \hat{H}\psi_u = \varepsilon_u\psi_u\,, \tag{4.3}$$

where $\varepsilon_g(R)$, $\varepsilon_u(R)$ are the energy eigenvalues of these states. We define the exchange interaction potential in this case as

$$\Delta(R) = \varepsilon_g(R) - \varepsilon_u(R)\,. \tag{4.4}$$

In order to determine this quantity at large distances between nuclei, we apply to the following method [76]. Let us multiply the first equation (4.3) by ψ_u^*, the second equation by ψ_g^*, take the difference of the obtained equations and integrate the result over the volume Ω which is a half-space bounded by the symmetry plane. Since the distance between the nuclei is large, the wave function ψ_2 is zero inside this volume and the wave function ψ_1 is zero outside this volume. Hence one obtains

$$\int_\Omega \psi_u^*\psi_g\,\mathrm{d}\mathbf{r} = \frac{1}{2}\,,$$

and the relation desired takes the form

$$\frac{\varepsilon_g(R) - \varepsilon_u(R)}{2} = \frac{1}{2}\int_\Omega \left(\psi_g\Delta\psi_g - \psi_u\Delta\psi_u\right)\mathrm{d}\mathbf{r} = \int_S \left(\psi_2\,\frac{\partial}{\partial z}\,\psi_1 - \psi_1\,\frac{\partial}{\partial z}\,\psi_2\right)\mathrm{d}\mathbf{s}\,,$$

where S is the symmetry plane which restricts the integration region; we use relations (4.2) with real wave functions, and the z-axis joins the nuclei. Take the origin of the coordinate system in the center of the line joining the nuclei. Since the electron is found in the s-state in the field of each atomic core, its wave functions in this coordinate system can be represented in the form

$$\psi_1 = \psi\left(\sqrt{\left(z + \frac{R}{2}\right)^2 + \rho^2}\right),$$
$$\psi_2 = \psi\left(\sqrt{\left(z - \frac{R}{2}\right)^2 + \rho^2}\right), \tag{4.5}$$

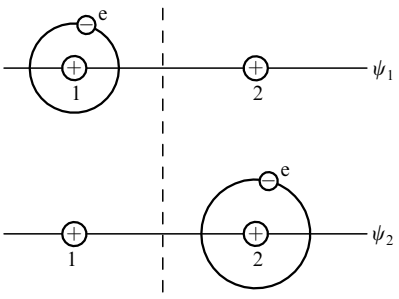

Figure 6. Electron in the field of two identical centers. Reflection in the symmetry plane corresponds to the transformation $\psi_1 \to \psi_2$, $\psi_2 \to \psi_1$. This yields the eigenfunctions of the system, so that the even electron wave function which retains its sign under reflection is $\psi_g = (\psi_1 + \psi_2)/\sqrt{2}$, and the odd wave function is $\psi_u = (\psi_1 - \psi_2)/\sqrt{2}$.

where ρ is the distance from the axis in the direction perpendicular to it. Since $d\mathbf{s} = 2\pi\rho\, d\rho$, we have from the above relation [76]:

$$\varepsilon_g(R) - \varepsilon_u(R) = \int_0^\infty 2\pi\rho\, d\rho \left[\psi\left(\sqrt{\left(z-\frac{R}{2}\right)^2+\rho^2}\right) \times \frac{\partial}{\partial z}\psi\left(\sqrt{\left(z+\frac{R}{2}\right)^2+\rho^2}\right) - \psi\left(\sqrt{\left(z+\frac{R}{2}\right)^2+\rho^2}\right) \times \frac{\partial}{\partial z}\psi\left(\sqrt{\left(z-\frac{R}{2}\right)^2+\rho^2}\right)\right]_{z=0}$$

$$= \pi R\int_0^\infty d\rho^2\, \frac{\partial}{\partial\rho^2}\,\psi^2\left(\sqrt{\frac{R^2}{4}+\rho^2}\right) = \pi R\psi^2\left(\frac{R}{2}\right). \quad (4.6)$$

In the course of the preparation of this formula we used the obvious relation

$$\frac{\partial}{\partial z}\left[\psi\left(\sqrt{\left(z-\frac{R}{2}\right)^2+\rho^2}\right)\right]_{z=0} = R\,\frac{\partial}{\partial\rho^2}\,\psi\left(\sqrt{\frac{R^2}{4}+\rho^2}\right).$$

Now let us connect the molecular wave function $\psi(r)$ of the s-electron with the atomic one ψ_{at} which is given by formula (3.7) at large electron distances from the atomic core and is determined by the Schrödinger equation

$$-\frac{1}{2}\,\frac{\partial^2}{\partial r^2}(r\psi_{at}) - \frac{1}{r}\,\psi_{at} = -\frac{\gamma^2}{2}\,\psi_{at},$$

where $\gamma^2/2$ is the electron binding energy. The solution of this equation is given by formula (3.7):

$$\psi_{at}(r) = Ar^{1/\gamma-1}\exp(-r\gamma).$$

Take the molecular wave function in the form $\psi(\mathbf{r}) = \chi(\mathbf{r})\psi_{at}(r)$ and compare the Schrödinger equations for molecular and atomic wave functions near the axis and far from nuclei, where one can use the asymptotic form of the interaction potential $V(r) = -1/r$ in formula (4.1) for the electron Hamiltonian. So, we have from the Schrödinger equation for ψ on neglecting the second derivative of χ near the axis:

$$\gamma\,\frac{\partial\chi}{\partial r_1} + \left(\frac{1}{R}-\frac{1}{r_2}\right)\chi = 0.$$

Solving this equation, we connect the molecular wave function of the s-electron near the axis with the atomic wave function that allows us to express the ion–atom exchange interaction potential through asymptotic parameters of the valence s-electron in the atom [13]:

$$\Delta = A^2R^{2/\gamma-1}\exp\left(-R\gamma-\frac{1}{\gamma}\right). \quad (4.7)$$

In particular, this formula yields for the exchange interaction potential of the proton and hydrogen atom in the ground state [4, 77]:

$$\Delta = \frac{4}{e}\,R\exp(-R).$$

Formula (4.7) shows the asymptotic expression for the exchange interaction potential of a one-electron atom with a valence s-electron and its atomic core. The criterion of validity of this formula has the form

$$R\gamma \gg 1, \qquad R\gamma^2 \gg 1. \quad (4.8)$$

Formula (4.7) admits a generalization. Consider the interaction of a one-electron atom with the parent ion for an electron angular momentum l and its projection μ onto the molecular axis. Then the electron wave function is $\psi(\mathbf{r}) = Y_{l\mu}(\theta,\varphi)\Phi(r)$, where r, θ, φ are the spherical coordinates of the electron if its center coincides with the corresponding nucleus, and the z-axis is directed along the molecular axis. In determination of the exchange interaction potential we may draw on the preparation of formula (4.7) for the s-electron and would have to make changes in the integration over $d\rho$. Then we arrive at

$$\Delta \sim \int_0^\infty \left|Y_{l\mu}(\theta,\varphi)\right|^2\Phi^2(r)\rho\, d\rho,$$

where $r = \sqrt{R^2/4+\rho^2}$ is the distance from each nucleus for the electron located in the symmetry plane. Since $\Phi(r) \sim \exp(-\gamma r)$, the integral converges at small ρ ($\rho \sim \sqrt{R/\gamma} \ll R$) (see also Fig. 7). Then one finds

$$\Phi(r) = \Phi\left(\frac{R}{2}\right)\exp\left(-\frac{\gamma\rho^2}{R}\right).$$

This corresponds to small angles $\theta = 2\rho/r$, and since $Y_{l\mu}(\theta,\varphi) \sim \theta^\mu$ for $\theta \ll 1$, we have

$$\Delta_\mu = \Delta_0\int_0^\infty \exp\left(-\frac{2\gamma\rho^2}{R}\right)\left|\frac{Y_{l\mu}(\theta,0)}{\theta^\mu}\right|^2\left|\frac{2\rho}{R}\right|^{2\mu}\frac{4\gamma\rho}{R}\, d\rho,$$

where Δ_0 is the exchange interaction potential defined by formula (4.7) in the case of zero angular momentum of the valence electron which has the same radial wave function. Since the exchange interaction potential does not depend on the sign of μ, we take the momentum projection to be positive. Thus, we find for the exchange interaction potential of a one-electron atom with the parent ion [10, 14]:

$$\Delta_\mu = A^2R^{2/\gamma-1-\mu}\exp\left(-R\gamma-\frac{1}{\gamma}\right)\frac{(2l+1)(l+\mu)!}{(l-\mu)!\mu!(2\gamma)^\mu}. \quad (4.9)$$

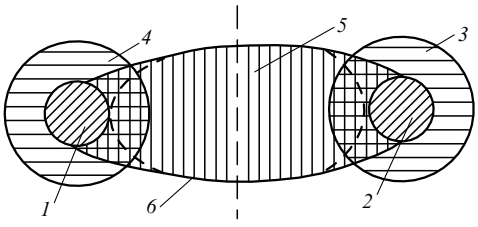

Figure 7. Electron regions which determine the exchange interaction potential of the ion and its parent atom at large distances between nuclei. *1*, *2* are internal regions of the atoms where the electrons are located; *3*, *4* are regions where the asymptotic expressions for the atomic wave functions are valid; *5* is the region where the quasi-classical approach is valid for valence electrons (it is restricted by the dotted line); *6* is the region which gives the main contribution to the exchange interaction potential of these atomic species. Since the volume of region *6* is of the order of R^2, where R is the distance between nuclei, and regions *1*, *2* occupy a volume of the order of the atomic value, on the basis of the asymptotic data for atomic wave functions one can evaluate the exchange interaction potential with an accuracy of the order of $1/R^2$.

In this way for the case of structureless cores and nonzero electron momentum, the ion–atom exchange interaction potential is characterized by the electron momentum projection m onto the molecular axis and is given by [10, 14, 78, 79]

$$\Delta_{lm} = \Delta_0 \frac{(2l+1)(l+|m|)!}{(l-|m|)!|m|!(R\gamma)^{|m|}}, \tag{4.10}$$

where l is the electron orbital momentum, and Δ_0 is the exchange interaction potential of the s-electron with the same asymptotic radial wave function (3.7) of the transiting electron. From this follows the ratio of the exchange interaction potential in the case of transition of a p-electron with one momentum projection to that with another projection:

$$\frac{\Delta_{11}(R)}{\Delta_{10}(R)} = \frac{2}{R\gamma}. \tag{4.11}$$

This ratio is small at large separations. Formula (4.11) describes the ion–atom exchange interaction potential if the atom has one valence electron at large separations according to the criterion (4.8). This interaction potential is determined by the overlapping of electron wave functions which correspond to the location of the electron in the field of the first and second cores (see Fig. 7). According to the criterion (4.8), this formula is not suitable for highly excited atoms and relates to the ground and lower excited atomic states.

4.2 Ion–atom exchange interaction for light atoms

In the case of light atoms one can neglect relativistic interactions and construct an atom within the framework of the LS-coupling scheme for the atom. This means that the energy difference for various orbital momentum projections of electrons onto the molecular axis connecting the atom and ion significantly exceeds the fine-structure splitting for the atom or ion. Then the quantum numbers of the molecular ion are the atomic quantum numbers L, S, M_L, M_S and the quantum numbers of the ion l, s, m, m_s. We sum up the electron momenta l_e, $1/2$ and the momenta of the atomic core l, s into the atomic momenta L, S, and then the atomic spin S and the spin of another atomic core s are summed into the total spin I of the molecular ion. Using formula (3.1) for the atomic wave function within the framework of the fractional parentage scheme and substituting it into the expression for the exchange interaction potential, we obtain [10, 11, 14, 79]

$$\begin{aligned}
\Delta &= n(G_{ls}^{LS})^2 \sum_{\mu,m',M_L'} \sum_{\sigma,\sigma',m_s,m_s'} \sum_{M_S,M_S'} \begin{bmatrix} l_e & l & L \\ \mu & m & M_L' \end{bmatrix} \\
&\quad \times \begin{bmatrix} l_e & l & L \\ \mu & m' & M_L \end{bmatrix} \begin{bmatrix} \frac{1}{2} & s & S \\ \sigma & m_s & M_S \end{bmatrix} \begin{bmatrix} \frac{1}{2} & s & S \\ \sigma' & m_s' & M_S' \end{bmatrix} \\
&\quad \times \begin{bmatrix} s & S & I \\ m_s & M_S & M \end{bmatrix} \begin{bmatrix} s & S & I \\ m_s' & M_S' & M \end{bmatrix} \Delta_\mu \\
&= n(G_{ls}^{LS})^2 \sum_\mu \begin{bmatrix} l_e & l & L \\ \mu & m & m+\mu \end{bmatrix} \begin{bmatrix} l_e & l & L \\ \mu & M_L-\mu & M_L \end{bmatrix} \\
&\quad \times (2S+1) \begin{Bmatrix} s & \frac{1}{2} & S \\ s & I & S \end{Bmatrix} \Delta_\mu \\
&= n \frac{I+1/2}{2s+1} (G_{ls}^{LS})^2 \sum_\mu \begin{bmatrix} l_e & l & L \\ \mu & m & m+\mu \end{bmatrix} \\
&\quad \times \begin{bmatrix} l_e & l & L \\ \mu & M_L-\mu & M_L \end{bmatrix} \Delta_\mu .
\end{aligned} \tag{4.12}$$

Here, M is the projection of the total spin I onto the molecular axis; the result obtained does not depend on this quantity because the influence of the spin on the exchange interaction is determined by the Pauli exclusion principle only, and the fine-structure splitting is assumed to be small. We applied to the properties of the Clebsch–Gordan coefficients. Note that the summation of the Clebsch–Gordan coefficients over spin projections leads to the $6j$-Wigner symbol which is denoted by braces, and its known value was used. Formula (4.12) gives the asymptotic expression for the exchange interaction potential of an atom with its atomic ion within the framework of the LS-coupling scheme. The criterion of validity of this expression is also given by formula (4.8).

This exchange interaction potential weakly depends on the total molecular spin I. Indeed, the level splitting corresponding to the different total spin of the quasi-molecule varies at large separations R as $\exp(-2\gamma R)$, because this exchange interaction potential is determined by the overlapping of the wave functions of electrons which are centered on different atomic particles. Since this interaction potential is relatively small, one can average formula (4.12) over the molecular total spin. Next, since the exchange interaction potential Δ_μ decreases with increasing μ as $R^{-\mu}$, one can restrict its consideration to the term in the sum (4.12) with the minimal μ, and formula (4.12) then takes the form [10, 11, 14, 79]

$$\begin{aligned}
\Delta(l_e\mu, lm\,s, LM_L S) &= \frac{\bar{I}+1/2}{2s+1} n(G_{ls}^{LS})^2 \\
&\quad \times \begin{bmatrix} l_e & l & L \\ \mu & m & m+\mu \end{bmatrix} \begin{bmatrix} l_e & l & L \\ \mu & M_L-\mu & M_L \end{bmatrix} \Delta_\mu ,
\end{aligned} \tag{4.13}$$

where Δ_μ is given by formula (4.9). Formula (4.13) relates to case 'a' of Hund coupling scheme when relativistic interactions are small. The method used allows us to express the ion–atom exchange interaction potential through asymptotic parameters of the radial wave function of a valent atomic electron. The above formulas give the first term of the asymptotic expansion of the ion–atom exchange interaction potential at large distances between nuclei. The next terms of the potential expansion in a power series of a small parameter of the theory are of order $1/R$ relative to the first term.

4.3 Ion–atom exchange interaction for valence p-electrons of light atoms

Formula (4.13) for the ion–atom exchange interaction potential is valid in the limit when relativistic interactions are small. This means that the energy level splitting for the molecular ion due to the long-range ion–atom interaction significantly exceeds the spin–orbit interaction for colliding ion and atom. This allows us to take the quantum numbers L, M_L, S of the atom and l, m, s of the ion as quantum numbers of the quasi-molecule, and the quantization axis is the line joining the atom and ion. Below we derive the criterion of validity of this approach. The energy level splitting over the projection of orbital momenta of atom and ion is determined by a long-range ion–atom interaction potential having the form

$$U(R) = \frac{Q_{at}}{R^3} + \frac{Q_{at}Q_i}{R^5}, \tag{4.14}$$

where Q_{at} and Q_i are the projections of the atomic and ion quadrupole moment tensor onto the axis joining the nuclei, R

is the distance between the atom and ion, and formula (4.14) is an expansion in the small parameter $1/R$. The first term of this expansion corresponds to interaction of the ion charge with the atomic quadrupole moment, while the second term represents the interaction of the atomic and ion quadrupole momenta. Formula (4.13) is valid if the first term of formula (4.14) is large compared to the atomic fine-structure splitting, and the second term of this formula significantly exceeds the ion fine-structure splitting.

The quadrupole moment of an atomic particle is represented by [80, 81]

$$Q = 2\sum_i \langle r_i^2 P_2(\cos\theta_i)\rangle = 2\sum_i \frac{l_i(l_i+1)-3m_i^2}{(2l_i-1)(2l_i+3)}\,\overline{r_i^2}\,, \quad (4.15)$$

where r_i, θ_i are the spherical coordinates of ith electron, l_i, m_i are the angular momentum of this electron and its projection on the field direction. Since

$$\sum_{l=-m}^{m}\left[l(l+1)-3m^2\right] = 0\,,$$

filled electron shells do not give a contribution to the atomic quadrupole moment, and it is determined by valence (outer) electrons.

Using expression (3.1) for the atomic wave function, we obtain for the atomic quadrupole moment after summation over spin projections:

$$Q(LSM_L) = n\sum_{ls\mu} q_\mu \left|G_{ls}^{LS}(l_e,n)\right|^2 \begin{bmatrix} l_e & l & L \\ \mu & M_L-\mu & M_L \end{bmatrix}^2 . \quad (4.16)$$

Here, L, M_L, S are the orbital momentum, its projection on the field direction, and the atomic spin, correspondingly, l_e is the momentum of the valence electron, μ is its projection onto the field direction, n is the number of identical valence electrons, l and s are the orbital momentum and spin of the atomic core, and the one-electron quadrupole moment in conventional units is equal to (e is the electron charge)

$$q_\mu = 2e\,\frac{l_e(l_e+1)-3\mu^2}{(2l_e-1)(2l_e+3)}\,\overline{r^2}\,. \quad (4.17)$$

where the quantity $\overline{r^2}$ relates to a valence electron. Considering the case of the p^n electron shell, we have

$$Q(p^n, LSM_L) = \frac{2n}{5}\,e\overline{r^2}\sum_{ls\mu}(2-3\mu^2)\left|G_{ls}^{LS}(p^n)\right|^2 \times \begin{bmatrix} 1 & l & L \\ \mu & M_L-\mu & M_L \end{bmatrix}^2 . \quad (4.18)$$

Table 9 contains the values of reduced quadrupole momenta for the ground-state atoms with valence p-electrons.

Table 9. Values $Q(p^n, LS, M_L)/\overline{r^2}$ for the ground states of atoms with p^n-electron shells.

State	$(p)^2P$	$(p^2)^3P$	$(p^3)^4S$	$(p^4)^3P$	$(p^5)^2P$
$M_L = 0$	4/5	−4/5	0	4/5	−4/5
$\lvert M_L\rvert = 1$	−2/5	2/5	–	−2/5	2/5

From formula (4.16) one can explain the general properties of the atomic quadrupole moment. The first property

$$Q(p^n, LS, M_L) = Q(p^n, LS, -M_L) \quad (4.19a)$$

follows from the transformation $\mu, M_L \to -\mu, -M_L$ in the above expression for the atomic quadrupole moment.

The second property of the atomic quadrupole moment uses the analogy between an electron and hole. This gives

$$Q(p^n, LS, M_L) = -Q(p^{6-n}, LS, M_L)\,. \quad (4.19b)$$

Notice that the quadrupole momenta of one electron and one hole with identical quantum numbers have a different sign. This can also be explained by the different charge sign for an electron and hole.

The third property relates to summation over projections of the atomic momentum, that is analogous to averaging over the field direction and gives

$$\sum_{M_L} Q(p^n, LS, M_L) = 0\,. \quad (4.19c)$$

Formula (4.18) for the atomic quadrupole momentum allows one to determine this quantity for nonzero-momentum atoms containing several electrons. In particular, Table 9 contains the reduced quadrupole momenta for the ground states of atoms with a unfilled p-shell, and the above consideration is valid if the following criteria hold true:

$$\frac{Q_{at}}{R^3} \gg \Delta_f^{at}\,, \qquad \frac{Q_{at}Q_i}{R^5} \gg \Delta_f^{i}\,, \quad (4.20)$$

where Δ_f^{at}, Δ_f^{i} are the fine-structure splitting energies for the atom and ion, correspondingly. Note that the energy of the molecular ion under consideration is degenerate over the momentum directions, i.e. it depends on $|M_L|$ and $|m|$ in accordance with Eqn (4.19a).

We now consider the ion–atom exchange interaction potential under the condition (4.20) in the case of valence p-electrons. We use the analogy of the exchange interaction potentials for elements of groups III and VIII, for elements of groups IV and VII or for elements of groups V and VI of the periodic table, which follows from the analogy in transitions of a valence electron and hole. Correspondingly, we obtain identical expressions for the exchange interaction potentials in these cases.

In the case of atoms of group III with one valence p-electron and ions of group VIII with one valence p-hole, when the ground states of the atom and ion are ^1S and ^2P, respectively, the exchange interaction potential of the interacting atom and ion depends only on the momentum projection of a transferring electron (hole), and according to formula (4.13) it has the form

$$\Delta_{M_L} = \begin{array}{|c|c|c|} \hline M_L=-1 & M_L=0 & M_L=+1 \\ \hline \Delta_{11} & \Delta_{10} & \Delta_{11} \\ \hline \end{array}\,, \quad (4.21)$$

while the connection between one-electron exchange interaction potentials that correspond to different momentum projections onto the molecular axis is given by formula (4.11).

If we take the direction on which the projection of the electron momentum is zero as a quantization axis, and denote the angle between this and molecular axes by θ, the exchange

interaction potential of an atom and parent ion in the case of groups III and VIII of the periodic table of elements is defined by the expression

$$\Delta(\theta) = \Delta_{10}\cos^2\theta + \Delta_{11}\sin^2\theta\,. \tag{4.22}$$

For elements of group IV of the periodic table, we have the ground states $(p^2)^3P$ and $(p)^2P$ for the atom and ion, correspondingly, i.e. the ion and atomic orbital momenta are $l = L = 1$ in this case. We specify the following parameters in formula (4.13): $n = 2$, $G_{ls}^{LS} = 1$, and the total spin of the molecular ion can take the values $I = 1/2,\ 3/2$ with the probabilities of these states being $1/3$ and $2/3$, correspondingly. This yields $\bar{I} + 1/2 = 5/3$. Using the values of the Clebsch–Gordan coefficients, we find the matrix of the reduced ion–atom exchange interaction potential Δ_{mM_L}:

$$\Delta(m, M_L) = \frac{5}{3}\begin{array}{|c|c|c|c|}\hline & M_L=-1 & M_L=0 & M_L=1\\ \hline m=-1 & \Delta_{10} & \Delta_{11} & \Delta_{10}\\ \hline m=0 & \Delta_{11} & 2\Delta_{11} & \Delta_{11}\\ \hline m=1 & \Delta_{10} & \Delta_{11} & \Delta_{10}\\ \hline\end{array}\,. \tag{4.23}$$

Here, m, M_L are the initial projections of the angular ion and atomic momenta, so that after transition of an electron with the projection μ of the angular momentum onto the molecular axis these final values become $m + \mu$ and $M_L - \mu$ for the atom and ion, correspondingly. Because of the relation

$$\begin{bmatrix}1 & 1 & 1\\ 0 & 0 & 0\end{bmatrix} = 0\,,$$

the momentum projection of the electron making transition is nonzero for zero initial momentum projections of the atom and ion. Matrix (4.23) brings about the exchange interaction potential as a function of the angles between the quantization and molecular axes:

$$\Delta(\theta) = \frac{5}{3}\left[\Delta_{10}\sin^2\theta_1\sin^2\theta_2 + \Delta_{11}(\cos^2\theta_1 + \cos^2\theta_2)\right], \tag{4.24}$$

where θ_1, θ_2 are the angles between the molecular axis which joins nuclei and the quantization axes for the atom and ion, correspondingly, so that the electron momentum projection onto the quantization axis is zero.

In the case of atoms of group VII of the periodic table of elements, we have the atomic ground state $(p^5)^2P$, the ion ground electronic state $(p^4)^3P$, and the parameters of the expression for the ion–atom exchange interaction potential are $n = 5$, $G_{ls}^{LS} = \sqrt{3/5}$. Though these values differ from those for elements of group IV of the periodic table, the matrix Δ_{mM_L} of the ion–atom exchange interaction potential is the same as for elements of group IV. This testifies the analogy in transition of a p-electron and p-hole for the exchange interaction potential.

In the case of atoms of group V of the periodic table of elements, we are dealing with the atomic ground electronic state $(p^3)^4S$, the ion ground electronic state $(p^2)^3P$, and $M_L = 0$. The parameters of the ion–atom exchange interaction potential are $n = 3$, $G_{ls}^{LS} = 1$. The total quasi-molecular spin can take the values $I = 1/2,\ 3/2,\ 5/2$ with the probabilities of these states being $1/6$, $1/3$ and $1/2$, correspondingly, so that $\bar{I} = 11/6$. From this we find for the ion–atom interaction potential on the basis of formula (4.13):

$$\begin{aligned}\Delta(m) &= 3\left(\bar{I} + \frac{1}{2}\right)\begin{bmatrix}1 & 1 & 0\\ \mu & m & 0\end{bmatrix}\begin{bmatrix}1 & 1 & 0\\ \mu & -\mu & 0\end{bmatrix}\Delta_\mu\\ &= 7\begin{bmatrix}1 & 1 & 0\\ \mu & m & 0\end{bmatrix}\begin{bmatrix}1 & 1 & 0\\ \mu & -\mu & 0\end{bmatrix}\Delta_\mu\,,\end{aligned} \tag{4.25}$$

where μ is the momentum projection onto the molecular axis for the electron making transition, m is the analogous parameter for the ion, and according to the character of momentum coupling $\mu = -m$. In this case we obtain the following matrix of the reduced ion–atom exchange interaction potential as a result of its averaging over the total spin I:

$$\Delta(m) = \frac{7}{3}\begin{array}{|c|c|c|}\hline m=-1 & m=0 & m=1\\ \hline \Delta_{11} & \Delta_{10} & \Delta_{11}\\ \hline\end{array}\,. \tag{4.26}$$

This matrix is similar to that for the transition of a p-electron between two structureless atomic cores.

Introducing an angle θ between the molecular axis and quantization axis onto which the projection of the ionic momentum is zero, we obtain for the ion–atom exchange interaction potential

$$\Delta(\theta) = \frac{7}{3}(\Delta_{10}\cos^2\theta + \Delta_{11}\sin^2\theta)\,. \tag{4.27}$$

With an accuracy up to a numerical factor, this matrix of the exchange interaction potential is identical to that of a p-electron in the field of two structureless atomic cores (4.21), and this analogy also relates to the exchange interaction potential for atoms of groups III and VIII of the periodic table of elements, which is given by formula (4.22).

In the case of the interaction event involving atoms of group VI of the periodic table of elements, we are concerned with the atomic ground state $(p^4)^3P$, the ion ground electronic state $(p^3)^4S$, and the parameters of the expression for the ion–atom exchange interaction potential being $n = 4$, $G_{ls}^{LS} = 1/\sqrt{3}$. In this case we obtain the same form of the matrix of the exchange interaction potential as for elements of group V. Thus we see the analogy between the transition of a p-electron and p-hole for the ion–atom exchange interaction potential.

Though we are restricted to the ground states of the ion and parent atom, this is a general scheme of construction of the ion–atom exchange interaction potential. Being averaged over the total quasi-molecular spin I, the exchange interaction potential depends on the ion m and atom M_L angular momentum projections onto the molecular axis. This corresponds to the LS-coupling scheme for atoms and ions, i.e. we neglect the spin–orbit interaction. Hence, the above expressions correspond to the following hierarchy of the interaction potentials:

$$V_{ex} \gg U(R) \gg \Delta(R)\,, \tag{4.28}$$

where V_{ex} is a typical exchange interaction potential for valence electrons inside the atom or ion, $U(R)$ is the long-range interaction potential between the atom and ion at large separations R, and $\Delta(R)$ is the exchange interaction potential between the atom and ion. Within the framework of the LS-coupling scheme for atoms and ions, we assume the excitation energies inside the electron shell to be relatively large, and this criterion is fulfilled for light atoms and ions. In the same

manner one can construct the exchange interaction potential matrix for excited states within a given electron shell.

Because the exchange interaction potential is determined by the transition of one electron from a valence electron shell and a transferring electron carries a certain momentum and spin, additional selection rules occur for the one-electron interaction. In particular, in the case of transition of a p-electron, the selection rules take the form

$$|L-l| \leqslant 1\,, \qquad |S-s| \leqslant \frac{1}{2}\,. \tag{4.29}$$

These selection rules follow from the properties of the Clebsch – Gordan coefficients in formula (4.13). If these conditions are violated, the ion – atom exchange interaction potential is zero on the scale of one-electron interaction potentials. In particular, this interaction potential is zero for atoms of group V in the ground state $(p^3)^4S$ and their ions in the excited states $(p^2)^1D$ and $(p^2)^1S$, and also for atoms of group VI in excited states $(p^4)^1D$ and $(p^4)^1S$, when the ion is found in the ground state $(p^3)^4S$. In these cases, the addition of one electron to the ion does not allow formation of an atom with a given spin, that is, criterion (4.29) is violated. In the same manner, the one-electron exchange interaction potential of atoms of group V in the excited state $(p^3)^2S$ with their ion in the excited state $(p^2)^1D$ is zero.

4.4 Ion – atom exchange interaction potential for case 'c' of Hund coupling scheme

The above consideration relates to case 'a' of Hund coupling scheme [7, 8] when the fine splitting of levels is relatively small, and criterion (4.20) allows us to choose the momentum projections M_L, m of the interacting ion and atom onto a joining line as quantum numbers of the molecular ion consisting of the given ion and atom. We now take a look at the other possibilities of momentum coupling which relate to another cases of Hund coupling of momenta in the molecule. Following Hund's analysis [7, 8], we consider three types of interaction in a diatomic molecule. The first type is described by the interaction potential V_e that corresponds to the so-called interaction between the orbital angular momentum of electrons and the molecular axis. This includes both the electron exchange interaction potential V_{ex} inside atoms and the interaction potential between atoms $U(R)$ on neglecting the relativistic effects. Above we considered the case of these interactions only, and then the electronic terms were characterized by a certain projection of the molecular orbital angular momentum onto the molecular axis. The second type of interaction whose potential is denoted by Δ_f corresponds to the spin – orbit interaction and some other relativistic interactions. The third type of interaction in a diatomic molecule is denoted by V_r and accounts for an interaction between the orbital or spin electron momenta and rotation of the molecular axis. Often this interaction is called the Coriolis one, and it is determined by the rotation of the molecular axis. Depending on the ratio between the potentials of these interactions, a certain character of coupling of the molecular momenta is realized, thus leading to appropriate quantum numbers of this molecule. Possible types of the ratio between the above interaction potentials determine the various limiting cases which are known as the Hund coupling cases. The various cases of Hund coupling scheme are summarized in Table 10 together with the quantum numbers which describe the electronic terms of the molecule in respective cases.

Table 10. Cases of the Hund coupling scheme.

Hund case	Relation	Quantum numbers
a	$V_e \gg \Delta_f \gg V_r$	Λ, S, S_n
b	$V_e \gg V_r \gg \Delta_f$	Λ, S, S_N
c	$\Delta_f \gg V_e \gg V_r$	Ω
d	$V_r \gg V_e \gg \Delta_f$	L, S, L_N, S_N
e	$V_r \gg \Delta_f \gg V_e$	J, J_N

Note. In the notation used **L** is the electron angular momentum, **S** is the total electron spin, **J** is the total electron momentum, Λ is the projection of the electron angular momentum onto the molecular axis, Ω is the projection of the total electron momentum **J** onto the molecular axis, S_n is the projection of the electron spin onto the molecular axis, and L_N, S_N, J_N are the projections of these momenta onto the direction of the nuclear rotation momentum **N**.

Table 10 represents the standard classification of Hund coupling of momenta as it was given by R S Mulliken in 1930. Considering the problem of the resonant charge exchange process, one can restrict oneself to cases 'a' and 'c' only. Above we analyzed case 'a' of Hund coupling scheme for the exchange ion – atom interaction potential at large separations. Note that because of the weak ion – atom interaction in comparison with the electron exchange interaction inside the atomic particles, the quantum numbers of individual atomic particles become the quantum numbers of the quasi-molecule. In addition, at large separations degeneracy of the electronic terms arises both for the projection of the total electron spin of the molecular ion and also its total spin because of the weak ion – atom interaction, so that the quantum numbers of the quasi-molecule at large separations are l, m, s, L, M_L, S, as we took above.

In case 'c' of Hund coupling scheme we consider only the spin – orbit interaction and neglect other relativistic interactions. This allows us to use the *jj*-coupling scheme for an individual atomic particle, and because the ion – atom interaction potential is small in comparison with the exchange interaction potential of electrons inside atomic particles, and this in turn is small compared to the spin – orbit interactions, the quantum numbers of the individual ion and atom remain the quantum numbers of the quasi-molecule at large separations. Thus, the quantum numbers of the quasi-molecule under consideration for case 'c' of Hund coupling scheme are J, M_J, the total atomic electron momentum and its projection onto the molecular axis, and also j, m_j, i.e. relevant quantum numbers for the ion.

We now examine the ion – atom exchange interaction potential in case 'c' of Hund coupling scheme and for one p-electron making transition between structureless cores. In this case, the spin – orbit splitting of electronic levels is large compared to the electrostatic ion – atom interaction, and the quantum numbers of the molecular ion are j, m_j — the total electron momentum and its projection onto the quasi-molecular axis. We have the following relations between the exchange interaction potential Δ_{jm_j} for case 'c' of Hund coupling and the exchange interaction potentials Δ_{lm} for case 'a' of Hund coupling, which are given by formula (4.10):

$$\Delta_{1/2,\,1/2} = \frac{1}{3}\,\Delta_{10} + \frac{2}{3}\,\Delta_{11}\,, \qquad \Delta_{3/2,\,1/2} = \frac{2}{3}\,\Delta_{10} + \frac{1}{3}\,\Delta_{11}\,,$$

$$\Delta_{3/2,\,3/2} = \Delta_{11}\,. \tag{4.30}$$

This connection is established in a simple way on the basis of the relation between the electron wave functions for these states. Thus, the behavior of the electronic term of a quasi-molecule consisting of an ion and parent atom depends on the character of coupling between electron momenta.

Introducing an angle θ between the quantization axis for the electron momenta and molecular axis, we arrive at the following expressions for the ion – atom exchange interaction potentials of a p-electron and structureless cores in case 'c' of Hund coupling scheme:

$$\Delta_{1/2} = \frac{1}{3}\Delta_{10} + \frac{2}{3}\Delta_{11}\,,$$
$$\Delta_{3/2}(\theta) = \left(\frac{1}{6} + \frac{1}{2}\cos^2\theta\right)\Delta_{10} + \left(\frac{1}{3} + \frac{1}{2}\sin^2\theta\right)\Delta_{11}\,, \quad (4.31)$$

where the quantities Δ_{10} and Δ_{11} correspond to case 'a' of Hund coupling scheme and are determined by formula (4.10).

Evidently, in case 'c' of Hund coupling of momenta when the spin – orbit interaction dominates, it is correct to use the *jj*-coupling scheme for electron momenta in the atom and ion. In this case the character of coupling of electron momenta is simpler than in the case of the *LS*-coupling scheme because of a lower symmetry of electron shells. Hence, the ion – atom exchange interaction potential is expressed through the one-electron exchange interaction potential in a simpler way. Table 11 contains parameters of electron shells for the ground electronic states of atoms and ions having a p-electron shell. Note that in the case of *jj*-coupling, the analogy in transitions of a p-electron and p-hole is lost because of the different sign of the spin – orbit interaction potential for an electron and hole. Hence, the ion – atom exchange interaction potential is different for the cases when a p-electron shell of an atom and its ion are replaced by shells consisting of identical p-holes.

Table 11. Ground states of atoms with p-electron shells within the framework of *LS*- and *jj*-coupling schemes. Δ is the ion – atom exchange interaction potential for case 'c' of Hund coupling scheme.

Shell	J	*LS*-term	*jj*-shell	Δ
p	1/2	$^2P_{1/2}$	$[1/2]^1$	$\Delta_{1/2}$
p^2	0	$^3P_0$	$[1/2]^2$	$\Delta_{1/2}$
p^3	3/2	$^4S_{3/2}$	$[1/2]^2[3/2]^1$	$\Delta_{3/2}$
p^4	2	$^3P_2$	$[1/2]^1[3/2]^3$	0
p^5	3/2	$^2P_{3/2}$	$[1/2]^2[3/2]^3$	$\Delta_{1/2}$
p^6	0	$^1S_0$	$[1/2]^2[3/2]^4$	$\Delta_{3/2}$

In the case of group VI of the periodic table of elements, the one-electron exchange interaction potential is zero if the atom and ion are found in the ground states, since the exchange interaction can result from the transition of two electrons only. Note that for all the groups of the periodic table of elements with an incomplete p-electron shells, when atoms and their ions are found in the ground state, the one-electron exchange interaction potential is not zero for case 'a' of Hund coupling scheme.

The principal difference between cases 'a' and 'c' of Hund coupling scheme for the exchange interaction potential of an atom and its ion with unfilled p-shells is due to the lower symmetry for case 'c'. Then the electron shell is divided into two independent subshells with $j = 1/2$ and $j = 3/2$. Therefore, the criterion of one-electron transition requires, instead of Eqn (4.29), that the difference in the number of electrons of a given j for the interacting atom and ion does not exceed one. This criterion is violated more often than the criterion (4.29) because of the lower atomic symmetry.

Thus, the exchange interaction potential of an atom with its ion is determined by electron transfer between cores, and at large separations this interaction potential decreases exponentially with increasing distance between nuclei. The interaction potential is governed by the character of coupling of the electron making transition with cores, and this in turn is connected with the symmetry of interacting atomic particles.

5. Resonant charge exchange in slow collisions

5.1 Peculiarities of the resonant charge exchange process

The resonant charge exchange process proceeds according to the scheme

$$A^+ + A \rightarrow A + A^+\,. \quad (5.1)$$

As a result of this process, a valence electron passes from the field of one atomic core to another. In slow collisions, when the collision velocity is small compared to an atomic velocity, the rate of this process is expressed through electronic terms of the quasi-molecule constituted from the colliding particles. This process was first analyzed by Massey et al. [82, 83] on the basis of the phase theory of collisional processes. Sena [84–86] applied to the classical character of motion of colliding particles that allowed him to ascertain the physical nature of the process and find the dependence of the cross section on collisional parameters. In particular, the resonant charge exchange cross section σ_{res} depends on the relative velocity of collision v as [84, 87]

$$\sigma_{res} = \frac{\pi}{2\gamma^2}\ln^2\frac{v_0}{v}\,. \quad (5.2)$$

Here, $\gamma = \sqrt{2I}$, I is the ionization potential of an atom A, and the parameter $v_0 \gg 1$. Since this formula may be rewritten in the form

$$\sigma_{res} = \frac{\pi}{2\gamma^2}(\gamma R_0)^2\,,$$

we obtain a weak dependence of the cross section on the collision energy because $\gamma R_0 \gg 1$, and $1/\gamma R_0$ is a small parameter of the asymptotic theory. The data of Table 12 demonstrate this fact. In this table the relative variation of the cross section for process (5.1) is given for an increase in the collision energy by ten times. One can see that the greater the relative cross section of this process, the weaker the energy dependence. Therefore, the weakest energy dependence of the cross section occurs at small collision energies.

The cross section of a slow collision process can be expressed through the parameters of the electronic terms which are responsible for the process. The eigenstates of the

Table 12. Relative decrease $\Delta\sigma_{res}/\sigma_{res}$ of the cross section of resonant charge exchange for an increase in the collision energy by an order of magnitude ($E/E_0 = 10$) and for a decrease in the asymptotic coefficient by 20% ($A/A_0 = 0.8$).

γR_0	6	8	10	12	14	16
$\Delta\sigma_{res}/\sigma_{res}$ ($E/E_0 = 10$)	0.347	0.267	0.217	0.183	0.158	0.139
$\Delta\sigma_{res}/\sigma_{res}$ ($A/A_0 = 0.8$)	0.143	0.108	0.087	0.073	0.063	0.055
$\bar{\sigma}_{res}/\sigma_0$	1.17	1.09	1.05	1.03	1.02	1.01

quasi-molecule A_2^+ are divided into odd and even in accordance with the properties of the wave functions of these states to conserve or change the sign as a result of electron reflection with respect to the symmetry plane which is perpendicular to the molecular axis and bisects it. If at the beginning an atom A and ion A^+ have only one electronic state, there are only one even and one odd quasi-molecular state with the wave functions $\psi_g(\mathbf{r}, R)$, $\psi_u(\mathbf{r}, R)$, and energies $\varepsilon_g(R)$, $\varepsilon_u(R)$ [see formulas (4.2), (4.3)]. Here, $\mathbf{r}$ defines the electron coordinates, and R is the distance between the nuclei. At large separations we have

$$\psi_g = \frac{1}{\sqrt{2}}(\psi_1 + \psi_2)\,, \qquad \psi_u = \frac{1}{\sqrt{2}}(\psi_1 - \psi_2)\,, \tag{5.3}$$

where the wave functions ψ_1, ψ_2 correspond to the electron location in the field of the first or second ion, correspondingly.

Assuming the absence of inelastic transitions, one can construct a molecular wave function Ψ, if before the collision $t \to -\infty$ the electron is bound to the first atomic core $[\Psi(\mathbf{r}, \mathbf{R}, -\infty) = \psi_1(\mathbf{r})]$. Because the two quasi-molecular states are developed independently, we get

$$\Psi(\mathbf{r}, \mathbf{R}, t) = \frac{1}{\sqrt{2}}\,\psi_g(\mathbf{r}, \mathbf{R}) \exp\left[-\mathrm{i}\int_{-\infty}^{t} \varepsilon_g(t')\,\mathrm{d}t'\right] + \frac{1}{\sqrt{2}}\,\psi_u(\mathbf{r}, \mathbf{R}) \exp\left[-\mathrm{i}\int_{-\infty}^{t} \varepsilon_u(t')\,\mathrm{d}t'\right]. \tag{5.4}$$

Here, the relative motion of nuclei $R(t)$ is given, and for free motion it has the form $R = (v^2t^2 + \rho^2)^{1/2}$, where v is the collision velocity, and ρ is the impact parameter of the collision. From this we obtain for the probability P_{res} of the charge exchange process and its cross section [76]:

$$P_{\mathrm{res}} = \sin^2\zeta(\rho)\,, \qquad \zeta(\rho) = \int_{-\infty}^{\infty} \frac{\Delta(R)}{2}\,\mathrm{d}t\,,$$

$$\Delta(R) = \varepsilon_g - \varepsilon_u\,; \qquad \sigma_{\mathrm{res}} = \int_0^{\infty} 2\pi\rho\,\mathrm{d}\rho\,\sin^2\zeta(\rho)\,. \tag{5.5}$$

Formula (5.5) expresses the parameters of the charge exchange process through electronic terms $\varepsilon_g(R)$, $\varepsilon_u(R)$ of the quasi-molecule consisting of colliding particles. This connection was first established by Firsov [76] and Demkov [87].

One more peculiarity of this slow-collision process is the large cross section in comparison to the typical atomic value. This allows us to construct an asymptotic theory [12–14] which treats the cross section as a result of an expansion in terms of a small parameter $1/(\sqrt{\sigma}\gamma)$. In this case, restricting ourselves to two terms in the expansion over the small parameter, we have for the charge exchange cross section [12–14]:

$$\sigma_{\mathrm{res}} = \frac{\pi R_0^2}{2}\,, \qquad \text{where} \quad \zeta(R_0) = \frac{\exp(-C)}{2} = 0.28\,. \tag{5.6}$$

Here $C = 0.577$ is the Euler constant.

Thus, within the asymptotic theory of the resonant charge exchange process, we suppose the electron transition to proceed at large distances between nuclei compared to the orbit size of a transferring electron. Then we can use the asymptotic expression of the exchange interaction potential of the ion and atom, $\Delta(R) = \varepsilon_g - \varepsilon_u$, and this quantity is expressed in turn through asymptotic parameters of the atomic wave function at large distances of the electron from its atomic core. Hence, in this version of the asymptotic theory we do not use the electron distribution inside the atom, and information about the electron behavior inside the atom is included in the theory indirectly through the asymptotic coefficient of a valence electron. According to Fig. 7, the contribution of internal atomic regions to the overlap integral is of order $1/R^2$. Therefore, representing the cross section of the resonant charge exchange as an expansion in terms of a small parameter $1/R$, one may consider only the first two terms of this expansion, and accounting for the subsequent terms is not correct. Formula (5.6) takes into account two terms of the power expansion in a small parameter. Hence, this asymptotic theory is characterized by a certain accuracy, and this accuracy cannot be improved within the framework of the information used.

Because of the simplicity and high accuracy, the asymptotic theory can be used for evaluation of the cross sections of resonant charge exchange for many elements of the periodic table, that has been considered repeatedly [88–91]. We note that formula (5.6) relates to the case of transition of an s-electron (or s-hole) between structureless cores, when only two quasi-molecular terms partake in the process. If the colliding ion and atom have unfilled electron shells, the charge exchange process proceeds simultaneously with transitions between atomic or ion states, in particular, charge exchange can be accompanied by rotation of electron momenta of colliding atomic particles. Unfortunately, this fact was ignored in some calculations [92–95]. Below we analyze various cases of the resonant charge exchange process.

5.2 Cross section of resonant charge exchange with the transition of s-electron

First we consider the resonant charge exchange process (5.1) when an s-electron makes transition from one atomic core to the other. In this case, from formula (4.7) for the potential of the exchange interaction we obtain for the phase of the charge exchange process, on the assumption of free motion of nuclei $(R^2 = \rho^2 + v^2t^2)$, the following expression

$$\zeta_0(\rho) = \int_{-\infty}^{\infty} \frac{\Delta(R)}{2}\,\mathrm{d}t = \frac{1}{v}\sqrt{\frac{\pi\rho}{2\gamma}}\,\Delta(\rho) = \frac{1}{v}\sqrt{\frac{\pi}{2\gamma}}\,A^2 \exp\left(-\frac{1}{\gamma}\right)\rho^{2/\gamma - 1/2}\exp(-\rho\gamma)\,, \tag{5.7}$$

and the cross section according to formula (5.5) is equal to [12]

$$\sigma_{\mathrm{res}} = \frac{\pi R_0^2}{2}\,, \qquad \text{where} \quad \frac{1}{v}\sqrt{\frac{\pi}{2\gamma}}\,A^2 \exp\left(-\frac{1}{\gamma}\right)R_0^{2/\gamma - 1/2} \times \exp(-R_0\gamma) = 0.28\,. \tag{5.8}$$

In particular, the velocity dependence (5.2) follows from this formula if we assume the basic dependence $\zeta(R_0)$ to be exponential.

In order to ascertain the accuracy of the asymptotic theory, we examine the charge exchange of a proton on a hydrogen atom at a collision energy of 1 eV in the laboratory coordinate system and analyze the various versions of the

asymptotic theory. In this case, formula (5.8) takes the form

$$\sigma_{\text{res}} = \frac{\pi R_0^2}{2}\,, \quad \text{where} \quad \zeta(R_0) = \frac{1}{v}\frac{4}{\text{e}}\sqrt{\frac{\pi}{2}}\,R_0^{3/2}\exp(-R_0) = 0.28\,. \tag{5.9a}$$

One can account for the next term of the expansion of the phase $\zeta(R_0)$ in terms of the small parameter $1/R_0$. Then formula (5.8) assumes the form

$$\sigma_{\text{res}} = \frac{\pi R_0^2}{2}\,, \quad \text{where} \quad \zeta(R_0) = \frac{1}{v}\frac{4}{\text{e}}\sqrt{\frac{\pi}{2}}\,R_0^{3/2}\left(1+\frac{7}{8R_0}\right) \times \exp(-R_0) = 0.28\,. \tag{5.9b}$$

One can evaluate the exchange phase $\zeta(\rho)$ on the basis of the exchange interaction potential $\Delta(R)$, directly using formula (5.5). This gives for the charge exchange cross section:

$$\sigma_{\text{res}} = \frac{\pi R_0^2}{2}\,, \quad \text{where} \quad \zeta(R_0) = \frac{4R_0^2}{v\,\text{e}}\left[K_0(R_0) + \frac{1}{R_0}\,K_1(R_0)\right] = 0.28\,. \tag{5.9c}$$

Finally, one can find the charge exchange cross section directly on the basis of formula (5.5):

$$\sigma_{\text{res}} = \int_0^\infty 2\pi\rho\,\mathrm{d}\rho\,\sin^2\zeta(\rho)\,, \tag{5.9d}$$

where the charge exchange phase is given by formulas (5.9a), (5.9b) and (5.9c). Calculation of the cross section in the hydrogen case at an energy of 1 eV in the laboratory coordinate system gives, on the basis of the above formulas for the values of the charge exchange cross section: 172, 175, and 175, correspondingly, in atomic units, if we use formulas (5.9a), (5.9b) and (5.9c), and also 170, 173, and 174, if we use formula (5.9d) with the above expressions for the phase of charge exchange. The statistical treatment of these data gives 173 ± 2 for the average cross section, i.e. the error in this case, which can be considered as the best accuracy of the asymptotic theory, comes to approximately 1%.

In reality, the accuracy of the asymptotic theory is determined by the small parameter $1/(R_0\gamma)$ and the above accuracy is of the order of $1/(R_0\gamma)^2$. Table 13 lists the values of the parameter $R_0\gamma$ for some cases of resonant charge exchange with the transition of an s-electron at an energy of 1 eV in the laboratory coordinate system. These values confirm that the best accuracy of the asymptotic theory is of the order of 1%.

The asymptotic theory leans upon the asymptotic coefficient A for the radial wave function (3.7) of a transferring electron, and this coefficient can be found by comparison of the calculated wave function and that of formula (3.7) in the range where both wave functions are valid. The accuracy of this operation is better, the more accurate the calculation. The error ΔA in this quantity influences the accuracy of the cross section. From formula (5.8) follows the relative accuracy of the cross section $\Delta\sigma$:

$$\frac{\Delta\sigma_{\text{res}}}{\sigma_{\text{res}}} = \frac{4}{R_0\gamma}\,\frac{\Delta A}{A}\,. \tag{5.10}$$

One can see that this error arises in the first approximation of the power expansion of the charge exchange cross section in a small parameter. In particular, if the error in the asymptotic coefficient is $\Delta A/A = 10\%$, the error in the cross section is 3–4 % for the cases of Table 13, as follows from formula (5.10) and Table 12. In particular, the asymptotic coefficient for the ground-state helium atom is 2.8 ± 0.3, as was found in Section 3.3 on the basis of the hydrogenlike electron wave functions. According to formula (5.10), this corresponds to an accuracy of 4% at a collision energy of 1 eV. Thus, the accuracy of the asymptotic coefficients is of importance for the accuracy of the asymptotic theory in relation to the cross section of resonant charge exchange, and the accuracy of the cross sections of resonant charge exchange with the transition of an s-electron lies in reality between 1% and 5% at small collision energies.

Figures 8 and 9 give the cross sections of resonant charge exchange for collisions of rubidium and cesium atoms with their ions depending on the collision energy, and Fig. 10 depicts the cross sections of the resonant charge exchange process involving negative ions of alkali metal atoms. The cross section is evaluated in these cases on the basis of formula (5.8). Note that the resonant charge exchange process with the transition of an s-electron proceeds not only in the case of valence s-electrons, but in most cases of atoms and ions with unfilled d-electron shells in the ground states. For the ground states of these atoms and ions, the resonant charge exchange process is determined by the transition of an s-electron. Such cases are included in the tables of Figs 11, 12 for the cross sections of resonant charge exchange for the ground atomic and ion states and for most elements of the periodic table.

Table 13. Values of the parameter $R_0\gamma$ for resonant charge exchange accompanied by the transition of an s-electron at an energy of 1 eV in the laboratory coordinate system.

Element	H	He	Li	Be	Na	Mg	K	Ca	Cu
$R_0\gamma$	10.5	10.5	13.6	12.7	14.9	13.8	15.7	14.7	14.3
Element	Zn	Rb	Sr	Ag	Cd	Cs	Ba	Au	Hg
$R_0\gamma$	14.0	16.3	15.4	14.5	14.4	16.8	16.0	14.5	14.5

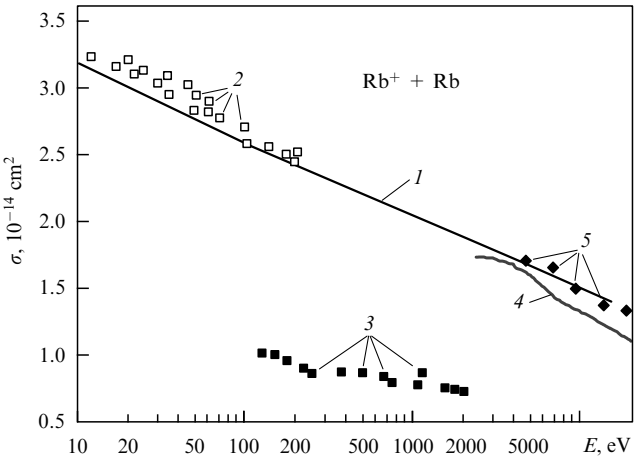

Figure 8. Cross sections of resonant charge exchange for rubidium. Curve *1* corresponds to formula (5.8); *2* —experimental data [99], *3* — [96], *4* — [98], *5* — [97].

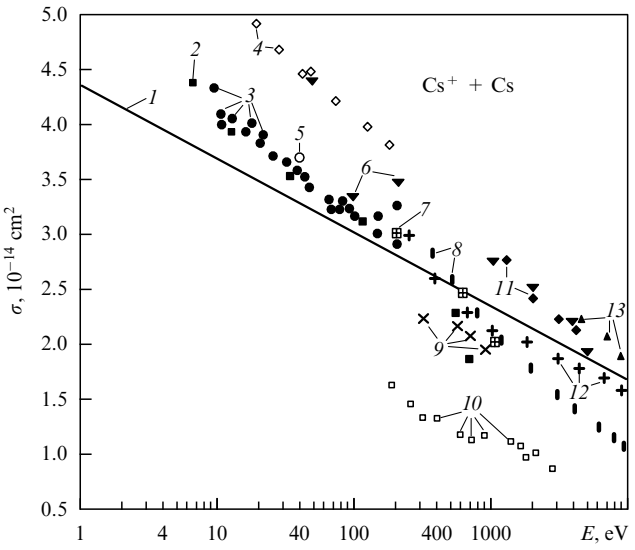

Figure 9. Cross sections of resonant charge exchange for cesium. Curve *1* corresponds to formula (5.8); *2* —experimental data [100], *3* — [99], *4* — [96], *5* — [106], *6* — [104], *7* — [105], *8* — [97], *9* — [98], *10* — [103], *11* — [101], *12* — [127], *13* — [102].

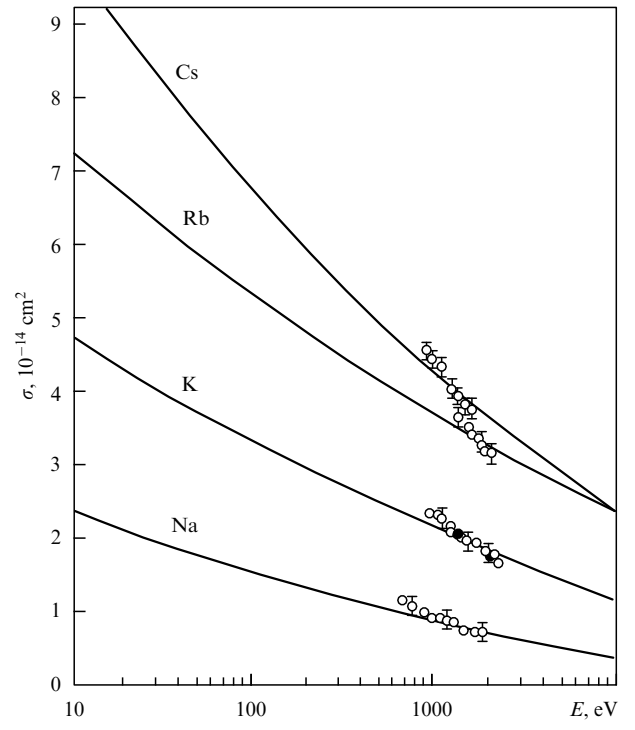

Figure 10. Cross sections of resonant charge exchange for negative ions of alkali metals. The solid curve corresponds to formula (5.8), ○ — experimental data [107].

5.3 Cross section of resonant charge exchange with the transition of p-electron

The asymptotic theory is rather simple for the transition of an s-electron, when the exchange phase $\zeta(\rho)$ is given by formulas (5.5) and (5.7). The cross section of the resonant charge exchange process is determined by formula (5.5), which accounts for two terms in the power expansion in a small parameter of the asymptotic theory. When a valence p-electron makes transition from one atomic core to the other in the course of a collision, the processes of charge exchange and rotation of the electron momentum are entangled. One can partially separate these processes because charge exchange proceeds in a narrow range of internuclear distances, where the molecular axis turns through a small angle of the order of $1/\sqrt{R_0\gamma}$. Indeed, the range of distances between nuclei ΔR, where the phase of charge exchange ζ varies significantly, is $\Delta R \sim 1/\gamma$, and this corresponds to an angle of rotation $\vartheta \sim vt/R \sim 1/\sqrt{R\gamma} \ll 1$. Therefore, one can neglect the depolarization process in the course of the electron transition, but this lowers the accuracy of the asymptotic theory. Below we consider the case of transition of a p-electron in the resonant charge exchange process.

Separating in this way the depolarization of colliding atom and ion from the charge exchange process, we average the cross section over the directions of the molecular axis with respect to the quantization axis. Considering the transition of a p-electron, we introduce an angle θ between the quantization axis for the electron momenta and the molecular axis of the colliding atom and ion, and this quantity varies in the course of a collision because of rotation of the molecular axis. We denote this angle by ϑ at the distance of closest approach of colliding particles, and the average cross section $\bar{\sigma}$ of resonant charge exchange is equal to

$$\bar{\sigma}_{\rm res} = \frac{1}{2}\int_{-1}^{1} \sigma(\vartheta)\, {\rm d}\cos\vartheta\,, \tag{5.11}$$

where $\sigma(\vartheta)$ is the cross section of charge exchange at an angle ϑ between the impact parameter of collision and the quantization axis. Figure 13 shows the geometry of a collision in a center-of-mass coordinate system, when the configuration of colliding particles is close to that at the distance of closest approach. We have the following relation which connects the current angle θ between the molecular and quantization axes and the angle ϑ between these axes at the distance of closest approach:

$$\cos\theta = \cos\vartheta\cos\alpha + \sin\vartheta\sin\alpha\cos\varphi\,, \tag{5.12}$$

where α, φ are the polar angles of the molecular axis, so that $\sin\alpha = vt/R$, where v is the collision velocity, t is time, and R is a distance between colliding particles.

A small parameter of the theory $1/\rho\gamma$ simplifies the determination of the phase and cross section of this process. Formulas (4.22) and (4.24) give the expressions for the exchange interaction potentials of atoms and their ions with unfilled p-shells, neglecting the spin – orbit interaction. These expressions, accounting for the relation (4.11), can be considered as a power expansion of the exchange interaction potentials in a small parameter $1/\rho\gamma$. Then on the basis of formula (5.6) we have for the charge exchange phase in the case of atoms of groups III, V, VI, and VIII of the periodic table of elements:

$$\zeta(\rho,\vartheta,\varphi) = \zeta(\rho,0)\left[\cos^2\vartheta - \frac{1}{\gamma\rho}\cos^2\vartheta + \frac{1}{\gamma\rho}\sin^2\vartheta(2+\cos^2\varphi)\right]. \tag{5.13}$$

This expression relates to large impact parameters of the collision, and $\zeta(\rho,0)$ is the phase of the charge exchange process when a quantization axis has the same direction as the

Periodic table of elements (cross sections of resonant charge exchange)

Period	Group I	Group II	Group III	Group IV	Group V	Group VI	Group VII	Group VIII		
1	1.008 $1s\ ^2S_{1/2}$ $_1$**H** 1.000 6.12 2.00 4.82 Hydrogen 3.65	$1s^2\ ^1S_0$ 4.003 3.4 1.344 2.7 2.87 2.1 $_2$**He** Helium								
2	6.491 $2s\ ^2S_{1/2}$ $_3$**Li** 0.630 26 0.82 22 Lithium 18	9.012 $2s^2\ ^1S_0$ $_4$**Be** 0.828 13 1.6 10 Berillium 8.2	$2p\ ^2P_{1/2}$ 10.81 13 0.781 $_5$**B** 11 0.88 8.5 Boron	$2p^3\ ^3P_0$ 12.011 9.9 0.910 $_6$**C** 8.6 1.3 6.9 Carbon	$2p^3\ ^4S_{3/2}$ 14.007 7.6 1.034 $_7$**N** 6.2 1.5 5.0 Nitrogen	$2p^4\ ^3P_2$ 15.999 8.1 1.000 $_8$**O** 6.6 1.3 5.3 Oxygen	$2p^5\ ^2P_{3/2}$ 18.998 6.0 1.132 $_9$**F** 4.9 1.6 4.0 Fluorine	$2p^6\ ^1S_0$ 20.179 4.1 1.259 $_{10}$**Ne** 3.3 1.8 2.6 Neon		
3	22.990 $3s\ ^2S_{1/2}$ $_{11}$**Na** 0.615 31 0.74 26 Sodium 21	24.305 $3s^2\ ^1S_0$ $_{12}$**Mg** 0.750 18 1.3 15 Magnesium 12	$3p\ ^2P_{1/2}$ 26.982 22 0.663 $_{13}$**Al** 19 0.61 15 Aluminium	$3p^2\ ^3P_0$ 28.086 18 0.774 $_{14}$**Si** 15 1.1 12 Silicon	$3p^3\ ^4S_{3/2}$ 30.974 13 0.878 $_{15}$**P** 11 1.6 9.2 Phosphorus	$3p^4\ ^3P_2$ 32.06 12 0.873 $_{16}$**S** 10 1.1 8.4 Sulfur	$3p^5\ ^2P_{3/2}$ 35.453 10 0.976 $_{17}$**Cl** 8.4 1.8 6.9 Chlorine	$2p^6\ ^1S_0$ 39.948 7.0 1.076 $_{18}$**Ar** 5.8 2.0 4.7 Argon		
4	39.098 $4s\ ^2S_{1/2}$ $_{19}$**K** 0.565 40 0.52 34 Potassium 28	40.08 $4s^2\ ^1S_0$ $_{20}$**Ca** 0.670 25 0.95 21 Calsium 17	44.956 $3d4s^2\ ^2D_{3/2}$ $_{21}$**Sc** 0.693 24 1.1 20 Scandium 16	47.88 $3d^24s^2\ ^3F_2$ $_{22}$**Ti** 0.708 22 1.2 19 Titanium 15	50.942 $3d^34s^2\ ^4F_{3/2}$ $_{23}$**V** 0.704 23 1.2 19 Vanadium 16	51.996 $3d^54s\ ^7S_{5/2}$ $_{24}$**Cr** 0.705 22 1.1 19 Chromium 15	54.938 $3d^54s^2\ ^6S_{5/2}$ $_{25}$**Mn** 0.739 20 1.3 17 Manganese 14	55.847 $3d^64s^2\ ^5D_4$ $_{26}$**Fe** 0.762 18 1.4 15 Iron 13	58.933 $3d^74s^2\ ^4F_{9/2}$ $_{27}$**Co** 0.760 19 1.4 16 Cobalt 13	58.69 $3d^84s^2\ ^3F_4$ $_{28}$**Ni** 0.749 20 1.4 17 Nickel 14
	$3d^{10}4s\ ^2S_{1/2}$ 63.546 19 0.754 $_{29}$**Cu** 16 1.3 13 Copper	$4s^2\ ^1S_0$ 65.38 15 0.831 $_{30}$**Zn** 12 1.7 10 Zinc	$4p\ ^2P_{1/2}$ 69.72 24 0.664 $_{31}$**Ga** 20 0.60 16 Gallium	$4p^2\ ^3P_0$ 72.59 21 0.762 $_{32}$**Ge** 18 1.3 15 Germanium	$4p^3\ ^4S_{3/2}$ 74.922 16 0.850 $_{33}$**As** 13 1.6 11 Arsenic	$4p^4\ ^3P_2$ 78.96 16 0.847 $_{34}$**Se** 13 1.5 11 Selenium	$4p^5\ ^2P_{3/2}$ 79.904 12 0.932 $_{35}$**Br** 10 1.8 8.2 Bromine	$4p^6\ ^1S_0$ 83.80 9.0 1.014 $_{36}$**Kr** 7.5 2.1 6.2 Krypton		
5	85.468 $5s\ ^2S_{1/2}$ $_{37}$**Rb** 0.554 45 0.48 38 Rubidium 32	87.62 $5s^2\ ^1S_0$ $_{38}$**Sr** 0.647 29 0.86 25 Strontium 20	88.906 $4d5s^2\ ^2D_{3/2}$ $_{39}$**Y** 0.682 25 1.0 21 Yttium 18	91.22 $4d^25s^2\ ^3F_2$ $_{40}$**Zr** 0.709 23 1.2 20 Zirconium 16	92.906 $4d^45s\ ^6D_{1/2}$ $_{41}$**Nb** 0.711 23 1.2 20 Niobium 16	95.94 $4d^55s\ ^7S_3$ $_{42}$**Mo** 0.722 22 1.2 19 Molibdenum 15	[98] $4d^55s^2\ ^6S_{5/2}$ $_{43}$**Tc** 0.731 22 1.3 18 Technetium 15	101.07 $4d^75s\ ^5F_5$ $_{44}$**Ru** 0.736 21 1.2 17 Ruthenium 14	102.91 $4d^85s\ ^4F_{9/2}$ $_{45}$**Rh** 0.741 21 1.2 17 Rhodium 14	106.42 $4d^{10}\ ^1S_0$ $_{46}$**Pd** 0.783 18 2.1 16 Palladium 13
	$4d^{10}5s\ ^2S_{1/2}$ 107.87 20 0.746 $_{47}$**Ag** 17 1.2 14 Silver	$5s^2\ ^1S_0$ 112.41 16 0.813 $_{48}$**Cd** 14 1.6 11 Cadmium	$5p\ ^2P_{1/2}$ 114.82 26 0.652 $_{49}$**In** 22 0.58 18 Indium	$5p^2\ ^3P_0$ 118.69 23 0.735 $_{50}$**Sn** 19 1.0 16 Tin	$5p^3\ ^4S_{3/2}$ 121.75 20 0.797 $_{51}$**Sb** 17 1.7 14 Antimony	$5p^4\ ^3P_2$ 127.60 19 0.814 $_{52}$**Te** 16 1.6 13 Tellurium	$5p^5\ ^2P_{3/2}$ 126.90 16 0.876 $_{53}$**I** 13 1.9 11 Iodine	$5p^6\ ^1S_0$ 131.29 12 0.944 $_{54}$**Xe** 10 2.2 8.2 Xenon		
6	132.90 $6s\ ^2S_{1/2}$ $_{55}$**Cs** 0.535 51 0.41 44 Cesium 36	137.33 $6s^2\ ^1S_0$ $_{56}$**Ba** 0.619 35 0.78 29 Barium 25	138.90 $5d6s^2\ ^2D_{3/2}$ $_{57}$**La** 0.640 32 0.90 27 Lanthanum 23	178.49 $5d^26s^2\ ^3F_2$ $_{72}$**Hf** 0.740 22 1.3 18 Hafnium 15	180.95 $5d^36s^2\ ^4F_{3/2}$ $_{73}$**Ta** 0.762 20 1.4 17 Tantalum 14	183.85 $5d^46s^2\ ^5D_0$ $_{74}$**W** 0.766 20 1.4 17 Tungsten 14	186.21 $5d^56s^2\ ^6D_{5/2}$ $_{75}$**Re** 0.761 20 1.4 17 Rhenium 14	190.2 $5d^66s^2\ ^5D_4$ $_{76}$**Os** 0.801 18 1.7 15 Osmium 13	192.22 $5d^76s^2\ ^4F_{9/2}$ $_{77}$**Ir** 0.816 17 1.7 14 Iridium 12	195.08 $5d^96s^3\ ^3D_3$ $_{78}$**Pt** 0.812 17 1.5 14 Platinum 12
	$5d^{10}6s\ ^2S_{1/2}$ 196.97 16 0.823 $_{79}$**Au** 14 1.6 11 Gold	$5d^{10}6s^2\ ^1S_0$ 200.59 14 0.876 $_{80}$**Hg** 12 1.9 10 Mercury	$6p\ ^2P_{1/2}$ 204.38 24 0.670 $_{81}$**Tl** 21 0.55 17 Thallium	$6p^2\ ^3P_0$ 207.2 24 0.738 $_{82}$**Pb** 20 1.1 17 Lead	$6p^3\ ^4S_{3/2}$ 208.98 26 0.732 $_{83}$**Bi** 22 1.4 19 Bismuth	$6p^4\ ^3P_2$ [209] 21 0.788 $_{84}$**Po** 18 1.5 15 Polonium	$6p^5\ ^2P_{3/2}$ [210] 20 0.813 $_{85}$**At** 17 1.9 15 Astatine	$6p^6\ ^1S_0$ [222] 15 0.889 $_{86}$**Rn** 12 2.3 10 Radon		
z 7	[223] $7s\ ^2S_{1/2}$ $_{87}$**Fr** 0.542 53 0.49 45 Francium 38	226.02 $7s^2\ ^1S_0$ $_{88}$**Ra** 0.623 35 0.78 30 Radium 25	227.03 $6d7s^2\ ^2D_{3/2}$ $_{89}$**Ac** 0.636 32 0.70 27 Actinium 22							

Actinides

$6d^27s^2\ ^3F_2$ 232.04 0.675 28 $_{90}$**Th** 0.94 24 Thorium 20	$5f^26d7s^2\ ^4K_{11/2}$ 231.04 0.647 30 $_{91}$**Pa** 0.70 25 Protactinium 21	$5f^36d7s^2\ ^5L_6$ 238.03 0.670 28 $_{92}$**U** 0.89 24 Uranium 20	$5f^46d7s^2\ ^6L_{11/2}$ 237.05 0.580 46 $_{93}$**Np** 0.70 39 Neptunium 33	$5f^67s^2\ ^7F_0$ [244] 0.612 38 $_{94}$**Pu** 0.73 32 Plutonium 27	$5f^77s^2\ ^8S_{7/2}$ [243] 0.569 49 $_{95}$**Am** 0.70 42 Americium 36

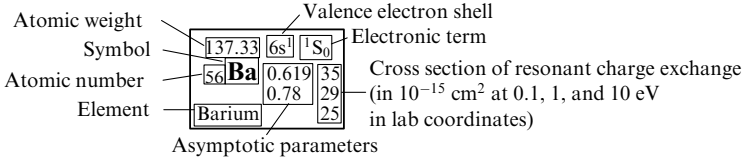

Figure 11. Cross sections of resonant charge exchange for basic elements of the periodic table.

Lanthanides

$4f5d\ 6s^2\ {}^1G_4$			$4f^36s^2\ {}^4I_{9/2}$			$4f^46s^2\ {}^5I_4$			$4f^56s^2\ {}^6H_{5/2}$			$4f^66s^2\ {}^7F_0$			$4f^76s^2\ {}^8S_{7/2}$			$4f^75d\ 6s^2\ {}^9D_2$		
140.12	0.638	32	140.91	0.634	32	144.24	0.637	32	[145]	0.640	32	150.36	0.644	31	151.96	0.646	31	157.25	0.672	28
$_{58}$**Ce**	0.88	27	$_{59}$**Pr**	0.84	28	$_{60}$**Nd**	0.85	27	$_{61}$**Pm**	0.86	27	$_{62}$**Sm**	0.88	26	$_{63}$**Eu**	0.89	26	$_{64}$**Gd**	1.0	24
Cerium		23	Praseodymium		23	Neodymium		23	Promethium		22	Samarium		22	Europium		22	Gadolinium		20

$4f^96s^2\ {}^6H_{15/2}$			$4f^{10}6s^2\ {}^5I_8$			$4f^{11}6s^2\ {}^5I_{15/2}$			$4f^{12}6s^2\ {}^3H_6$			$4f^{13}6s^2\ {}^2F_{7/2}$			$4f^{14}6s^2\ {}^1S_0$			$4f^{14}5d\ 6s^2\ {}^2D_{3/2}$		
158.92	0.657	30	162.50	0.661	29	164.93	0.665	29	167.26	0.670	28	168.93	0.674	28	173.04	0.678	27	174.97	0.632	34
$_{65}$**Tb**	0.93	25	$_{66}$**Dy**	0.94	25	$_{67}$**Ho**	0.96	24	$_{68}$**Er**	0.98	24	$_{69}$**Tm**	0.99	23	$_{70}$**Yb**	1.0	23	$_{71}$**Lu**	0.92	29
Terbium		21	Dysprosium		20	Holmium		20	Erbium		20	Thulium		19	Ytterbium		19	Lutetium		24

Figure 12. Cross sections of resonant charge exchange for lanthanides.

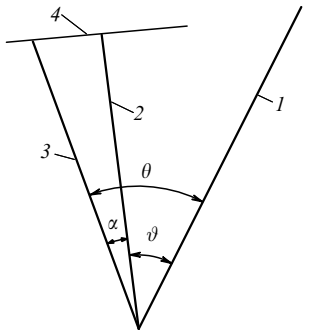

Figure 13. Geometry of the nuclear trajectory in the centre-of-mass coordinate system. *1* — quantization axis, *2* — molecular axis at the distance of closest approach, *3* — current molecular axis, *4* — trajectory of nuclear motion. θ, ϑ are the angles between the quantization and molecular axes, current and at the distance of closest approach, α, φ are the polar angles of the current molecular axis with respect to that for the distance of closest approach.

molecular axis at the distance of closest approach. The quantity $\zeta(\rho,0)$ can be expressed through the charge exchange phase ζ_0 which is given by formula (5.7) and relates to the transition of an s-electron with the same asymptotic parameters γ, A. This connection for the resonant charge exchange process involving atoms of groups III and VIII of the periodic table of elements has the form

$$\zeta(\rho,0)=3\zeta_0(\rho)\,, \tag{5.14a}$$

and for atoms of groups V and VI this connection becomes

$$\zeta(\rho,0)=7\zeta_0(\rho)\,. \tag{5.14b}$$

Note that our analysis relates to the ground state of the colliding atom and ion.

In the case of atoms of groups IV and VII of the periodic table of elements, the expression for the charge exchange phase at large collision impact parameters takes the form

$$\begin{aligned}\zeta(\rho,\vartheta,\varphi)=5\zeta_0(\rho)\Big\{&\sin^2\vartheta_1\sin^2\vartheta_2+\frac{1}{\gamma\rho}\big[2\cos^2\vartheta_1\\&+2\cos^2\vartheta_2+\sin^2\vartheta_1\cos^2\vartheta_2+\cos^2\vartheta_1\sin^2\vartheta_2\\&-\sin^2\vartheta_1\sin^2\vartheta_2(\cos^2\varphi_1+\cos^2\varphi_2)\\&+\sin 2\vartheta_1\sin 2\vartheta_2\cos\varphi_1\cos\varphi_2\big]\Big\}\,,\end{aligned} \tag{5.15}$$

where ϑ_1, φ_1 and ϑ_2, φ_2 are the polar angles of the quantization axes of the atom and ion, correspondingly, with respect to the molecular axis at the distance of closest approach.

We can use formula (5.6) for the resonant charge exchange cross section at $\vartheta=0$ and take into account that the angular dependence of the cross section is logarithmic, according to formula (5.2), so that the average cross section of this process is close to that at zero angle. Hence, the average cross section can be determined as an expansion over the small parameter of the theory. Indeed, taking the basic dependence of the exchange phase $\zeta(\rho,\vartheta,\varphi)$ on the collision impact parameter ρ to be exponential $\zeta(\rho,\vartheta)\sim\exp(-\gamma\rho)$, we have in the case of atoms of groups III, V, VI, VIII of the periodic table of elements:

$$R_0(\vartheta,\varphi)=R_0(0)+\frac{1}{\gamma}\ln\frac{\zeta(\rho,\vartheta,\varphi)}{\zeta(\rho,0)}\,. \tag{5.16}$$

We account for the atom and ion in the ground states, including the S-state, so that the angles ϑ, φ characterize the quantization axis direction for an atomic particle with a nonzero momentum. This gives for the average cross section of resonant charge exchange according to formula (5.11):

$$\bar\sigma_{\rm res}=\frac{1}{4}\int_0^1\int_0^{2\pi}\left[R_0(0)+\frac{1}{\gamma}\ln\frac{\zeta(R_0,\vartheta,\varphi)}{\zeta(R_0,0)}\right]^2\mathrm{d}\cos\vartheta\,\mathrm{d}\varphi\,. \tag{5.17}$$

In essence, formula (5.17) means that the dependence of the exchange phase ζ on the collision impact parameter ρ has the form $\zeta\sim\exp(-\gamma\rho)$. This formula is the basis for determination of the average cross section of the resonant charge exchange, when this process results from the transition of a p-electron. This formula is valid for elements of groups III, V, VI, VIII of the periodic table when the atoms and ions are in the ground states, and one of these states is the S-state, so that the phase of the charge exchange depends on two angles ϑ, φ. In the same manner one can find the charge exchange phase for elements of groups IV and VII, which depends now on 4 angles: ϑ_1, φ_1, ϑ_2, φ_2. The data for the cross sections of resonant charge exchange for these cases are compiled in the table of Fig. 11.

Let us compare the cross sections of resonant charge exchange for transitions of s and p valence electrons if these electrons are characterized by the same asymptotic parameters γ and A. Supposing the dependence of the charge exchange phase $\zeta(\rho,\vartheta,\varphi)$ on the collision impact parameter ρ to be exponential $\zeta(\rho,\vartheta,\varphi)\sim\exp(-\gamma\rho)$ and neglecting the momentum rotation during the electron transition, we obtain for the average cross section $\bar\sigma_{\rm res}$ of the resonant charge exchange process:

$$\bar\sigma_{\rm res}=\sigma_0\int_0^1\mathrm{d}\cos\vartheta\int_0^{2\pi}\frac{\mathrm{d}\varphi}{2\pi}\left[1+\frac{1}{\gamma R_0}\ln\frac{\zeta(\rho,\vartheta,\varphi)}{\zeta_0(\rho)}\right]^2.$$

Here, σ_0 is the cross section for resonant charge exchange for an s-electron making transition with the same asymptotic parameters, and $\zeta_0(\rho)$ is the charge exchange phase for an s-electron, which is given by formula (5.7). Table 12 contains the ratios of the cross sections for elements of groups III and VIII of the periodic table depending on a small parameter of the asymptotic theory. The use of additional assumptions for evaluating the charge exchange cross sections with a transition of a p-electron decreases the accuracy of the asymptotic theory in this case.

Note that the above considerations relate to the ground states of colliding atom and ion. In the case of excited atoms and ions with valence p-electrons, the cross section may be significantly different for various states. For example, in the case of the process

$$O^+(^4S) + O \to O + O^+(^4S),$$

where the ion is found in the ground state, the cross section is zero for excited atomic ^2D and ^2S states of this p^3-valent shell. Because the statistical weight of the atom in the ground state is $3/5$ with respect to the total number of atomic states for this electron shell, the cross section of the process under consideration significantly depends on the method of initial preparation of atoms and ions.

5.4 Resonant charge exchange in case 'c' of Hund coupling scheme

The above analysis corresponds to the criterion (4.28) on neglecting the relativistic effects. In reality, depending on the hierarchy of interaction potentials and characteristic energies in a system, we have a certain character of description of interactions and processes. In the case of an atom, we considered two types of interactions: V_{ex}, the exchange interaction potential involving identical valence electrons, and Δ_f, the fine-structure splitting of energy levels due to spin–orbit interaction for each valence electron. Different relations between these interaction potentials lead to the *LS*- or *jj*-coupling schemes in the atomic case. For a molecule, a system of two interacting atomic particles, the rotational energy V_r is added to these interaction potentials, and we have six different cases of Hund coupling scheme for this system, depending on the relation between these potentials, which are given in Table 10. In the case of the collision of two atomic particles, the number of the limiting cases increases due to the new energy parameters $1/\tau$ and $\Delta\varepsilon$, where τ is a typical collision time, and $\Delta\varepsilon$ is the transition energy. In this case the analysis of the limiting cases between the interaction potentials becomes more complex. Nikitin [9] introduced the hierarchy of typical energy parameters in the analysis of collisional processes [9–11, 108]. Below we apply to this analysis for the resonant charge exchange process.

Thus, we have the following typical interaction potentials and energies for the process of interest:

$$V_{ex}, \Delta_f, V_r, \frac{1}{\tau}, U(R), \Delta(R), E. \tag{5.18}$$

Here, along with the above parameters, we included in this list the long-range interaction potential of colliding atomic particles $U(R)$, the ion–atom exchange interaction potential $\Delta(R)$, and the collision energy E. We consider slow collisions when $\Delta(R_0) \sim 1/\tau$ is small compared to a typical atomic energy ~ 1, so that inelastic transitions involving the valence electron shells of the atom and ion are absent. This criterion takes the form

$$\tau \sim \frac{1}{v}\sqrt{\frac{R_0}{\gamma}} \gg 1, \quad \text{or} \quad E \ll m\frac{R_0}{\gamma}, \tag{5.19}$$

where v is the collision velocity, $R_0 \sim \sqrt{\sigma_{res}}$, σ_{res} is the resonant transfer cross section, and m is the mass of colliding particles. The other criterion

$$mR_0 v \gg 1 \tag{5.20}$$

allows us to use the classical law of nuclear motion. In addition to this, the rotational energy is

$$V_r \sim \frac{d\theta}{dt} \sim \frac{v}{R_0} \sim \frac{1}{\tau\sqrt{R_0\gamma}} \sim \frac{\Delta}{\sqrt{R_0\gamma}} \ll \Delta. \tag{5.21}$$

The above consideration corresponds to the conditions

$$V_{ex} \gg U(R_0) \gg \Delta(R_0) \gg V_r \quad \text{and} \quad \Delta_f \ll V_{ex}, U(R_0). \tag{5.22}$$

Under these conditions one can neglect the spin–orbit interaction, and the orbital momentum projections of an atom and ion are the quantum numbers. This corresponds to case 'a' of Hund coupling scheme. Within the framework of this coupling mechanism, one can change the ratio between V_{ex} and Δ. In particular, in the case $\Delta \gg V_{ex}$ or $V_{ex}\tau \ll 1$ the states of the initial electron and ion shells are mixed in collisions. This requires attraction of another model of the electronic states of atoms and ions, like that of Fig. 1, i.e. in this case we observe the other quantum numbers of the states, which correspond to a lower symmetry of atomic particles, but the character of the charge exchange process is identical in these cases.

Now we consider the resonant charge exchange process within the framework of case 'c' of Hund coupling scheme, when

$$\Delta_f \gg V_{ex} \gg V_r \tag{5.23}$$

according to the data of Table 10. This criterion leads to the *jj*-coupling scheme in the atom and ion that in turn corresponds to a transition of one electron with a given total momentum j in the process of resonant charge exchange. Below we analyze the character of resonant charge transfer for atoms and ions with valence p-electrons. In case 'c' of Hund coupling scheme with the transition of a p-electron or p-hole between two filled atomic cores, we have only one electronic term, if the electron momentum is $1/2$. The exchange interaction potential for this fine-structured state of the atom or ion is given by formula (4.30), thus leading to the following charge exchange phase

$$\zeta_{1/2}(\rho, \vartheta) = \zeta_0(\rho)\left(1 + \frac{4}{\rho\gamma}\right), \tag{5.24}$$

where $\zeta_0(\rho)$ is the charge exchange phase defined according to formula (5.7), so that $3\zeta_0(\rho)$ is the charge exchange phase for zero projection of the electron momentum onto the impact parameter of collision in case 'a' of Hund coupling scheme. In the case when the total electron momentum is $3/2$, the exchange phase within the framework of case 'c' of Hund

coupling scheme follows from formulas (4.31):

$$\zeta_{3/2}(\rho,\vartheta)=\zeta_0(\rho)\left[\frac{1}{2}+\frac{3}{2}\cos^2\vartheta+\frac{1}{\rho\gamma}\left(\frac{1}{2}+\frac{9}{2}\sin^2\vartheta+\frac{3}{2}\sin^2\vartheta\cos^2\varphi\right)\right], \quad (5.25)$$

where ϑ, φ are the polar angles of the collision impact parameter or the molecular axis at the distance of closest approach with respect to the quantization axis.

In order to understand the sensitivity of the cross section of the charge exchange process to different schemes of coupling of electron momenta, in Table 14 we give the corresponding cross sections of this process for rare gases, i.e. $\bar{\sigma}$ is the average cross section for case 'a' of Hund coupling scheme, $\sigma(\vartheta=0)$ is the cross section of this process when the projection of the orbital momentum of the hole on the impact parameter direction is zero, and $\sigma_{1/2}$ and $\sigma_{3/2}$ are the charge exchange cross sections for the total ion momenta $1/2$ and $3/2$, correspondingly. We take the atomic ionization potential for the formation of an ion in different fine-structured states to be identical, so that the difference in the cross sections under consideration is solely determined by the process dynamics. According to the data of Table 14, the difference in the average cross sections for different coupling schemes is small and is lower than the accuracy of these evaluations which is determined by the accuracy of asymptotic coefficients of the wave function of an atomic valence electron. Hence, in spite of the significant dependence of the cross section of resonant charge exchange on the direction of the orbital momentum, the average cross section of this process is not sensitive to the scheme of coupling of electron momenta if the process is allowed in the one-electron approach. Hence, the cross sections averaged over initial states weakly depend on the coupling scheme for atoms of groups III and VIII. The difference between the cross sections of this process can be dramatic for certain initial atomic and ion states because of the different selection rules for one-electron transitions within the framework of these coupling schemes. Some calculated results of the cross sections for resonant charge transfer are given in the tables of Figs 11, 12 which are based on case 'a' of Hund coupling scheme.

Table 14. Resonant charge exchange cross sections for rare gases at an ion energy 1 eV.

Element	Ne	Ar	Kr	Xe	Rn
$\bar{\sigma}_{\rm res}/\sigma_{\rm res}(\vartheta=0)$	0.85	0.86	0.888	0.87	0.87
$\sigma_{1/2}/\bar{\sigma}_{\rm res}$	1.02	1.02	1.02	1.02	1.02
$\sigma_{1/2}/\sigma_{3/2}$	0.995	0.995	0.995	0.995	0.995
$\bar{\sigma}_{\rm res}$, 10^{-15} cm^2	3.3	5.8	7.5	10	12

Let us consider the charge exchange process of rare gas atoms and ions if the ions are found in the ground state ($j=3/2$) at the beginning. Then at small collision velocities only the ion ground state partakes in the process, and the transition into the ion state $j=1/2$ is forbidden. At high collision velocities this channel is opened, and the resonant charge exchange process corresponds to case 'a' of Hund coupling scheme. Let us assume that these coupling schemes leads to an identical cross section, so that the variation of the cross section in the course of transition between cases 'c' and 'a' of Hund coupling scheme is due to the different atomic ionization potentials corresponding to various fine-structured ion states. The jump in the cross section due to this effect is

$$\Delta\bar{\sigma}_{\rm res}=\frac{1}{3}\,\frac{\Delta I}{I}\,\bar{\sigma}_{\rm res}\,, \quad (5.26)$$

where the first factor is the probability of the ion state $j=1/2$, and the second factor accounts for the dependence (5.2) of the cross section on the electron binding energy. According to this formula, the relative variation of the cross section is about 0.4% for Ar, about 2% for Kr and about 4% for Xe. First this effect was examined experimentally in Ref. [109]. A collision velocity v for this transition can be estimated from the expression for a typical time of the process:

$$\tau\sim\frac{1}{v}\sqrt{\frac{R_0}{\gamma}}\sim\Delta_f\,,$$

as follows from formula (5.7), and a typical collision energy for this transition is estimated as ~ 10 eV for Ar, ~ 100 eV for Kr, and ~ 600 eV for Xe. Figures 14–16 depict the cross sections of resonant charge exchange as a function of the collision energy for Ne, Kr, and Xe.

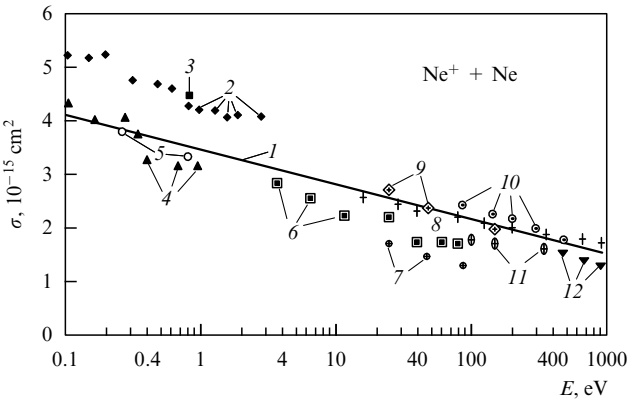

Figure 14. Cross sections of resonant charge exchange for neon. *1* — formulas (5.13), (5.17); experiment: *2* — [123], *3* — [111], *4* — [118], *5* — [119], *6* — [114], *7* — [117], *8* — [110], *9* — [115], *10* — [112], *11* — [113], *12* — [120].

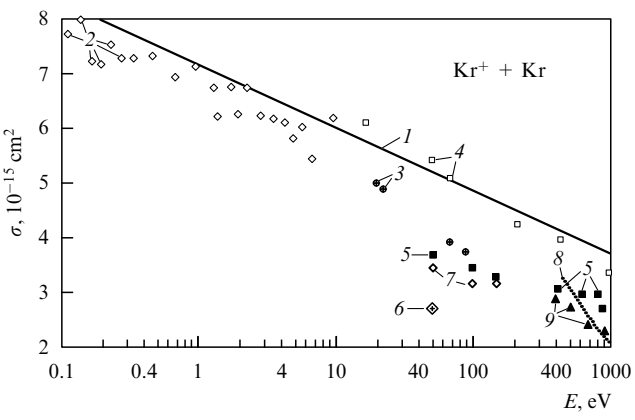

Figure 15. Cross sections of resonant charge exchange for krypton. *1* — formulas (5.13), (5.17); experiment: *2* — [116], *3* — [117], *4* — [100], *5* — [115], *6* — [122], *7* — [113], *8* — [120], *9* — [121].

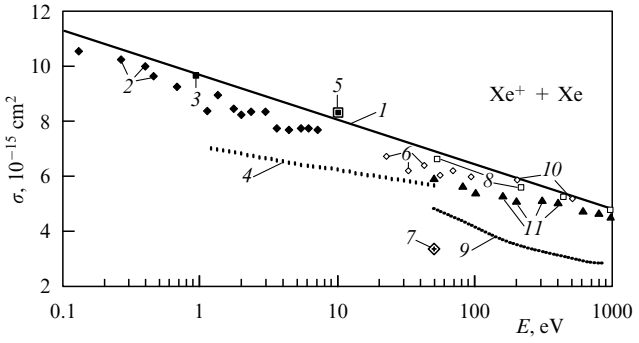

Figure 16. Cross sections of resonant charge exchange for xenon. *1* — formulas (5.13), (5.17); experiment: *2* — [123], *3* — [111], *4* — [126], *5* — [100], *6* — [117], *7* — [122], *8* — [124], *9* — [112], *10* — [125], *11* — [113].

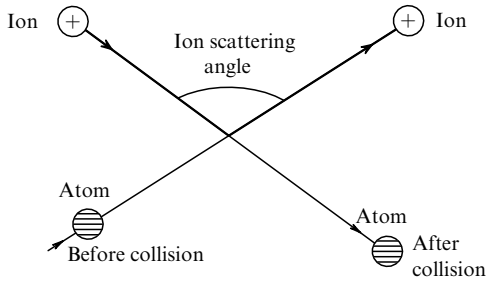

Figure 17. Sena effect for the scattering of an ion by an atom as a result of charge exchange in the absence of elastic scattering.

5.5 Experimental aspects of resonant charge exchange

When we constructed the table of the cross sections of the resonant exchange process for various elements of the periodic table (Figs 11 and 12), we applied to the theoretical data only for the following reasons. First, the accuracy of the asymptotic theory is better than the experimental results (excluding the case of helium). Second, the experimental data are restricted to certain elements, and the collision energies for some elements are limited. Third, in many cases we cannot determine the accuracy of the experimental data. Hence, the experimental studies give a restricted contribution to the data on resonant charge transfer, and below we consider them rather briefly.

The experimental methods of measuring the resonant charge exchange cross sections lean upon the fact that the cross section of this process significantly exceeds the cross section of ion–atom elastic scattering at the collision energies under consideration. Then the simple version of the experiment is based on the passage of an ion beam through a gas or vapor of parent atoms in a collisional chamber or drift tube, where the mean free path of ions with respect to the process is large or comparable with the paths of ions in a gas or vapor. Then the resonant charge exchange cross section is determined from a decrease in the ion beam intensity after passage through a gas. The above measurements of the cross sections of resonant charge transfer for rare gases (Figs 14–16) are based on this technique.

In some cases it is problematic to create an atomic vapor of a given element. Then atoms are taken in the form of a beam, and charge exchange event results from intersection of the ion and atomic beams, or when the ion beam overtakes the atomic beam. In particular, crossing beam methods are used for measurement of the cross section of resonant charge exchange of a proton or deuteron in collisions with the hydrogen atom [104, 128, 129], and in some experiments for rubidium and cesium (see Figs 8, 9). This can also be achieved by using merging beams [130, 131].

The resonant charge exchange process governs the mobility of ions in the parent gas. Because at not low temperatures elastic ion–atom scattering gives a small contribution to the ion mobility in the parent gas, the charge transfer is determined by the resonant charge exchange process according to the Sena effect, as is shown in Fig. 17. The mobility of ions in a gas at small electric field strengths in the first Chapman–Enskog approximation [132, 133] is expressed through the diffusion cross section of ion–atom scattering:

$$\sigma^* = \int (1 - \cos\theta)\, \mathrm{d}\sigma\,, \tag{5.27}$$

where θ is the scattering angle in the center-of-mass coordinate system. If we neglect the elastic cross section, the scattering angle of the ion due to the resonant charge transfer process in the center-of-mass coordinate system is equal to $\theta = \pi$, so that we have [134]

$$\sigma^* = 2\sigma_{\mathrm{res}}\,,$$

where σ_{res} is the cross section of resonant charge exchange. According to formula (5.2), this cross section weakly depends on the collision velocity and that leads in the first Chapman–Enskog approximation to the following expression for the ion mobility in the parent gas at low electric field strengths [135]:

$$K = \frac{3\sqrt{\pi}\, e}{16N\sqrt{Tm}\,\sigma_{\mathrm{res}}(2.2v_T)}\,. \tag{5.28}$$

Here, N is the number density of atoms in the gas, T is the gas temperature expressed in energy units, m is the ion or atom mass, e is the electron charge, and the argument in the cross section of resonant charge exchange shows the velocity at which this cross section is taken, so that $v_T = \sqrt{2T/m}$. Here we use the conventional units.

The second term of the power expansion in a numerical parameter of the Chapman–Enskog approximation gives a correction of 2% to the ion mobility and to the diffusion coefficient of the ion in a gas, if the cross section does not depend on the collision velocity [132, 133]. Taking this into account, for the ion mobility in the parent gas in the limiting case of low electric field strengths [136, 137] we arrive at

$$K = \frac{0.341e}{N\sqrt{Tm}\,\sigma_{\mathrm{res}}(2.1v_T)}\,. \tag{5.29}$$

Correspondingly, the ion drift velocity w and its diffusion coefficient D in the gas in this case assume the form

$$w = KE\,, \qquad D = \frac{eK}{T}\,,$$

where E is the electric field strength.

Usually the mobility is reduced to the number density of gas atoms under normal conditions [138, 139], i.e. $N = 2.69 \times 10^{19}$ cm^{-3}. Hence, it is convenient to rewrite

formula (5.29) in the form

$$K = \frac{1340}{\sqrt{Tm}\,\sigma_{\rm res}(2.1v_T)}\,, \tag{5.30}$$

where the mobility is expressed in $\mathrm{cm}^2\ (\mathrm{V\ s})^{-1}$, the temperature T is given in Kelvin, the mass m of atoms and ions is expressed in atomic mass units, and the resonant charge exchange cross section is given in $10^{-15}\ \mathrm{cm}^2$.

Above we neglected the elastic scattering of the colliding ion and atom in the course of the resonant charge exchange process. At large distances R between the colliding ion and atom, the polarization interaction acts between them, and the cross section of ion – atom elastic scattering varies with the collision velocity v as $\sim 1/v$. The resonant charge exchange cross section weakly depends on the collision velocity. Therefore, elastic scattering can influence the charge transfer during ion – atom collisions at small velocities, and this effect has to be taken into account for the ion mobility at low temperatures. The size of this effect can be understood from Table 15 where a decrease ΔK of the ion mobility in the parent gas is given due to elastic ion – atom scattering, which is determined by the polarization interaction. This effect is taken into account in Fig. 18, where the mobility of atomic helium ions in helium in the limit of low electric field strengths, which is evaluated on the basis of formula (5.30), is compared with available experimental data [140 – 144].

Table 15. Relative decrease of the ion mobility $\Delta K/K$ in the parent gases at room temperature due to elastic ion – atom scattering [137].

Ion, gas	He	Ne	Na	Ar	K	Kr	Rb	Xe	Cs
$\Delta K/K$, %	6	9	8	9	9	18	9	21	7

The drift velocity of atomic ions in the parent gases is given by formula (5.30) in the limit of low electric field strengths, when the drift velocity is small in comparison with the thermal velocity of the atomic ion, so that

$$eE\lambda \ll T\,, \tag{5.31}$$

where $\lambda = 1/(N\sigma_{\rm res})$ is the mean free path of ions in the parent gas. Let us consider the other limit of high electric field strengths and, following Refs [85, 86], we find the ion drift velocity under the assumption that the charge exchange cross section $\sigma_{\rm res}$ does not depend on the collision velocity. According to Fig. 17, ions are accelerated in the direction of the electric field, and the velocity in the field direction is large in comparison with that in transverse directions. We introduce the distribution function $f(v_x)$ of ions over velocities v_x in the field direction, which is analogous to the probability $P(t)$ of absence of charge exchange during a time t after the previous exchange event. This probability satisfies the equation

$$\frac{{\rm d}P}{{\rm d}t} = -\nu P\,,$$

where $\nu = Nv_x\sigma_{\rm res}$ is the rate of the resonant charge exchange process. The solution of this equation is

$$P(t) = \exp\left(-\int_0^t \nu\ {\rm d}t'\right).$$

The equation of motion for the ion, viz.

$$m\,\frac{{\rm d}v_x}{{\rm d}t} = eE\,,$$

connects the ion velocity and the time after the last charge exchange event by the expression

$$v_x = \frac{eEt}{m}\,,$$

so that $P(t)$ gives the velocity distribution function for the ions. Assuming the cross section of the resonant charge transfer process $\sigma_{\rm res}$ to be independent of the collision velocity, we obtain for this distribution function

$$f(v_x) = C\exp\left(-\frac{mv_x^2}{2eE\lambda}\right), \qquad v_x > 0\,,$$

where C is a normalization factor, and the mean free path of ions in the parent gas is $\lambda = 1/(N\sigma_{\rm res})$. From this we have for the ion drift velocity

$$w = \langle v_x\rangle = \sqrt{\frac{2eE\lambda}{\pi m}}\,, \tag{5.32}$$

and according to the criterion, which is reciprocal with respect to (5.31), this drift velocity significantly exceeds the thermal velocity of atoms. The drift ion velocity in the intermediate region of electric field strengths can be determined from the solution of the kinetic equation for the ion distribution function [145, 146]. It is convenient to approximate the ion drift velocity in the form

$$w = \sqrt{\frac{2T}{m}}\,\frac{0.48x}{(1+0.22x^{3/2})^{1/3}}\,,$$

where x is the solution of the equation

$$x = \frac{eE}{2TN\sigma_{\rm res}\sqrt{(4.5+1.8x)2T/m}}\,,$$

and is essentially a weak velocity dependence on $\sigma_{\rm res}$. Figure 19 compares this formula with experimental data [147 – 149]. Thus, the resonant charge exchange process whose nature is closely connected with the structure of atomic particles is of importance for ion transport processes in parent gases. The

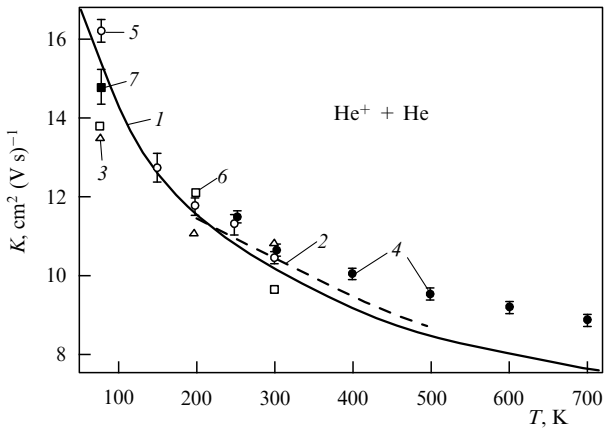

Figure 18. Mobility of He^+ in helium in weak fields. Theory: *1* — formula (5.28), *2* — [139]; experiment: *3* — [140], *4* — [141], *5* — [142], *6* — [143], *7* — [144].

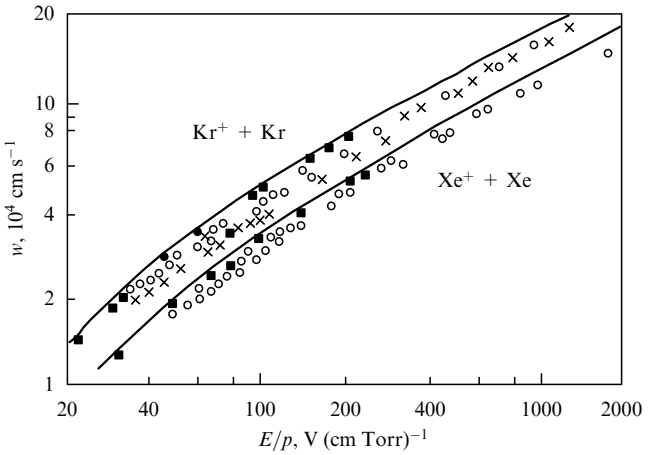

Figure 19. Drift velocity of Kr^+ and Xe^+ in parent gases as a function of the reduced electric field strength. Solid curve — formula (5.33), experiment: ■ — [147], ○ — [148], × — [149].

asymptotic theory accounts for the nature of the process, simplifies the analysis of the process and permits one to evaluate its parameters with an acceptable accuracy under various real conditions.

6. Conclusions

We have considered the character of coupling of electron momenta in atoms and its role in the process of resonant charge exchange. The analysis shows that the *LS*-scheme of momentum coupling, which is valid for light atoms, is useful for the description of valence electron shells of individual atoms. Since some relativistic interactions are not taken into account within the framework of the *jj*-scheme of momentum addition, this scheme is not accurate for the description of heavy atoms, so that the *LS*-scheme of coupling of electron momenta may be used for a qualitative description of these atoms alongside other coupling schemes. We note the importance of correlation effects in atoms due to the violation of the one-electron approach for atoms. In particular, neglecting these effects in atoms leads to an error in the asymptotic coefficient which characterizes the amplitude of the wave function of a valence electron far from the nucleus.

All the above problems of electron coupling and correlations between electrons are of importance for the analysis of processes involving atomic particles. Then additional problems occur due to the motion of atomic particles and their interaction. From this standpoint resonant charge exchange in slow collisions is the simplest of such processes, since the electron transition proceeds at large internuclear distances where interaction between colliding particles is weak, the molecular axis turns by a small angle during the electron transition, and nuclear motion has a classical character. The weakness of interaction allows us to use a specific perturbation method and to extract different effects, considering them separately. In spite of this simplicity, the process of resonant charge exchange is characterized by several limiting cases with respect to the coupling of atom and ion momenta, to the rotation of the molecular axis, and to the ion–atom interaction. According to the experience acquired from the above analysis, in reality case 'a' of Hund coupling scheme, which is a generalization of the *LS*-coupling scheme of addition of electron momenta in an atom with respect to molecular particles, is suitable for evaluation of the resonant charge exchange cross sections for light elements, while case 'c' of Hund coupling scheme is preferable for heavy atoms when the *jj*-coupling scheme is better for composing momenta in individual atomic particles. Nevertheless, the resonant charge exchange cross sections, evaluated on the basis of these coupling schemes and averaged over the momentum projections of the colliding ion and atom, are not sensitive to the coupling scheme if the one-electron transition is allowed for different channels of this process. If this transition is forbidden for some channels, the difference in the cross sections within the framework of cases 'a' and 'c' of Hund coupling scheme can be significant.

This analysis exhibits the general problems of the theory of slow atomic collisions for quasi-resonant processes if the electron transfer proceeds at large separations between colliding atomic particles, where these atomic particles conserve their individuality. Because the cross sections of such processes are expressed through asymptotic parameters of colliding atomic particles, this analysis shows the connection between the problems of physics of individual atomic particles and the physics of atomic collisions.

The author thanks R S Berry who showed the author the importance of correlation effects for two-electron atoms. This paper is partially supported by RFBR (grant # 00-02-17090).

References

1. Condon E U, Shortley G H *The Theory of Atomic Spectra* (Cambridge: The University Press, 1951)
2. Bethe H A *Intermediate Quantum Mechanics* (New York: W A Benjamin, 1964) [Translated into Russian (Moscow: Mir, 1965)]
3. Sobel'man I I *Vvedenie v Teoriyu Atomnykh Spektrov* (Moscow: Nauka, 1977) [Translated into English: *Atomic Spectra and Radiative Transitions* (Berlin: Springer-Verlag, 1979)]
4. Landau L D, Lifshitz E M *Kvantovaya Mekhanika* (Quantum Mechanics) (Moscow: Nauka, 1974) [Translated into English (Oxford: Pergamon Press, 1980)]
5. Veselov M G, Labzovskiĭ L N *Teoriya Atoma*: *Stroenie Elektronnykh Obolochek* (Theory of the Atom: Structure of Electron Shells) (Moscow: Nauka, 1986)
6. Pauli W *Z. Phys.* **31** 765 (1925)
7. Mulliken R S *Rev. Mod. Phys.* **2** 60 (1930)
8. Hund F *Z. Phys.* **36** 637 (1936)
9. Nikitin E E *Opt. Spektrosk.* **22** 379 (1966)
10. Nikitin E E, Smirnov B M *Usp. Fiz. Nauk* **124** 201 (1978) [*Sov. Phys. Usp.* **21** 95 (1978)]
11. Nikitin E E, Smirnov B M *Atomno-Molekulyarnye Protsessy v Zadachakh s Resheniyami* (Atomic and Molecular Processes in Problems with Solutions) (Moscow: Nauka, 1988)
12. Smirnov B M *Zh. Eksp. Teor. Fiz.* **46** 1017 (1964) [*Sov. Phys. JETP* **19** 692 (1964)]
13. Smirnov B M *Zh. Eksp. Teor. Fiz.* **47** 518 (1965) [*Sov. Phys. JETP* **20** 345 (1965)]
14. Smirnov B M *Asimptoticheskie Metody v Teorii Atomnykh Stolknoveniĭ* (Asymptotic Methods in the Theory of Atomic Collisions) (Moscow: Atomizdat, 1973)
15. Hartree D R *Proc. Cambr. Phil. Soc.* **24** 89 (1928)
16. Fock V A *Z. Phys.* **61** 126 (1930)
17. Hartree D R *The Calculation of Atomic Structures* (New York: J Wiley, 1957)
18. Smirnov B M *Fizika Atoma i Iona* (Physics of Atoms and Ions) (Moscow: Energoatomizdat, 1986)
19. Bashkin S, Stoner J *Atomic Energy Levels and Grotrian Diagrams* Vols 1–4 (Amsterdam: North-Holland, 1975–1982)
20. Martin W C, Zalubas R *J. Phys. Chem. Ref. Data* **12** 323 (1983)

21. Radzig A A, Smirnov B M *Reference Data on Atoms, Molecules, and Ions* (Heidelberg: Springer-Verlag, 1985)
22. Schiff L I *Quantum Mechanics* (New York: McGraw-Hill, 1955) [Translated into Russian (Moscow: IL, 1960)]
23. Bethe H A, Salpeter E E *Quantum Mechanics of One- and Two-Electron Atoms* (Berlin: Springer-Verlag, 1957) [Translated into Russian (Moscow: Fizmatgiz, 1960)]
24. Greiner W *Quantum Mechanics* (Berlin: Springer-Verlag, 1989)
25. Fermi E *Notes on Quantum Mechanics* (Chicago: Univ. of Chicago Press, 1961)
26. Hylleraas E A *Z. Phys.* **48** 469 (1928)
27. Hylleraas E A *Z. Phys.* **54** 347 (1929)
28. Chandrasekhar S, Herzberg G *Phys. Rev.* **98** 1050 (1955)
29. Eckardt C *Phys. Rev.* **36** 878 (1930)
30. Hylleraas E A, Undheim B *Z. Phys.* **65** 759 (1930)
31. Galitskiĭ V M, Karnakov B M, Kogan V I *Zadachi po Kvantovoĭ Mekhanike* (Problems of Quantum Mechanics) (Moscow: Nauka, 1981)
32. Blokhintsev D I *Osnovy Kvantovoĭ Mekhaniki* (Grounds of Quantum Mechanics) (Moscow: Vysshaya Shkola, 1961)
33. Davydov A S *Kvantovaya Mekhanika* (Quantum Mechanics) (Moscow: Nauka, 1963) [Translated into English (Oxford: Pergamon Press, 1965)]
34. Wiese W L, in *Progress in Atomic Spectroscopy* Pt. B (Eds W Hanle, H Kleinpoppen) (New York: Plenum Press, 1979) p. 1101
35. Hylleraas E A *Z. Phys.* **63** 291 (1930)
36. Hylleraas E A *Nordske Vidensk. Akad. Skrift., Mat.-natur Kl.* (Oslo) (6) (1932); *Die Grundlagen der Quantenmechanik mit Anwendungen auf atomtheoretische Ein- and Mehrelectron Probleme* (Oslo, 1932)
37. Pekeris C L *Phys. Rev.* **126** 1470 (1962)
38. Fock V A *Izv. Akad. Nauk SSSR Ser. Fiz.* **18** 161 (1954)
39. Sochilin G B *Int. J. Quantum Chem.* **3** 297 (1969)
40. Kellmann M E, Herrick D R *J. Phys. B* **11** L755 (1978)
41. Herrick D R, Kellmann M E *Phys. Rev. A* **21** 418 (1980)
42. Kellmann M E, Herrick D R *Phys. Rev. A* **21** 1536 (1980)
43. Herrick D R, Kellmann M E, Poliak R D *Phys. Rev. A* **22** 1517 (1980)
44. Herrick D R *Adv. Chem. Phys.* **52** 1 (1982)
45. Berry R S *Contemp. Phys.* **30** 1 (1989)
46. Hunter J E, Berry R S *Phys. Rev. A* **36** 3042 (1987)
47. Hunter J E, Berry R S *Phys. Rev. Lett.* **59** 2959 (1987)
48. Berry R S, Krause J L *Adv. Chem. Phys.* **70** 35 (1988)
49. Berry R S, in *Structure and Dynamics of Atoms and Molecules: Conceptual Trends* (Eds J L Calais, E S Kryachko) (Dordrecht: Kluwer Acad. Publ., 1995) p. 155
50. Batka J J, Berry R S *J. Phys. Chem.* **97** 2435 (1993)
51. Berry R S, Ceraulo S C, Batka J, in *Dimensional Scaling in Chemical Physics* (Eds D R Herschbach, J Avery, O Goscinski) (Dordrecht: Kluwer Acad. Publ., 1993) p. 485
52. Hund F *Linienspektren und Periodisches System der Elemente* (Berlin: J Springer, 1927)
53. Hund F *Geschichte der Quantentheory* (Mannheim: Bibliographishes Inst., 1975) [Translated into Russian (Kiev: Naukova Dumka, 1980)] [Translated into English: *The History of Quantum Theory* (New York: Barnes & Noble Books, 1974)]
54. El'yashevich M A *Usp. Fiz. Nauk* **122** 673 (1977) [*Sov. Phys. Usp.* **20** 465 (1977)]
55. Racah G *Phys. Rev.* **61** 186 (1942); **62** 438 (1942)
56. Kaplan I G *Simmetriya Mnogoelektronnykh Sistem* (Symmetry of Many-Electron Systems) (Moscow: Nauka, 1969) [Translated into English (New York: Acad. Press, 1975)]
57. Clementi E, Roetti C *Atom. Data Nucl. Data Tabl.* **14** 177 (1974)
58. McLean A D, McLean R S *Atom. Data Nucl. Data Tabl.* **26** 197 (1981)
59. Evseev A I, Radzig A A, Smirnov B M *Opt. Spektrosk.* **44** 833 (1978) [*Opt. Spectrosc.* **44** 495 (1978)]
60. Ema I et al. *Atom. Data Nucl. Data Tabl.* **72** 57 (1999)
61. Massey H S W *Negative Ions* 3rd ed. (Cambridge: Cambridge Univ. Press, 1976)
62. Smirnov B M *Negative Ions* (New York: McGraw-Hill, 1982)
63. Miller T M, in *Handbook of Chem. Physics* Vol. 10, 74th ed. (Ed. D R Lyde) (London: CRC Press, 1998 – 1999) p. 187
64. Scheer M, Haugen H K *Phys. Rev. Lett.* **76** 2870 (1997)
65. Scheer M, Bilodeau R C, Haugen H K *Phys. Rev. Lett.* **80** 2562 (1998)
66. Williams W W et al. *J. Phys. B* **31** L341 (1998)
67. Scheer M et al. *Phys. Rev. A* **58** 2844 (1998)
68. Sundholm D et al. *J. Phys. B* **32** 5893 (1999)
69. Andersen T, Haugen H K, Hotop H *J. Phys. Chem. Ref. Data* **28** 1511 (1999)
70. Chandrasekhar S *Astrophys. J.* **100** 176 (1944)
71. Drukarev G F *Stolknoveniya Elektronov s Atomami i Molekulami* (Collisions of Electrons with Atoms and Molecules) (Moscow: Nauka, 1978) [Translated into English (New York: Plenum Press, 1987)]
72. Bethe H *Phys. Rev.* **76** 38 (1947)
73. O'Malley T F *Phys. Rev.* **130** 1020 (1963)
74. Martynenko Yu V, Firsov O B, Chibisov M I *Zh. Eksp. Teor. Fiz.* **44** 225 (1963) [*Sov. Phys. JETP* **17** 143 (1963)]
75. Shevelko V P, Vinogradov A V *Phys. Scripta* **19** 275 (1979)
76. Firsov O B *Zh. Eksp. Teor. Fiz.* **21** 1001 (1951)
77. Hering C *Rev. Mod. Phys.* **34** 631 (1963)
78. Smirnov B M *Teplofiz. Vys. Temp.* **4** 429 (1966)
79. Duman E L, Smirnov B M *Zh. Tekh. Fiz.* **40** 91 (1970) [*Sov. Phys. Tech. Phys.* **15** 61 (1970)]
80. Heitler W, London F *Phys. Z.* **44** 445 (1927)
81. Wang S C *Phys. Z.* **28** 363 (1927)
82. Massey H S W, Smith R A *Proc. R. Soc. London Ser. A* **142** 142 (1933)
83. Massey H S W, Mohr C B *Proc. R. Soc. London Ser. A* **144** 88 (1934)
84. Sena L A *Zh. Eksp. Teor. Fiz.* **9** 1320 (1939)
85. Sena L A *Zh. Eksp. Teor. Fiz.* **16** 734 (1946)
86. Sena L A *Stolknoveniya Elektronov i Ionov s Atomami Gaza* (Collisions of Electrons and Ions with Gaseous Atoms) (Leningrad – Moscow: Gostekhizdat, 1948)
87. Demkov Yu N *Uch. Zap. Leningr. Gos. Univ. Ser. Fiz. Nauk* (146) 74 (1952)
88. Duman E L, Smirnov B M *Teplofiz. Vys. Temp.* **12** 502 (1974)
89. Duman E L, Smirnov B M *Teplofiz. Vys. Temp.* **17** 1328 (1979)
90. Duman E L et al., Preprint Kurchatov Institute of Atomic Energy No. 3532/12 (Moscow: IAE, 1982)
91. Smirnov B M *Phys. Scripta* **61** 595 (2000)
92. Rapp D, Francis W E *J. Chem. Phys.* **37** 2631 (1962)
93. Sakabe S, Izawa Y *Atom. Data Nucl. Data Tabl.* **49** 257 (1991)
94. Sakabe S, Izawa Y *Phys. Rev. A* **45** 2086 (1992)
95. Copeland F B M, Crothers D S F *Atom. Data Nucl. Data Tabl.* **72** 57 (1999)
96. Bukhteev A M, Bydin Yu F *Izv. Akad. Nauk SSSR Ser. Fiz.* **24** 964 (1960)
97. Chkuaseli D V, Nikolaĭshvili U D, Guldamashvili A I *Izv. Akad. Nauk SSSR Ser. Fiz.* **24** 970 (1960)
98. Perel J, Daley H L, Vernon R H *Phys. Rev.* **138** 937A (1965)
99. Gentry W R, Lee Y, Mahan B H *J. Chem. Phys.* **49** 1758 (1968)
100. Kushnir R M, Palyukh B M, Sena L A *Izv. Akad. Nauk SSSR Ser. Fiz.* **23** 1007 (1959)
101. Kushnir R M, Buchma L M *Izv. Akad. Nauk SSSR Ser. Fiz.* **24** 986 (1960)
102. Speiser R C, Vernon R *Am. Rocket Soc.* (2068-61) (1961)
103. Marino L L, Smith A C H, Caplinger E *Phys. Rev.* **128** 2243 (1962)
104. McClure G W *Phys. Rev.* **148** 47 (1966)
105. Marino L L *Phys. Rev.* **152** 46 (1966)
106. Palyukh B M, Savchin A S *Zh. Tekh. Fiz.* **38** 1055 (1968)
107. Bydin Yu F *Zh. Eksp. Teor. Fiz.* **46** 1612 (1964) [*Sov. Phys. JETP* **19** 1085 (1964)]
108. Nikitin E E, Umanskii S Ya *Theory of Slow Atomic Collisions* (Berlin: Springer-Verlag, 1984)
109. Gilbody H B, Hasted J B *Proc. R. Soc. London Ser. A* **238** 334 (1956)
110. Wolf F *Ann. Phys.* (Leipzig) **29** 33 (1937)
111. Zeigler B *Z. Phys.* **136** 108 (1953)
112. Dilon J A et al. *J. Chem. Phys.* **23** 776 (1955)
113. Grosh S N, Sheridan W F *J. Chem. Phys.* **26** 480 (1957); *Ind. J. Phys.* **31** 337 (1957)
114. Cramer W H *J. Chem. Phys.* **28** 688 (1958)
115. Gustafsson E, Lindholm E *Ark. Fys.* **18** 219 (1960)
116. Kaneko Y, Kobayashi N, Kanomata I *J. Phys. Soc. Jpn.* **27** 992 (1960)

117. Galli A, Giardani-Guidoni A, Volpi G G *Nuovo Cimento* **26** 845 (1962)
118. Kaneko Y, Kobayashi N, Kanomata I *J. Mass Spectrom.* **18** 920 (1970)
119. Kobayashi N *J. Mass Spectrom.* **20** 123 (1972)
120. Kikiani B I, Saliya Z E, Bagdasarova I G *Zh.Tekh. Fiz.* **45** 586 (1975)
121. Williams J F *Can. J. Phys.* **46** 2339 (1968)
122. Smith D L, Kevan L *Am. Chem. Soc.* **93** 2113 (1971)
123. Okuno K, Koizumi T, Kaneko Y *Phys. Rev. Lett.* **40** 1708 (1978)
124. Amme R C, Haugdjaa P O *Phys. Rev.* **165** 63 (1968)
125. Hishinuma N *J. Phys. Soc. Jpn.* **32** 1452 (1972)
126. Squires L, Baer T *J. Chem. Phys.* **65** 4001 (1976)
127. Kushnir R M *Ukr. Fiz. Zh.* **3** 788 (1958)
128. Fite W L, Smith A C, Stebbings R F *Proc. R. Soc. London Ser. A* **268** 527 (1962)
129. Newmann J H et al. *Phys. Rev. A* **25** 2976 (1982)
130. Belyaev V A, Brezhnev B G, Erastov E M *Zh. Eksp. Teor. Fiz.* **52** 1170 (1967) [*Sov. Phys. JETP* **25** 777 (1967)]
131. Belyaev V A, Brezhnev B G, Erastov E M *Zh. Eksp. Teor. Fiz.* **54** 720 (1968) [*Sov. Phys. JETP* **27** 924 (1968)]
132. Chapman S, Cowling T G *The Mathematical Theory of Non-Uniform Gases* 2nd ed.(Cambridge: The Univ. Press, 1952)
133. Ferziger J H, Kaper H G *Mathematical Theory of Transport Processes in Gases* (Amsterdam: North-Holland, 1972)
134. Holstein T *J. Chem. Phys.* **56** 832 (1952)
135. Mordvinov Yu P, Smirnov B M *Zh. Eksp. Teor. Fiz.* **48** 133 (1965) [*Sov. Phys. JETP* **21** 98 (1965)]
136. Smirnov B M *Dokl. Akad. Nauk SSSR* **168** 322 (1966)
137. Smirnov B M *Iony i Vozbuzhdennye Atomy v Plazme* (Ions and Excited Atoms in Plasma) (Moscow: Atomizdat, 1974)
138. McDaniel E W, Mason E A *The Mobility and Diffusion of Ions in Gases* (New York: Wiley, 1973)
139. Dalgarno A *Philos. Trans. R. Soc. London Ser. A* **250** 428 (1958)
140. Chanin L M, Biondi M A *Phys. Rev.* **106** 473 (1957)
141. Orient O J *Can. J. Phys.* **45** 3915 (1967)
142. Patterson P L *Phys. Rev. A* **2** 1154 (1970)
143. Courville G E, Biondi M A *J. Chem. Phys.* **37** 616 (1962)
144. Gerber R A, Gusinov M A *Phys. Rev. A* **4** 2027 (1971)
145. Perel' V I *Zh. Eksp. Teor. Fiz.* **32** 526 (1957) [*Sov. Phys. JETP* **5** 436 (1957)]
146. Smirnov B M *Dokl. Akad. Nauk SSSR* **181** 61 (1968)
147. Munson R J, Tyndal A M *Proc. R. Soc. London Ser. A* **177** 187 (1940)
148. Varney R N *Phys. Rev.* **88** 362 (1952)
149. Beaty E C *Phys. Rev.* **104** 17 (1956)